

5-17-2014

Verification of Post-glacial Speleogenesis and the Origins of Epigene Maze Caves in New York

Max P. Cooper

Follow this and additional works at: <https://scholarsjunction.msstate.edu/td>

Recommended Citation

Cooper, Max P., "Verification of Post-glacial Speleogenesis and the Origins of Epigene Maze Caves in New York" (2014). *Theses and Dissertations*. 4958.
<https://scholarsjunction.msstate.edu/td/4958>

This Graduate Thesis - Open Access is brought to you for free and open access by the Theses and Dissertations at Scholars Junction. It has been accepted for inclusion in Theses and Dissertations by an authorized administrator of Scholars Junction. For more information, please contact scholcomm@msstate.libanswers.com.

Verification of post-glacial Speleogenesis and the origins of Epigene Maze Caves in
New York

By
Max Cooper

A Thesis
Submitted to the Faculty of
Mississippi State University
in Partial Fulfillment of the Requirements
for the Degree of Master of Science
in Geoscience
in the Department of Geosciences

Mississippi State, Mississippi

May 2014

Copyright by

Max Cooper

2014

Verification of post-glacial Speleogenesis and the origins of Epigene Maze Caves in
New York

By

Max Cooper

Approved:

John E. Mylroie
(Major Professor)

Renee M. Clary
(Committee Member)

Darrel W. Schmitz
(Committee Member)

Michael E. Brown
(Graduate Coordinator)

R. Gregory Dunaway
Professor and Dean
College of Arts and Sciences

Name: Max Cooper

Date of Degree: May 1, 2014

Institution: Mississippi State University

Major Field: Geosciences

Major Professor: Dr. John E. Mylroie

Title of Study: Verification of post-glacial Speleogenesis and the origins of Epigene
Maze Caves in New York

Pages in Study: 180

Candidate for Degree of Master of Science

Dissolutional features called karst exist on the surface, and in the subsurface as caves. In glaciated regions caves were thought to be post-glacial in origin. Work in the 1970s demonstrated that pre-glacial caves existed, but did not answer if a cave could form post-glacially. A model proposed by Mylroie and Carew (1987) states that a post-glacial cave would be controlled entirely by glacial features and the deranged drainage of glaciated terrains. Caves known as maze caves form at maximum rates, and could form to navigable size in the time since deglaciation. Maze caves form in the shallow subsurface, allowing them to be removed in subsequent glaciations. GIS water flow analysis, and calculation of formation times using cross-section data demonstrates that maze caves in the glaciated region of New York are post-glacial in origin fitting in the deranged drainage and forming in the time since deglaciation.

ACKNOWLEDGEMENTS

This thesis would not be possible without a long list of people. I would like to acknowledge: Dr. John Mylroie, my advisor for his ideas and input, as well as guidance in life; my committee members Dr. Renee Clary and Dr. Darrell Schmitz for their input and edits; all of the northeast cavers who helped with access to caves particularly Emily Davis, Tony Hopkins, and Chuck Porter; as well as the staff at the DEC and Northbrook Energy for helping with access to Glen Park Labyrinth, particularly Carl Herzog and Angelena Ross from the DEC, and Chuck Ahlrichs of Northbrook Energy. I would also like to acknowledge my friends who helped with field work Daniel Dreyfus, and Kate Lawrence, as well as my friends who did not participate in field work but who supported me through my studies. Most of all I would like to acknowledge Dr. Alex Bartholomew of SUNY New Paltz who introduced me to caving, participated in field work for this project, and who has been a friend and mentor.

TABLE OF CONTENTS

ACKNOWLEDGEMENTS	ii
LIST OF TABLES	viii
LIST OF FIGURES	x
CHAPTER	
I. INTRODUCTION	1
II. LITERATURE REVIEW	7
Introduction.....	7
Caves and Karst	9
Cave formation.....	10
Passage geometry.....	10
Breakthrough time and growth rates of passages	11
Breakthrough time	11
Growth rate	12
Effects of glaciation	15
Effects on geology and topography	16
Effects on surface hydrology	20
Glaciated karst	21
Glaciated karst studies	22
Determination of pre-glacial origins for caves in glaciated karst.....	23
Flow routes as determination of pre-glacial origin of caves.....	23
Glacially derived sediment sequences within caves	24
Size of cave passage for determining development time.....	25
U/Th Age date determination of caves	26
Effects of glaciation on karst	28
General effects	28
Glacial advance effects	29
In situ glacial effects	30
Retreating glacial effects.....	31
Effects of post-glacial landscape on karst.....	33
Determination of sub-glacial origins of caves	34
Determination of post-glacial origins	34
Maze caves.....	36

Cave patterns.....	38
Network pattern	38
Anastomotic pattern	39
Spongework pattern	39
Branchwork cave speleogenetic origins.....	39
Maze cave speleogenetic origins	40
Maze caves of diffuse infiltration origin.....	41
Diffuse infiltration on soluble rock.....	41
Diffuse infiltration on a permeable, insoluble cap-rock	42
Maze caves of floodwater origin.....	45
Maze caves of hypogenic origin	46
Maze caves in glaciated karst	47
Mention of glaciation in maze cave literature.....	47
Onesquethaw Cave.....	47
Glaciated lowlands geographic province	47
Possible effects of glaciation	48
Sub-glacial origins of network maze caves in the stripe karst of Norway.....	48
Hypothesized effects of glaciation on maze caves	49
Removal of existing maze caves.....	49
Controls on speleogenetic origins.....	50
Initiation of caves.....	50
New York geology.....	51
New York glaciation and glacial landforms	51
Timing of glaciation.....	51
Glacial landforms.....	52
Deranged drainage of New York	53
New York karst areas.....	53
Grenville Marble.....	56
Cambro-Ordovician strata of the Ontario Lowlands	56
Black River Group	56
Trenton Group.....	57
Siluro-Devonian strata of the Appalachian Plateaus	57
Rondout Formation	58
Helderberg Group	58
Manlius Formation.....	58
Coeymans Formation	59
Kalkberg Formation	59
New Scotland Formation	59
Becraft, Alsen, and Port Ewen Formations.....	60
Oriskany Formation	60
Esopus Formation	60
Onondaga Formation	61
Structural geology of New York karst areas.....	61
III. STUDY AREAS AND CAVE DESCRIPTIONS	63

Introduction.....	63
Joralemon Park karst area	63
Geology of Joralemon Park	66
Hydrology of Joralemon Park.....	70
Caves of Joralemon Park	75
Joralemons Cave and Joralemons Backdoor.....	75
Active Caves	77
Hannacroix Maze.....	77
Hydrology	77
Depth of the cave	78
Presence of sediments	80
Cave geometry and passage shape	80
Merritts Cave	81
Depth of the cave	81
Hydrology	81
Cave geometry and passage shape	82
Skips Sewer.....	82
Depth of the cave	82
Hydrology	82
Cave geometry and passage shape	83
Helderberg Plateau, Barber Cave.....	83
Helderberg Plateau geology.....	83
Barber Cave	84
Surface geology and depth of the cave	84
Hydrology	85
Cave geometry and passage shape	85
Adirondacks region, Big Loop Cave	86
Big Loop Cave	87
Depth of the cave	88
Presence of sediments	89
Hydrology	89
Cave geometry and passage shape	89
Ontario Lowlands, the Black River, and the Glen Park Labyrinth.....	90
Black River	91
Glen Park Labyrinth.....	91
Surface geology and depth of the cave	93
Presence of sediment.....	94
Hydrology	94
Cave geometry and passage shape	95
 IV. METHODS	 96
Introduction.....	96
GIS Analysis	98
Creating the initial GIS Description	98
Field work.....	98

	Data from aerial imagery and LiDAR contours.....	99
	Water flow analysis.....	99
	Cave description, and surveying.....	100
	Cave Survey.....	101
	Passage cross-sectional data.....	102
	Measuring cross-sections.....	102
	Measurements.....	102
	Sampling.....	104
	Calculation of possible times of formation by wall-retreat rate.....	104
	Calculations of cross-sectional areas.....	106
	Calculation of possible formation times.....	107
	Evaluation of time in conduit-full conditions.....	109
	Comparison of recorded discharges to supported discharge.....	109
	Modeling of passage growth.....	112
V.	RESULTS.....	113
	Results of Fieldwork and GIS Analysis.....	113
	Description of the study area.....	113
	Topography.....	114
	Surficial karst.....	115
	Cave positions, hydrologic activity and base levels.....	116
	Tills and their position relative to cave entrances.....	118
	Results of GIS water flow analysis.....	119
	Possible times of passage formation.....	122
	Hannacroix Maze.....	123
	Merritts Cave.....	127
	Barber Cave.....	130
	Big Loop Cave.....	134
	Glen Park Labyrinth.....	137
VI.	DISCUSSION.....	144
	Verification of the post-glacial cave origin model.....	144
	Potential issues in methods determining post-glacial origins.....	146
	Use of time plots and calculations.....	146
	Sample size.....	147
	Time discrepancy between Hannacroix Maze and Merritts Cave.....	148
	Post-glacial origins of maze caves in glaciated areas.....	148
	Time and maze caves.....	151
	Transience of maze caves in glaciated areas.....	151
	Rapidity of growth.....	153
	Future work.....	154
VII.	CONCLUSIONS.....	156

REFERENCES158

APPENDIX

A. A PYTHON PROGRAM FOR PASSAGE GROWTH MODELING164

B. CROSS-SECTION SKETCHES, MEASUREMENTS, AND
CALCULATIONS.....168

LIST OF TABLES

2.1	Table showing U/Th from speleothems in caves within the glaciated Heldeberg Plateau.	27
2.2	Comparisons of caves of different time origins in a post-glacial landscape.	36
5.1	Time of glacial retreat and cross-sectional areas for each cave measured in this study.	123
5.2	Calculated times to form the current passage width in Hannacroix Maze depending on days in conduit full conditions.....	126
5.3	Calculated times to form the current passage width in Merritts Cave depending on days in conduit full conditions.....	130
5.4	Calculated times to form the current passage width in Barber Cave depending on days in conduit full conditions.....	132
5.5	Calculated times to form the current passage width in Big Loop Cave depending on days in conduit full conditions.....	137
5.6	Calculated times to form the current passage width in Glen Park Labyrinth depending on days in conduit full conditions.....	140
B.1	Measurements of Hannacroix Maze cross-section.....	169
B.2	Computations based on Equation 4.1 to compute cross-sectional passage area for Hannacroix Maze.....	170
B.3	Measurements of Merritts Cave cross-section.....	171
B.4	Computations based on Equation 4.1 to compute cross-sectional area for Merritts Cave.....	173
B.5	Measurements for cross-section BC- BC' in Barbers Cave.....	173
B.6	Computations for cross-sectional area along BC-BC' using Equation 4.1.....	174

B.7	Measurements for cross-section BLC-BLC' in Big Loop Cave.	175
B.8	Computations for cross-sectional area along BLC-BLC' using Equation 4.1.	176
B.9	Sketch of passage cross-section in Glen Park Labyrinth.	177
B.10	Measurements of passage cross-section in Glen Park Labyrinth.	178
B.11	Calculations of cross-sectional area for passage in Glen Park Labyrinth.	180

LIST OF FIGURES

1.1	The relationship between recharge, dominant type of porosity, and cave development showing that karst is a function of both recharge, and porosity.	2
1.2	Location map for this study.	4
2.1	The different maze cave patterns.	8
2.2	Log-log plot of breakthrough times (time required to reach maximum enlargement rate) depending on several factors. The time to reach maximum enlargement rate depends on flow length (L), temperature, hydraulic gradient (i), and P_{CO_2}	12
2.3	Log-log plot of radius of a tube in cm versus wall-retreat rate (S) in $cm\ a^{-1}$	14
2.4	Graph of mean scallop length (cm) versus mean flow velocity (cm/sec) holding temperature, P_{CO_2} , and diameter/width at various constants.	15
2.5	Photograph of striations on Devonian limestone in Schoharie County, New York State.	17
2.6	Section of the Ravena Quadrangle USGS topographic map (1953) showing the ponded water and connected streams typical of post-glacial deranged drainage.	18
2.7	Cave map of Barrack Zourie Cave system, and a rose diagram of joint orientations controlling the cave.	20
2.8	Flow routes through caves in the Cobleskill plateau proved by dye tracing (solid arrows), and potential flow routes (dotted arrows). These dye traces demonstrate a dendritic pattern of drainage in contrast to the deranged drainage of the surface.	24
2.9	A sequence of glacially derived sediment that is preserved in Howe's Caverns, New York (from Mylroie 1984).	25
2.10	Cave map of the Onesquethaw Cave System.	27

2.11	Map of Skull Cave in Albany County, New York.	32
2.12	Schematic diagram of a hypothetical drainage pattern that can show post-glacial cave origins.	33
2.13	Map of Crossroads Cave, Bath County, Virginia.	43
2.14	Cave map of Anvil Cave, Alabama.	44
2.15	Map indicating time of glacial retreat in calibrated years before present (in ka BP).	52
2.16	Map areas in which carbonates are exposed in New York State. From Engel (2009).	54
2.17	Stratigraphic column of New York State geologic units. Karst forming units are in red. From Engel (2009).	55
3.1	Map generated from the GIS results of the study area.	65
3.2	Cave map of Hannacroix Maze, Albany County, New York.	67
3.3	Map of the previously unmapped Merritts Cave.	68
3.4	Map of Skips Sewer, a floodwater maze cave of network pattern located in Joralemon Park.	69
3.5	Exaggerated DEM (6.5x) of the area around Joralemon Park showing ice-aligned (north-south in this area) ridges and swamps.	70
3.6	Photograph taken from looking upstream of surface stream at swamp adjacent to Hannacroix Maze in Fig. 3.1.	71
3.7	Photograph of limestone ridge containing Hannacroix Maze, which drains the swamp it is located in.	72
3.8	Photograph of the resurgence labeled in Fig. 3.1.	73
3.9	Photographs showing flow out of the entrance to Merritts Cave (Merritts Cave Overflow in Fig. 3.1).	74
3.10	Map of Joralemons Cave and Joralemons Backdoor.	76
3.11	Photograph of till cap.	79
3.12	(a) Photograph of consolidated till cap in Hannacroix Maze that acts as the roof of passage near the Sleeping Alligator entrance. (b) Emplaced glacial cobble located within Hannacroix Maze.	80

3.13	Location map of Barber Cave, Schoharie County, New York.....	84
3.14	Map of Barber Cave.	86
3.15	Location map of Big Loop Cave showing its location within the deranged drainage.	87
3.16	Map of Big Loop Cave.....	88
3.17	Map of the “Old Labyrinth” section of Glen Park Labyrinth.....	92
3.18	Photograph showing the small scallops in Glen Park Labyrinth.	93
4.1	Different methods of deriving cross-sectional area approximations.....	103
4.2	Picture of tripod and Disto used for measurements.	104
4.3	Graph of wall-retreat rates allowing uniform enlargement of passages and the formation of a maze cave.....	105
4.4	Diagram showing different conditions of conduit-full conditions at varying discharges.....	110
4.5	Joint spacing can be further extrapolated after downcutting of a channel.	111
5.1	Map of Minicroix Cave, a previously undescribed and unmapped cave in the Joralemon Park karst area.....	117
5.2	Flow map produced from flow accumulation tool.	120
5.3	Schematic map showing the position of Hannacroix Maze, Merritts Cave, and Skips.....	122
5.4	(a) Photograph of the cross-section of Fungus Footpath of Hannacroix Maze. (b) Transformed cross-section of Fungus Footpath from sketch and measurement data.	124
5.5	Plot of diameter of tube versus time to form at varying conduit-full days per annum for Hannacroix Maze.....	125
5.6	A model of possible growth path for Hannacroix Maze.	127
5.7	Transformed cross-section MC-MC’ (Fig. 4.8) in Merritts Cave.	128
5.8	Plot of width of fissure versus time to form at various conduit full days per annum for Merritts Cave.	129

5.9	Transformed cross-section along BC-BC' in Barber Cave showing fissure shaped passage.	131
5.10	Plot of width of fissure versus time at various conduit-full days per annum for Barber Cave.	132
5.11	Model for one path of Barber Cave growth.	134
5.12	Transformed cross-section of Big Loop Cave along BLC-BLC'	135
5.13	Plot of width of fissure versus time at various conduit-full days per annum for Big Loop Cave.	136
5.14	Transformed cross-section along GPL-GPL' in Glen Park Labyrinth.	138
5.15	Plot of width of fissure versus time at various conduit-full days per annum for Glen Park Labyrinth.	139
5.16	Map section of Glen Park Labyrinth with line indicating where passages were counted and measured for extrapolation across the channel.	141
5.17	Photograph showing typical passage cross-section in Glen Park Labyrinth.	142
5.18	Model of possible growth path of Glen Park Labyrinth.	143
6.1	Schematic model similar to the model given by Mylroie and Carew (1987).	145
6.2	Denudation rates as a function of climate type and precipitation minus evapotranspiration.	152
A.1	Code listing to generate points for Hannacroix Maze model.	165
A.2	Code listing to generate points for Barber Cave model.	166
A.3	Code listing to generate points for Glen Park Labyrinth.	167
B.1	Sketch of passage cross-section in Hannacroix Maze in Fungus Footpath.	169
B.2	Transformed cross-section sketch of Hannacroix Maze in Fungus Footpath.	170
B.3	Sketch of passage cross-section in Merritts Cave along MC-MC'	171
B.4	Transformed cross-section in Merritts Cave along MC-MC'	172

B.5	Sketch of passage cross-section along BC-BC' in Barbers Cave.	173
B.6	Transformed cross-section along BC-BC' in Barbers Cave.	174
B.7	Sketch of passage cross-section along BLC-BLC' in Big Loop Cave.....	174
B.8	Transformed cross-section along BLC-BLC' in Big Loop Cave.....	175
B.9	Transformed cross-section of passage in Glen Park Labyrinth.....	179

CHAPTER I

INTRODUCTION

Karst refers to a landscape formed by dissolutional processes. These are typically in the soluble rock, limestone. Karst can also occur in dolomite, marble, gypsum, and occasionally quartzites. Karst landscapes include surficial features such as karren, dissolutionally enlarged joints (grikes), and sinkholes. Karst landscapes also include enterable and navigable sub-surface features known as caves (as defined by Curl 1964), and their interfaces with the surface, such as sinking streams and springs. Patterns of these dissolutional features are controlled by geology, and by the type of recharge (Fig 1.1, A. Palmer 1991). Therefore, karst is partially a function of recharge and geology.

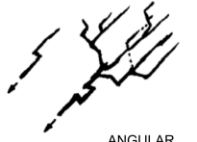






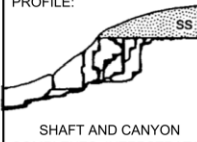




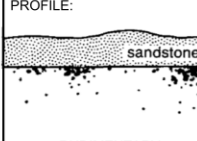


		TYPE OF RECHARGE				
		VIA KARST DEPRESSIONS		DIFFUSE		HYPOGENIC
		SINKHOLES (LIMITED DISCHARGE FLUCTUATION)	SINKING STREAMS (GREAT DISCHARGE FLUCTUATION)	THROUGH SANDSTONE	INTO POROUS SOLUBLE ROCK	DISSOLUTION BY ACIDS OF DEEP-SEATED SOURCE OR BY COOLING OF THERMAL WATER
BRANCHWORKS (USUALLY SEVERAL LEVELS) & SINGLE PASSAGES		SINGLE PASSAGES AND CRUDE BRANCHWORKS, USUALLY WITH THE FOLLOWING FEATURES SUPERIMPOSED:	MOST CAVES ENLARGED FURTHER BY RECHARGE FROM OTHER SOURCES	MOST CAVES FORMED BY MIXING AT DEPTH		
DOMINANT TYPE OF POROSITY	FRACTURES	 ANGULAR PASSAGES	 FISSURES, IRREGULAR NETWORKS	 FISSURES, NETWORKS	 ISOLATED FISSURES AND RUDIMENTARY NETWORKS	 NETWORKS, SINGLE PASSAGES, FISSURES
	BEDDING PARTINGS	 CURVILINEAR PASSAGES	 ANASTOMOSES, ANASTOMOTIC MAZES	PROFILE:  SHAFT AND CANYON COMPLEXES, INTERSTRATAL SOLUTION	 SPONGEWORK	 RAMIFORM CAVES, RARE SINGLE-PASSAGE AND ANASTOMOTIC CAVES
	INTERGRANULAR	 RUDIMENTARY BRANCHWORKS	 SPONGEWORK	PROFILE:  RUDIMENTARY SPONGEWORK	 SPONGEWORK	 RAMIFORM & SPONGEWORK CAVES

Figure 1.1 The relationship between recharge, dominant type of porosity, and cave development showing that karst is a function of both recharge, and porosity.

Different porosities create different patterns, and recharge controls how caves receive water. Intergranular porosities are common in eogenetic rock, where secondary porosity from bedding partings and fractures are common in telogenetic rock. Redrawn from A. Palmer (1991).

Recharge is the addition of water to a hydrologic system. This can be accomplished several categorical ways. These categories are epigenic, in which recharge is accomplished through surface waters (i.e. surface coupled), and hypogenic, where recharge is accomplished through deep waters with dissolutional potential (A. Palmer 1991). When applied to karst, epigene caves are formed by surface water through diffuse flow, or from a point source such as sinking streams and dolines; hypogene caves are

formed through rising thermal waters, or mixing of subsurface waters of different chemistry (A. Palmer 1991).

The geologic controls on caves depend on the type of porosity (Fig. 1.1, A. Palmer 1991), as well as other factors such as geologic structure and stratigraphy. Porosity can be affected by several factors: the age of the rock (and if and how it has been buried), and structural features such as partings from bedding, jointing, or faulting (A. Palmer 1991). Choquette and Pray (1970) presented three diagenetic categories for sedimentary rocks: eogenetic, mesogenetic, and telogenetic. Eogenetic rocks are young, unburied rocks with high intergranular porosity. Eogenetic limestones are typical of tropical and sub-tropical coastlines, and carbonate islands. Mesogenetic rocks have undergone burial, but have not been restored to the surface. These have undergone significant compaction and diagenesis, removing intergranular porosity. Once mesogenetic rocks have been restored to the surface they are categorized as telogenetic, and have very small (<1%) intergranular porosity, and thus their porosity is due to primary structures such as bedding planes, and secondary structures such as jointing. Mesogenetic and telogenetic rocks are typical of continental settings.

One control on geology and recharge is glaciation. Glaciation creates large-scale erosional and depositional features, as well as producing a derangement of the surficial drainage. The removal of large amounts of material, as well as crushing pressures, made early workers on caves in glaciated regions steer towards post-glacial origins for these caves (Myroie and Myroie 2004). This idea was demonstrated to be incorrect through studies performed in New York, specifically the Helderberg Plateau (Fig 1.2) (Baker 1973, 1976, Kastning 1975, M. Palmer 1976, Myroie 1977, Dumont 1995, Lauritzen and

Myroie 2000), as well as in Canada (Ford 1977, 1983, 1987) and Norway (Lauritzen 1981).



Figure 1.2 Location map for this study.

Noted are the caves visited, and the historically studied Helderberg Plateau. The main study area, Joralemon Park includes Hannacroix Maze, Merritts Cave, Skips Sewer, Joralemons Cave, and Joralemons Backdoor.

These studies showed the survival of large, pre-glacial cave systems. They demonstrated this survival through observation of large caves, dye tracing showing pre-glacial dendritic drainage patterns (Baker 1973, 1976, Kastning 1975, Myroie 1977, Dumont 1995), and the presence of glacial sediment sequences in caves (Myroie 1984, Dumont 1995). Final proof of pre-glacial origins comes from U/Th age dates on

speleothems performed by Dumont (1995) and by Lauritzen and Mylroie (2000). This research yielded dates all the way up to the maximum date obtainable through U/Th methods (350 ka), indicating survival through multiple glaciations. These studies additionally showed the effects of glaciation on the development of karst, including the mantling of some karst by glacial debris, and the infilling of insurgences and resurgences.

The question of pre-glacial caves has been answered, with caves remaining through multiple glaciations. One unanswered question however, is the existence of post-glacial caves, as the time since deglaciation is short, and therefore enterable and navigable caves have little time to form. A previously untested hypothesis postulated by Mylroie and Carew (1987) is that post-glacial caves would be completely aligned to current base levels, and be controlled by glacial landforms. One type of cave is a maze cave, which forms at maximum rates, and therefore can reach navigable size in the time since deglaciation. These can therefore be used to test the hypothesis of Mylroie and Carew (1987), which is the purpose of this research study. Additionally, the shallow nature of epigenic maze caves makes them prone to removal, and therefore another hypothesis that can be tested is the post-glacial origins of maze caves in glaciated regions, such as New York. Hypogene caves, while important to mention in any maze cave study, are not part of this study as their depth makes them less susceptible to removal, unless they have been brought to the shallow subsurface by uplift and erosion.

To test this hypothesis, GIS surface water flow analysis was performed, combined with cave mapping to verify the model proposed by Mylroie and Carew (1987). The water flow analysis was performed on the area in and around Joralemon Park near Ravena, New York; the primary study location (Fig. 1.2) with respect to the floodwater

maze caves, Hannacroix Maze, Merritts Cave, and Skips Sewer (selected because preliminary fieldwork revealed controls by swamps located in glacial depressions). Floodwater caves were selected as they are controlled directly by drainage and not through diffuse flow, as well as having set conditions for the rate at which they form. To determine whether the majority of maze caves in glaciated areas are post-glacial, cross-sectional data were collected from Hannacroix Maze, Merritts Cave, Big Loop Cave, Barber Cave, and Glen Park Labyrinth (chosen for accessibility reasons, and their locations in a complete range of New York stratigraphy and structure). These data, combined with wall-retreat rate (increase in passage width per year) for maze caves and times exposed to conduit-full conditions (i.e., time a passage is completely full of water), give a range of time required to form the current cross-sectional area of passage for these caves. These parameters can then be compared to data observed in the field, in the literature, from watershed areas and precipitation, and from United States Geological Survey (USGS) stream gages to determine how many days conduits are full, and which formation times are viable. Formation times less than the time since glacial retreat in each study area lends evidence to post-glacial origins for each cave.

CHAPTER II

LITERATURE REVIEW

Introduction

Glaciated terrains exist in the northern latitudes, including Canada, England, Russia, Scandinavia, and the northern United States. Within these glaciated terrains there are many karst terrains, including in Canada, England, Norway, and the northern United States (Jennings 1971, Walthem 1974, Ford 1977, 1983, 1987, Lauritzen 1981). Studies since the 1970s have been conducted to tie the post-glacial drainage characteristics to pre-glacial patterns in karst, especially within the glaciated karst terrain in central New York (Baker 1973, 1976, Kastning 1975, Mylroie 1977, Dumont 1995). Much of this work focuses on determining whether the caves in glaciated areas are of pre- or post-glacial origin, whether caves can survive repeated glaciation, and what effect glaciation has on modifying pre-glacial caves. These studies also relate the current drainage of karst areas to these pre-glacial caves. Through these studies, as well as through U/Th dating of speleothems (e.g. Lauritzen and Mylroie 2000), researchers demonstrated that caves could survive multiple glaciations, such as those seen in the Pleistocene.

The speleogenesis of maze caves is another area of karst research subjected to rigorous studies in the 1970s. A. Palmer's (1975) seminal maze cave paper discussed the geometries as well as the speleogenetic origins of maze caves. A. Palmer (1975) gave the following geometries of maze caves: branchwork pattern, network pattern, anastomotic

pattern, and spongework pattern (Fig. 2.1). Also provided were speleogenetic causes: diffuse flow through a non-soluble, permeable cap-rock, floodwater recharge, and “artesian” flow of water (later to be replaced by hypogenic recharge). Further work by A. Palmer (1991) connected the type of recharge to the patterns of these caves (Fig. 1.1).

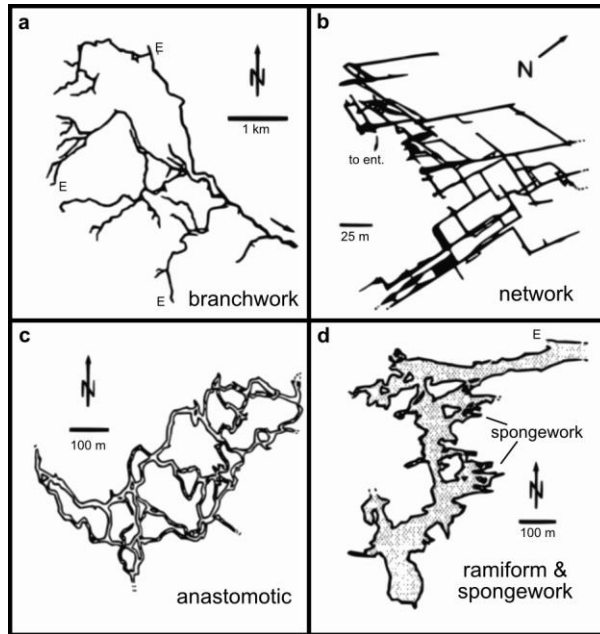


Figure 2.1 The different maze cave patterns.

Network patterns are more regular, typically following joint sets that are orthogonal or at a slight angle. Anastomotic patterns are similar to a braided stream pattern. Spongework pattern is “sponge-like” and irregular. Redrawn from A. Palmer (1999).

Both glaciated karst studies and maze cave studies referenced the other. Studies of glaciated karst mention maze caves (e.g. Mylroie 1977), and some give the cause of maze-like areas within larger caves to be related to flooding caused by flow blockage from glacial sediment (e.g. A. Palmer 1975). A. Palmer (1975) mentioned the glacial geographic provenance with respect to maze caves by giving the dominant maze pattern

as network, but did not give the dominant recharge type. None of this earlier work establishes whether maze caves in glaciated regions are pre-, post-, or sub-glacial in origin. Recent studies in Norway by Skoglund et. al. (2005, 2010, 2011) proposed sub-glacial origin of maze caves in the stripe karst of that country. These few studies, however, do not fully elucidate maze caves in glaciated regions, as they only exist in the contact karst end-member of stripe karst (Lauritzen 2001). The lack of study on the connection between glaciation and maze caves thus gives purpose to this study, as well as a return to the historically studied New York karst.

Caves and Karst

The process of karst formation in carbonate rocks involves the dissolution of soluble material. This dissolution occurs because of acids dissolving calcium carbonate (CaCO_3). The dissolutional potential of these acids vary with pH, with the partial pressure of CO_2 (P_{CO_2}), and with temperature (A. Palmer 1991, 2007). Unlike most minerals, CaCO_3 is more soluble in cold waters (Adams and Swinnerton 1937). Cold water also holds more CO_2 , the primary acidifier of surface and shallow subsurface waters (i.e. epigene). Dissolution processes are responsible for both surface features, and for caves.

Additional processes can also affect karst and caves. Caves in particular are shaped after initial development from mechanical weathering in the form of breakdown (A. Palmer 2007).

Cave formation

A subset of karst is the subsurface voids known as caves. These form in different overall patterns depending on recharge and geology (Fig. 1.1, A. Palmer 1991).

Geometry of individual cave passages is determined by amounts of water, and the position of the water table in relation to the passage (A. Palmer 2007). The rates at which these passages form depend on inception (breakthrough) times, and on wall-retreat rates (A. Palmer 1991).

Passage geometry

Passage geometry depends on the initial geologic structure controlling the passage, and how it grows. Growth can either be vertical, or around the perimeter of the passage. How growth occurs is determined by the movement of water through these passages.

Vertical growth is caused by water in the vadose zone. The vadose zone exists above the water table, permitting water to move laterally and vertically down to the water table under a continuous gravitational gradient. The result of vadose water is the creation of shafts, and canyon shaped passages (A. Palmer 1984). The growth of these passages is downward, dissolving the floor.

Growth around the perimeter of a passage is caused by water in the phreatic zone. The phreatic zone is below the water table, and water moves horizontally through passages under pressure. Passage growth is around the perimeter in these cases and forms fissure shape passage, or tube shape passage (A. Palmer 1984). Where the water table has moved downwards (i.e. changes in base level), these tubes can be downcut by canyons in the floor by the change to vadose conditions (A. Palmer 2007).

Breakthrough time and growth rates of passages

Breakthrough time

The time in which a passage is formed depends on the initiation of the passage, and then the enlargement rate afterwards. Breakthrough time is defined as the growth time until maximum enlargement rate (A. Palmer 2007), and is generally achieved when a fracture or tube width reaches 1 cm. This breakthrough time marks the transition between laminar and turbulent flow, and depends on the length of the passage, the initial width, the temperature of the water, the hydraulic gradient, and the initial P_{CO_2} (Fig. 2.2, A. Palmer 1991).

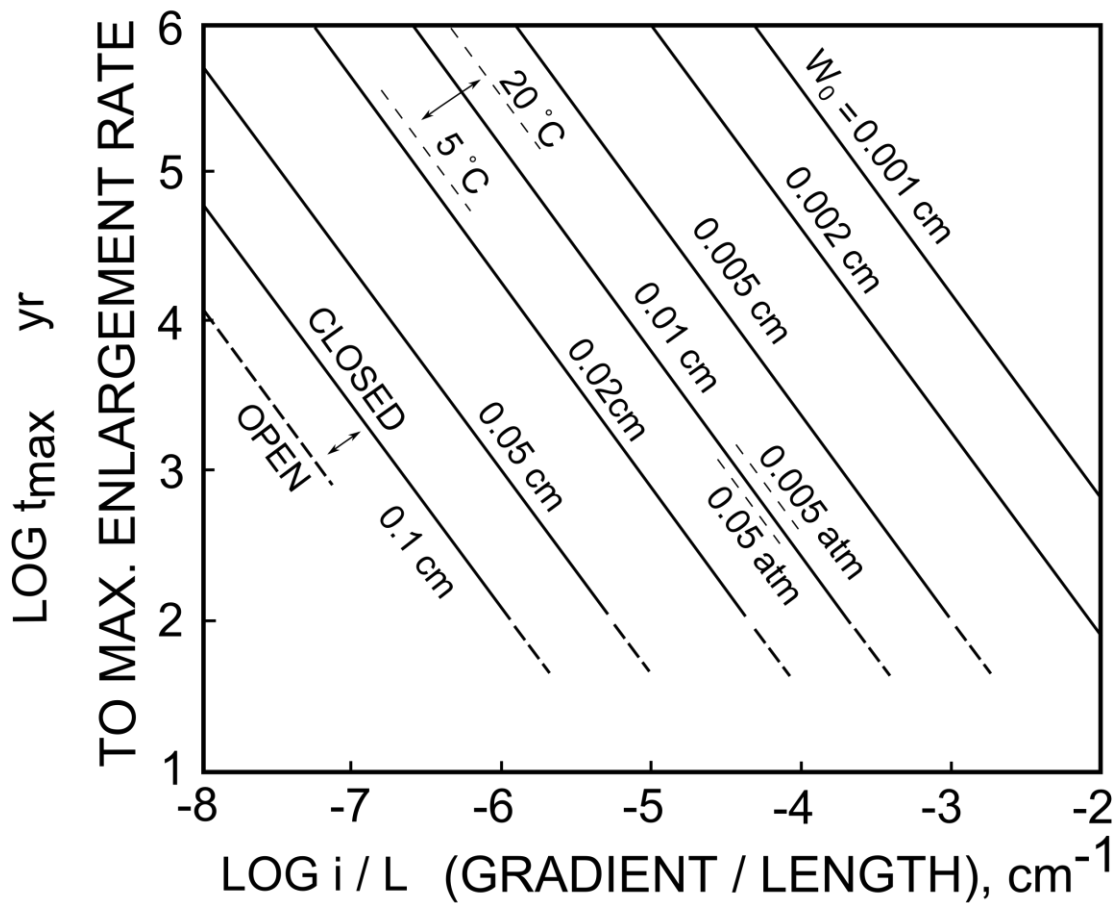


Figure 2.2 Log-log plot of breakthrough times (time required to reach maximum enlargement rate) depending on several factors. The time to reach maximum enlargement rate depends on flow length (L), temperature, hydraulic gradient (i), and P_{CO₂}.

Redrawn from A. Palmer (1991).

Growth rate

Once the initial passage is formed it enlarges at rates dependent on discharge (Q), flow length (L), and radius (r)/width (w) of the passage. This growth is either downwards in vadose passage, or by the perimeter in phreatic passage (A. Palmer 2007). Wall-retreat rates can be calculated by a variety of factors, and are generally between 0.001–0.01 cm

per year in non-floodwater conditions (A. Palmer 1991). Equation 2.1 can be used for calculating wall-retreat rates (A. Palmer 1991):

$$S = \frac{31.56Q(C - C_0)}{pL r_r} \text{ cm / year} \quad (2.1)$$

where S = wall-retreat rate in cm/year, C is the concentration of solutes, p is the wetted perimeter (related to the radius in tubes, or width in fissures), and r_r is rock density. The constant 31.56 converts units of the variables into cm/year. For tubes this retreat rate applies along the radius; for fissures this retreat rate applies to the half-width (w/2).

The relationship for wall-retreat rate is proportional to discharge, and inversely proportional to radius and flow length. The retreat rate also depends on the amount of time per year that a passage is full of water. Wall-retreat rates can be directly measured, or through calculations with Eq 2.1. Graphs (Fig. 2.3) generated from Eq 2.1 by holding groundwater conditions constant can be used to identify wall-retreat rates depending on discharge (Q), radius or width of fissure, and flow length (L).

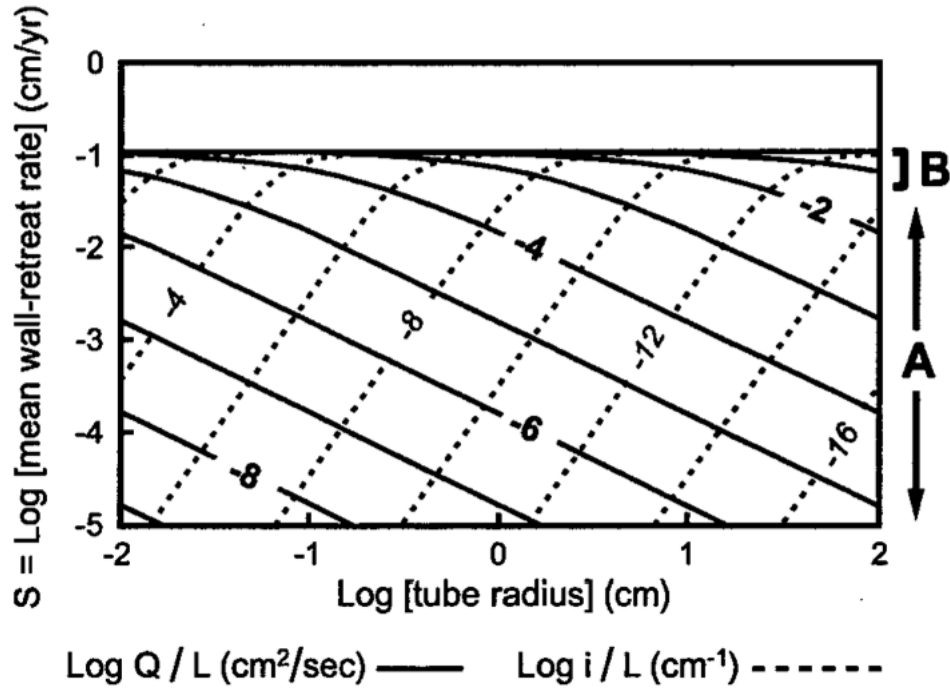


Figure 2.3 Log-log plot of radius of a tube in cm versus wall-retreat rate (S) in cm a^{-1} .

This function depends on either Q/L for turbulent flow, or i/L for laminar flow. From A. Palmer (1999).

To use these graphs, discharges must be obtained. Discharges can be obtained by measurements of flow velocities, and by the cross-sectional area of passage. If there is no current flow, paleo-discharges can be calculated using scallops. Scallops form by turbulent flow along passage walls, and their length is inversely proportional to velocity (A. Palmer 2007, Fig. 2.4). Other factors affecting size of scallops include temperature, and P_{CO_2} . There is some debate in the literature as to whether scallops represent mean flow, or peak flow (A. Palmer 2007). Mean flow velocity, as the cause for the generation of scallops, will be assumed in the calculations of this study.

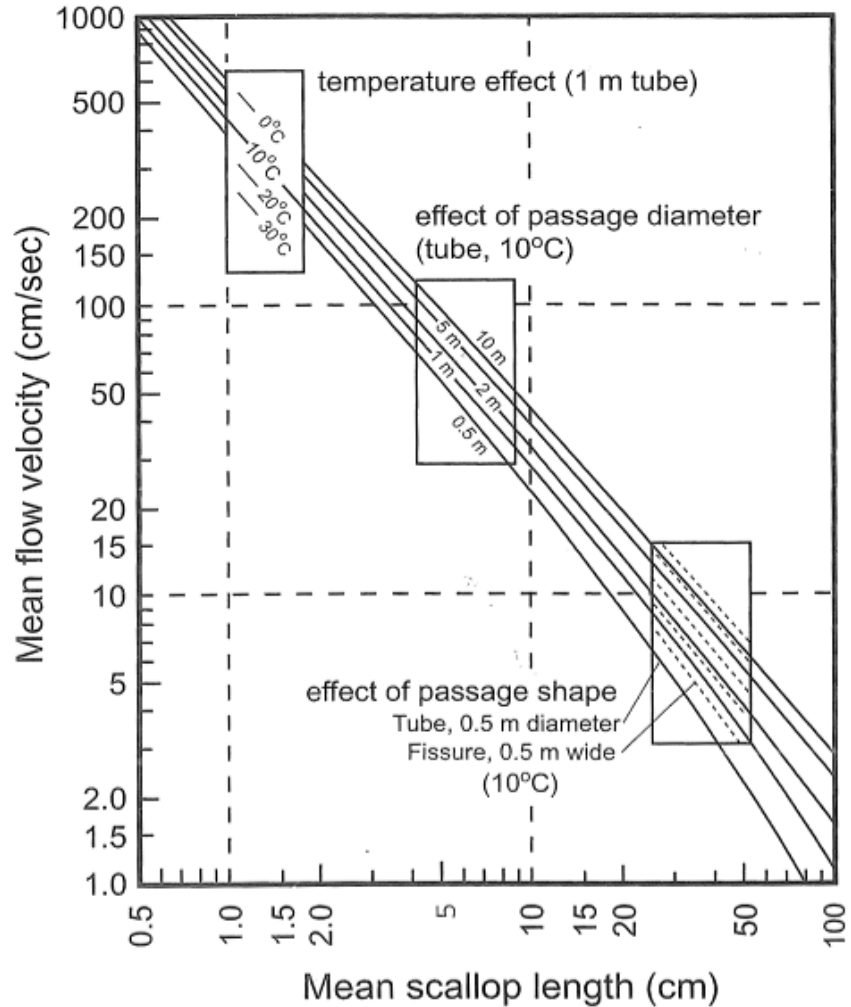


Figure 2.4 Graph of mean scallop length (cm) versus mean flow velocity (cm/sec) holding temperature, P_{CO_2} , and diameter/width at various constants.

From A. Palmer (2007).

Effects of glaciation

As karst is a function of geology and recharge it is important to understand the effects of glaciation on geology, topography, and hydrology in order to further understand glaciated karst. The effects are due to the quarrying of bedrock, the deposition of sediment in the form of till and outwash, the presence and draining of glacial lakes, and isostatic effects from glacial loading and unloading.

Effects on geology and topography

Glaciers are powerful erosional forces, especially the continental glaciers of the recent ice ages of the Pleistocene. These glaciers remove material irrespective of size, and have been known to produce house-sized erratics (Goldring 1943, Isacshen et. al. 2000). They produce large depressions in topography by excavation and by valley blockages; and remove soils as well as weaker clastic rocks such as sandstones and shales. The removal of this material is preferential to the strength of the materials, and can leave the more resistant karst-forming limestones and dolostones exposed (Myloie 1977). The scouring produces geologic and topographic features at the small scale, such as striations (Fig. 2.5), which can indicate ice-flow direction, as well as at the large scale with large depressions (also aligned with ice-flow direction) that can be visible on topographic quadrangle maps (e.g., Fig. 2.6, Goldring 1943).



Figure 2.5 Photograph of striations on Devonian limestone in Schoharie County, New York State.

These striations can indicate ice flow directions of advancing glaciers. Striations on limestone, such as seen here can be difficult to preserve due to dissolution and denudation. The light colored areas in the image show a lineation from left (NE) to right (SW). The striations were protected from karst dissolution by a layer of overlying till rich in carbonate clasts. The dark patches represent dissolution and removal of the glacial polish in the ~10 years since the outcrop was uncovered by excavation for quarrying purposes. Photo credit J.E. Mylroie.

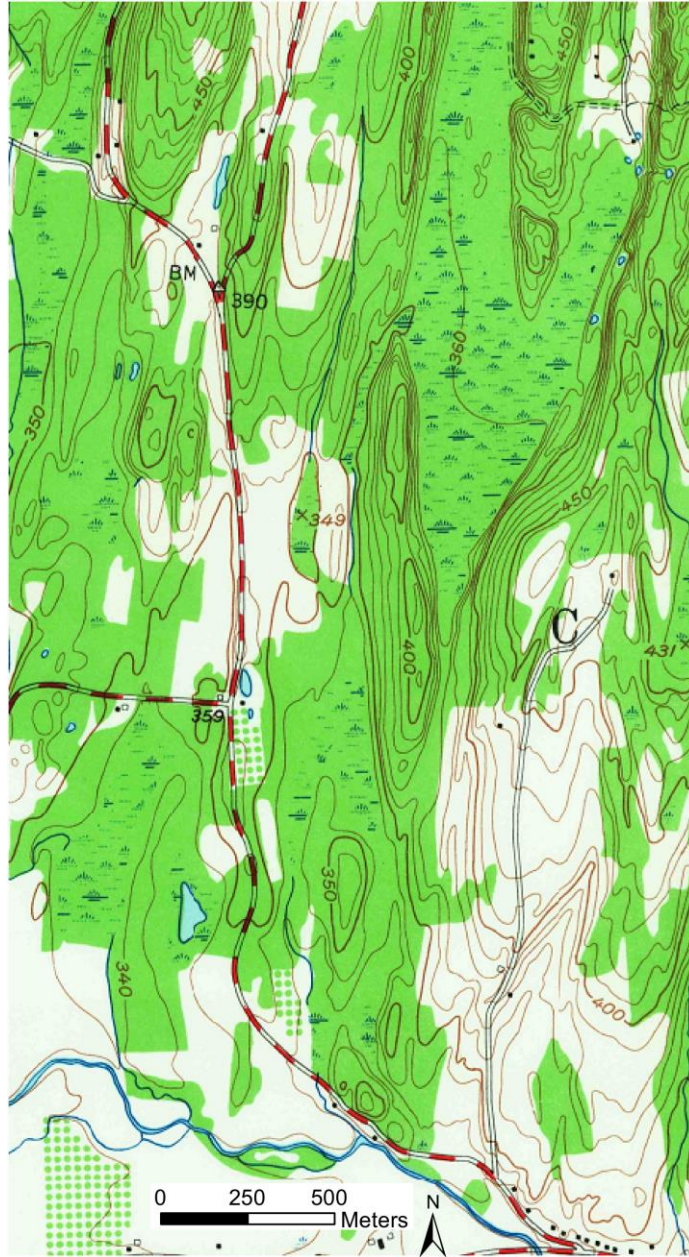


Figure 2.6 Section of the Ravenna Quadrangle USGS topographic map (1953) showing the ponded water and connected streams typical of post-glacial deranged drainage.

Depressions occupied by these swamps as well as hills and glacial landforms are aligned in a north-south orientation, congruent with ice flow in this area, about 30 miles (50 km) SW from the location of Figure 2.5. Additional factors for north-south orientation include the orientation of structures in this area, creating preexisting weaknesses for the north-south ice movement to remove.

Glaciers are also powerful depositional forces. Glaciers create landforms such as moraines and drumlins composed of tills, as well as a variety of glacial lake sediments and outwash debris. The tills are unsorted, and in some cases have had enough time to compact and begin diagenesis (Mylroie 1977). These till landforms are commonly visible on topographic maps in glaciated regions, and are aligned with ice-flow direction.

Other effects on geology include the release of stress on jointing. The release of pressure during glacial unloading and rebounding releases stress and can cause the expression of regional jointing (Harland 1957), as seen in Barrack Zourie Cave of the Helderberg Plateau (Dumont 1995, Fig. 2.7 A. Palmer 2007).

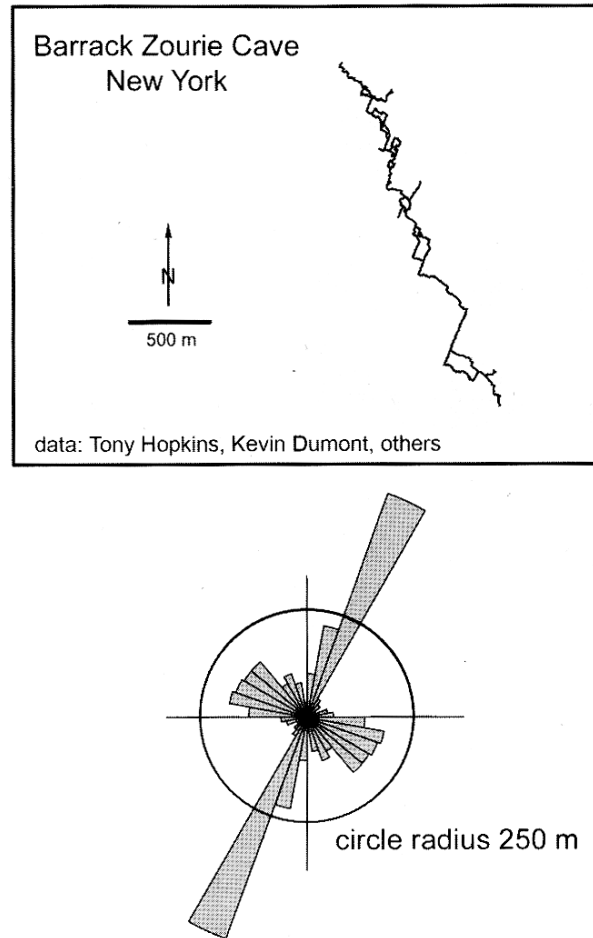


Figure 2.7 Cave map of Barrack Zourie Cave system, and a rose diagram of joint orientations controlling the cave.

These orientations are typical of caves found in the Helderberg Plateau. This rose diagram shows the magnitudes of joint lengths and their orientation. These joints may be mechanically enlarged from glacial unloading (Dumont 1995, A. Palmer 2007). Map and rose diagram from A. Palmer 2007.

Effects on surface hydrology

The removal and deposition of material by glaciers changes the drainage patterns of large areas. The creation of large-scale depressions, as well as the creation of large-scale sediment packages, changes the patterns from common dendritic patterns to a deranged drainage system. Irregularly shaped streams and pooled water in lakes and

swamps dammed by tills characterize this drainage (Kastning 1975, Twidale 2004). These deranged patterns can be seen on topographic and geologic maps in glaciated regions (e.g., Goldring 1943; Fig. 2.6). The patterns visible are small lakes connected by streams that do not seem to follow structural controls such as jointing, but instead follow the glacially modified topography.

Glaciation also causes large-scale drainage effects in stream valleys, with the creation of underfit streams and rivers, and the infilling of pre-glacial valleys (M. Palmer 1976). An underfit stream is a stream that occupies a valley that it itself could not create at its current or flood discharge levels. In glaciated regions this valley shape can result from the formation of a large U-shaped glacial valley as opposed to a V-shaped stream valley. These can also form through previously much larger discharges due the draining of a glacial lake (LaFleur 1968, Twidale 2004), or via discharges associated with glacial melt and retreat.

Glaciated karst

Due to changes in the geology, topography, and hydrology, glaciers have a varying impact on karst. This karst also has an impact on the drainage in these glaciated terrains. Original thoughts were that most caves in glaciated regions are post-glacial, and the presence of large caves was anomalous (e.g. Jennings 1971). This idea was shown to be erroneous through the glaciated karst studies from the 1970s to the recent (Baker 1973, 1976, Kastning 1975, Ford 1977, Mylroie 1977, Lauritzen 1981, Dumont 1995, Lauritzen and Mylroie 2000). These studies indicated that glaciers modified the pre-glacial karst drainage, but that the pre-glacial flow routes through large cave systems persist in post-glacial times.

Glaciated karst studies

Much of the work on glaciated karst has been conducted in central New York (Baker 1973, 1976, Kastning 1975, Mylroie 1977, Dumont 1995, Lauritzen and Mylroie 2000), as well as in Britain (Jennings 1971, Sweeting 1973, Waltham 1974, Ryder 1975), Canada (Ford 1977, 1983, 1987), and Norway (Lauritzen 1981). The studies performed in New York focused on the Helderberg and Cobleskill plateaus, and demonstrated the survival of pre-glacial flow routes through large cave systems such as McFails Cave, Howe Caverns, and the Barrack Zourie Cave System (Kastning 1975, Mylroie 1977, Dumont 1995). These studies demonstrated that large caves are able to be preserved over multiple glaciations, and retain their dendritic drainage characteristics with some modification from glaciation. Some of these modifications include quarrying away large entrances, creation of new resurgence points, deposition of sediment, and altering caves by damming of sediment to form maze-like elements (Mylroie 1977, A. Palmer 1975, Mylroie and Mylroie 2004).

These studies demonstrated the survival of these pre-glacial caves using several methods. Methods include the dye traces revealing dendritic flow paths of pre-glacial drainage (Baker 1973, 1976, Kastning 1975, Mylroie 1977, Dumont 1995), agreement with pre-glacial base levels (M. Palmer 1976), the presence of glacial sediments in caves (Mylroie 1984, Dumont 1995), large passage dimensions in contrast with the possible time allowed to form post-glacial caves (Mylroie and Carew 1987, Mylroie and Mylroie 2004), and by U/Th absolute age dating on speleothems (Dumont 1995, Lauritzen and Mylroie 2000).

While these studies have definitively revealed that pre-glacial caves survived glaciation, they do not demonstrate the characteristics of a cave that is post-glacial in origin. Potential post-glacial origins have been discussed based on passage dimensions, and by the connection to post-glacial deranged drainage (A. Palmer 1972, Mylroie and Carew 1987), but have not been documented through field work and methods such as dye tracing to reveal the post-glacial characteristics.

Determination of pre-glacial origins for caves in glaciated karst

Flow routes as determination of pre-glacial origin of caves

The studies of glaciated karst in the Helderberg and Cobleskill plateaus pay much attention to the determination of flow routes through caves systems via dye tracing. The dye tracing done by Baker (1973, 1976), Mylroie (1977), and Dumont (1995) demonstrate flow paths congruent with that of non-glaciated drainage. These flow paths show typical dendritic systems in contrast to the deranged drainage systems of glaciated terrains (Fig. 2.8). While dye tracing does reveal changes by glaciation of flow routes, these changes are to tributary passages by new post-glacial insurgences (Mylroie and Carew 1987, Mylroie and Mylroie 2004). The presence of these dendritic patterns reveals that these caves' speleogenetic configurations are related to pre-glacial drainage conditions, and these data serve as one piece of evidence for the survival of large cave systems through glaciation.

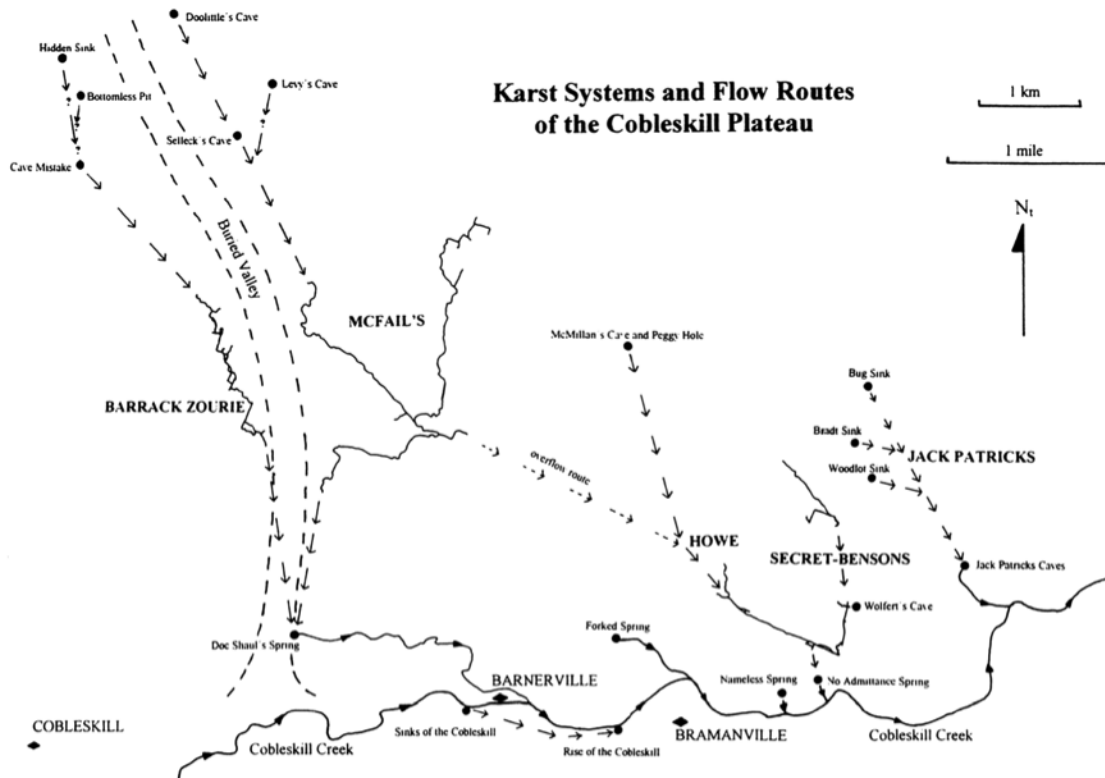


Figure 2.8 Flow routes through caves in the Cobleskill plateau proved by dye tracing (solid arrows), and potential flow routes (dotted arrows). These dye traces demonstrate a dendritic pattern of drainage in contrast to the deranged drainage of the surface.

Figure from Dumont (1995).

Glacially derived sediment sequences within caves

Several glaciated karst studies noted, and some analyzed, sediments within the caves (Myroie 1984, Dumont 1995, Weremeichik 2013). For caves to have glacially derived sequences of sediments within them, the caves themselves must have existed prior to the deposition of sediment. Sediments that are glacially derived and are present in these caves include glacial tills, cobbles, and laminated clays (Myroie 1984, White 2007). A sequence of glacially derived sediments is portrayed in Figure 2.9, and has been

demonstrated to be glacial lake deposits by Weremeichik (2013), thus requiring the cave to have been there before the glacial lake deposited the sequence. Glacially derived sediments have been used to both demonstrate the survival of caves through glaciations, and for paleoclimatic studies (White 2007).

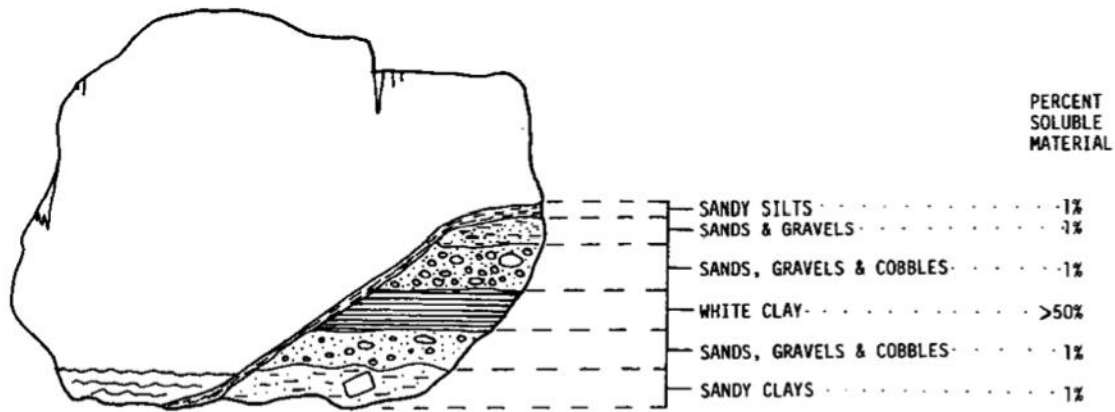


Figure 2.9 A sequence of glacially derived sediment that is preserved in Howe’s Caverns, New York (from Mylroie 1984).

This sequence is hypothesized to be a glacial lake deposit of Glacial Lake Schoharie (Weremeichik 2013).

Size of cave passage for determining development time

The earliest observation in glaciated karst regions were of passage dimensions. While it was earlier thought that large caves were anomalous in these glaciated areas (Mylroie and Mylroie 2004), it has been demonstrated there are many large caves in glaciated areas, such as Schoharie Caverns, Howe Caverns, McFail’s Cave, Skull Cave, the Barrack Zourie Cave System, and others (Baker 1973, 1976, Kastning 1975, Mylroie 1977, Dumont 1995). The time window from the last glacial maximum only allows for

the formation of cave passages with small cross-sectional areas (Myloie and Carew 1987) due to wall-retreat rates (A. Palmer 1991). Though some post-glacial passages exist in the large caves, they are restricted in cross-sectional area and are influenced by the post-glacial topography. These caves with large cross-sectional areas are simple yet effective indicators of pre-glacial cave origins.

U/Th Age date determination of caves

The most definitive evidence of pre-glacial cave origins in glaciated karst regions comes from absolute age dating of speleothems. U/Th dating on speleothems by Dumont (1995), and by Lauritzen and Myloie (2000) demonstrated that the large Helderberg caves are pre-glacial. Dumont (1995) performed U/Th dating on speleothems from the Barrack Zourie Cave System, and had results of 165 ± 10 ka and 277 ± 24 ka, both of which are pre-glacial dates. Data from Lauritzen and Myloie (2000) showed U/Th dates of speleothems in select Helderberg Plateau caves up to the maximum possible date possible from U/Th of 350 ka. Selected data from Lauritzen and Myloie (2000) are included in Table 2.1, and their complete data can be found in that paper. Lauritzen and Myloie (2000) also obtained recent, post-glacial speleothem dates in Onesquethaw Cave (Fig. 2.10; Table 2.1), which is a cave of floodwater origin with maze-like characteristics (A. Palmer 1972). While this U/Th age date does not prove that it is post-glacial, it does leave that possibility, as there are no other age dates from speleothems within that cave greater than that of the post-glacial time period.

Table 2.1 Table showing U/Th from speleothems in caves within the glaciated Heldeberg Plateau.

J.No	Sample	Cave	U(ppm)	235U/238U	230Th/234Th	230Th/ 232Th	Age (ka)	Corrected Age
931	BZ95-05 Rocky Road	Barrack Zourie	0.17±0.00 3	1.974±0.039	0.8077±0.0195	34	146.7±6.7	
935	S-1 A	Schoharie	0.51±0.01	1.639±0.047	1.0688±0.0413	61	>350	
941	C-5 A	Caboose	2.75±0.04	2.434±0.025	0.4318±0.0104	>1000	57.8±1.8	
979	O-1B	Onesquethaw	0.10±0.00 3	1.390±0.060	0.1105±0.0136	4.94	12.6±1.65	8.96±2.1
1655	NY-96- HH1-1	Hollyhock Hollow	0.09±0.00 3	1.497±0.071	0.5195±0.0400	4.44	75.8±8.3	56.32±10.2

These data range from the largest date possible with U/Th dating (350 ka) to a post-glacial date (8.96±2.1 ka). Selected data are from Lauritzen and Mylroie (2000).

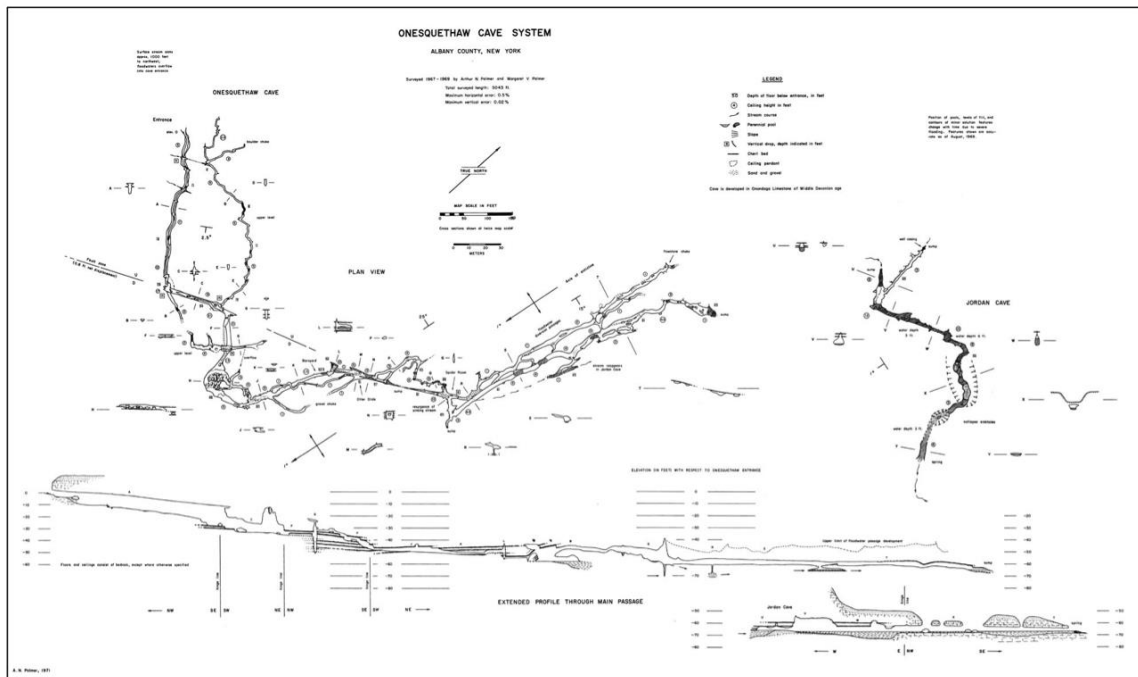


Figure 2.10 Cave map of the Onesquethaw Cave System.

This cave partially has the geometry of an anastomotic maze cave, and is of floodwater origin. U/Th dating gives a date of at least 8.96±2.1 ka (Lauritzen and Mylroie 2000). Map from A. Palmer (1972).

Effects of glaciation on karst

General effects

In addition to the determination of pre-glacial origins of caves in glaciated karst, the effects of the glaciation on karst were studied as well. These effects are related not only to the general action of glaciers on geology, topography, and hydrology, but also to the chemistry of glacial waters. The quarrying of weaker clastics as well as some limestones, and the deposition of material has impacts on the development and modification of karst (Kastning 1975, Baker 1976, Mylroie 1977). Additional effects include mechanical freeze-thaw weathering (Kastning 1975, Ford 1987), ice-contact speleogenesis (Lauritzen 1981), changes in water chemistry (Tranter et. al. 1993), and joint development from isostatic rebound (Harland 1957, Baker 1976, Faulkner 2006a). Mylroie (1977) summarized these effects as ice advance effects, in-place ice effects, and ice recession effects. Ford (1987) further classified these effects as destructive, inhibitive, preservative, and stimulative.

Glacial quarrying of material and the deposition of glacial sediments has a great impact on karst and cave development. This glacial quarrying removes limestone and removes near-surface karst development including karren and shallow caves (Kastning 1975, Mylroie 1977). This quarrying also removed weaker clastic sedimentary rocks such as sandstone and shale (potentially creating new limestone exposures for post-glacial karst development). The deposition of sediments buried surficial karst features, as well as surface-subsurface interfaces (Kastning 1975). Additionally, this deposition acts in ways to preserve pre-glacial karst by covering it with fairly impermeable materials (Ford 1987) as can be seen in Fig. 2.5, where deposited material protected striations from dissolution.

Glacial advance effects

Myroie (1977, 1984) categorized glacial effects according to the timeline of glaciation: advancing glaciers, glacial contact, and glacial recession. These stages affect karst differently with periglacial (the cold margins along glacial areas) effects in ice advance and ice retreat, and ice-contact and water filling effects during in-place ice periods.

Advancing glacial effects include both mechanical, and chemical (Kastning 1975, Baker 1976, Myroie 1977, 1984). Mechanical erosional effects include the quarrying of weaker rocks, as well as surficial and shallow sub-surface karst. Depositional effects come from the establishment of tills, moraines and drumlins (Myroie 1977). This deposition obstructs insurgences and resurgences (Kastning 1975, Baker 1976). Additional mechanical ice advance effects are due to the establishment of permafrost in the periglacial environment, and include freeze-thaw weathering (Ford 1977, 1987, Myroie 1977, 1984).

Chemical ice advance effects are mainly due to the periglacial environments at the edge of the advancing glaciers (Myroie 1977, 1984), especially the establishment of permafrost (Ford 1977, 1987). The establishment of permafrost reduces water flow, thus slowing down karstification (Ford 1977, Myroie 1984). An increased rate of dissolution may result due to calcium carbonate having a higher solubility in colder temperatures (Adams and Swinnerton 1937). This effect may be negated however due to the lowering of P_{CO_2} because of low organic activity in soils (Myroie 1977). Additional effects may include the shutting off of speleothem growth due to permafrost (Ford 1977, Lauriol et. al. 1997).

In situ glacial effects

In situ glacial effects, like advancing glacial effects are mechanical, hydrological and chemical. Mechanical effects include the further erosion and deposition of material, including obstruction of pre-glacial insurgences and resurgences. Hydrological and chemical effects include infilling of caves with ponded water, and establishing layered sequences of sediments in this water (Mylroie 1977, 1984; however see Weremeichik 2013 for an alternative explanation.). Hydrological and chemical effects also cause some karstification, and ice-contact speleogenesis. Additionally, they cause the sub-glacial initiation and development of certain caves (e.g. Lauritzen 2001).

Hydrological and chemical effects of glaciers on karst are varied. Glacial effects on water chemistry both hinder and amplify dissolutional ability. Rock flour from mechanical weathering decreases acidity by providing high amounts of soluble material surface area, which thus decreases the dissolutional ability of waters (Tranter et. al. 1993, Tranter 2003). High discharges from glacial meltwater however reduce this effect and still allows for karst development. These hydrochemical effects can increase karstification during ice-contact, and can increase wall-retreat by an order of magnitude (from 0.01-cma^{-1} to 0.1-cma^{-1} , Lauritzen 2013). Another driver of speleogenesis with *in situ* ice is the hydrologic effect of increased head within rock, especially within confined dipping beds as seen in the stripe karst of Norway (Mylroie 1984, Lauritzen 2001, 2013). This effect can also be possible in other rugged upland areas that have undergone deformation, such as the Adirondack Mountains of New York; however these are not direct analogues to stripe karst (Faulkner 2009).

Retreating glacial effects

Retreating glacial effects include the reestablishment of periglacial effects for a short period, as well as massive deposition of sediment from outwash (Myroie 1977, 1984). The massive deposition of sediment in the form of tills and outwash streams blocks insurgences and resurgences. Additionally the high discharges from meltwater entered caves and deposited glacially derived sediments within them. This deposition clogged certain cave passages and created inefficiencies (Myroie 1977), leading to backflooding and some establishment of floodwater mazes superimposed on pre-glacial caves, such as Skull Cave, New York (Fig. 2.11, A. Palmer 1975, 2007). Further effects from retreating glaciers include unloading and resulting tectonism (Harland 1957, A. Palmer 1975, Baker 1976, Faulkner 2006a). The removal of pressure due to unloading combined with tectonism releases joints to mechanically enlarge and allows new passages, or entire new caves, to form. These joints may be enlarged enough to cause initiation of caves to maximum enlargement (and thus are at a width of ~1 cm), without the need for chemical breakthrough (Faulkner 2006a).

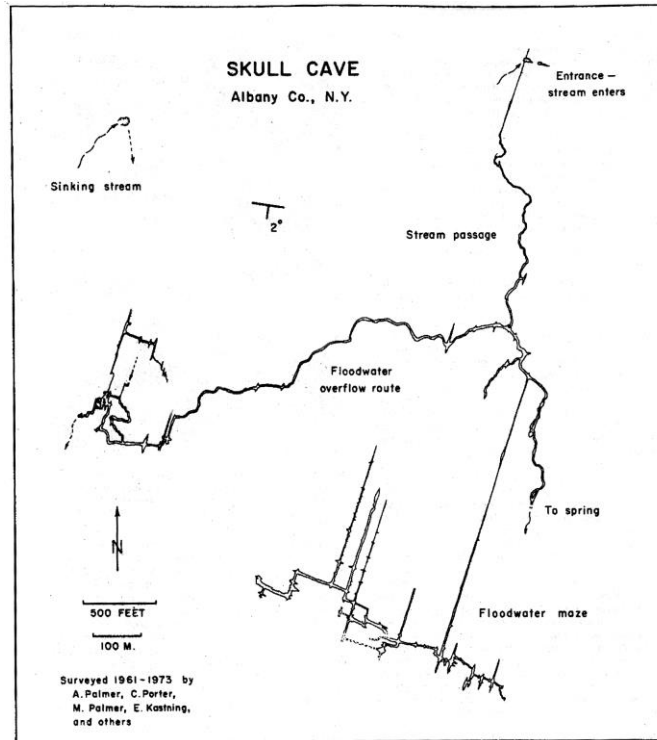


Figure 2.11 Map of Skull Cave in Albany County, New York.

This map shows joint controls on the cave, which were potentially mechanically enlarged by glacial unloading. Mechanical enlargement of joints, combined with glacial damming of resurgence is the hypothesized cause of the floodwater maze sections seen (A. Palmer 1975). The maze sections are overprinted on a simple dendritic pattern of pre-glacial origin. Map from A. Palmer (1975).

The combination of tectonic initiation and conditions directly after ice retreat may play a role in the formation of post-glacial caves. After retreat ice dammed lakes are created, tectonically initiated caves can enlarge under cold waters. This model of cave formation has been studied in marble caves of Norway and New England (Faulkner 2008, 2009). This model may also apply to limestone in glaciated areas.

Effects of post-glacial landscape on karst

The post-glacial landscape includes infilled insurgences and resurgences, as well as pre-glacial valleys with sediments. This infilling changes and buries previous base levels of flow for the pre-glacial cave systems (M. Palmer 1976), which caused the overprint of post-glacial deranged drainage onto the pre-glacial caves by establishing new insurgences and in-feeder shafts (Myroie and Carew 1987, Myroie and Myroie 2004). The waters in these drainages are ponded in glacial depressions and guided by glacial landforms such as drumlins, which will channelize them into sinkholes (Myroie and Carew 1987) (Figure 2.12).

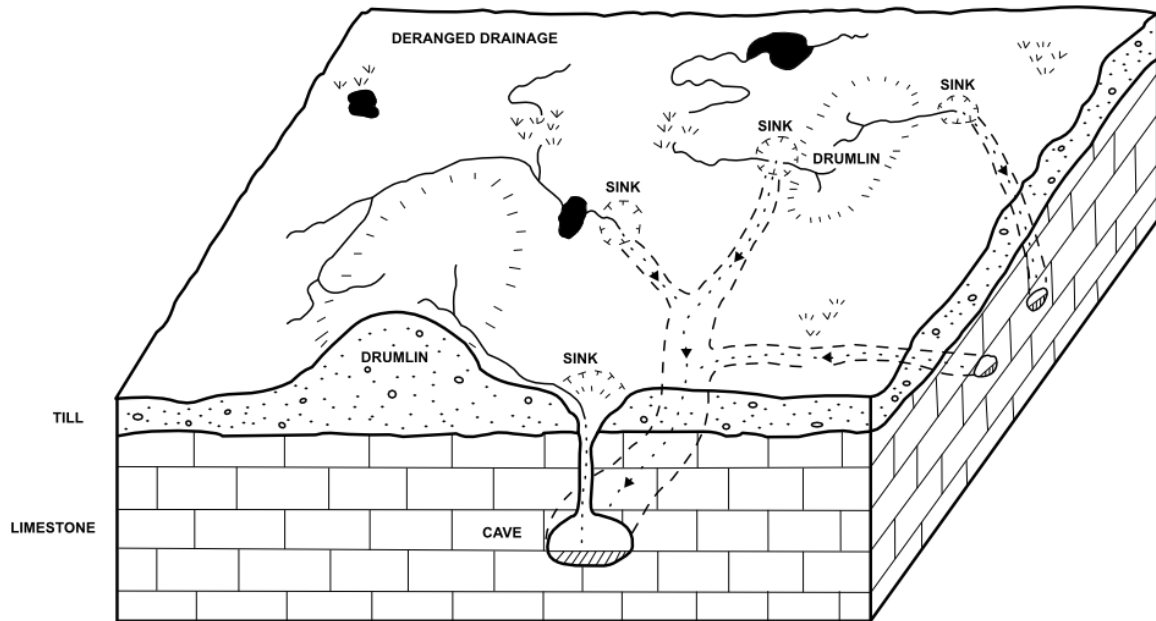


Figure 2.12 Schematic diagram of a hypothetical drainage pattern that can show post-glacial cave origins.

Redrawn from Myroie and Carew (1987).

Determination of sub-glacial origins of caves

The effects of glaciation during advancing, *in situ*, and retreating stages still allow for some speleogenesis due to sources of aggressiveness in meltwaters, and from meltwater mixing with other water sources (Tranter et. al. 1993, Tranter 2003, Skoglund and Lauritzen 2011). Direct observation of sub-glacial speleogenesis includes areas in Canada (Ford et. al. 1983), and in Norway (Lauritzen 1981, 1984, Skoglund and Lauritzen 2010, 2011).

Other evidence includes agreement with the hydrology of *intraglacial* periods (time periods with major continental glaciation) in the stripe karst of Norway (Skoglund and Lauritzen 2010, 2011). Skoglund and Lauritzen (2011) noted that maze caves in stripe karst are relict at a higher elevation, and that their flow paths agree with the flow and retreat of the glaciers. Additionally, scallop data and wall-retreat rates demonstrated that the development time agreed with intraglacial time lengths.

Determination of post-glacial origins

Caves of post-glacial origins have their initial speleogenetic development after the retreat of glaciers. Assigning a time period for initial karstification is fairly difficult, as there are no ways to directly date epigenic void initiation. Dates obtained by U/Th age dating and other methods only show that the voids must have existed prior to the establishment of the dated speleothems or sediments. These methods do not directly show the time of initiation of the void, and thus cannot be used to state whether a cave is post-glacial (though the presence of a pre-glacial date will invalidate post-glacial origin).

In order to define the origin of a cave, it is first important to define a cave, and specifically a karst cave. Curl (1964) reviewed definitions of caves. His definition

includes the ability of a human to enter and be surrounded by rock. This definition separates caves from the smaller subsurface voids such as simple intergranular pore space that is established after diagenesis and compaction. Karst caves in particular are caves that form by dissolution of soluble bedrock, and are humanly enterable.

For karst caves to be established there must be dissolution of initial material creating a void, requiring an initial porosity either through intergranular pores, or from partings via jointing or bedding planes (A. Palmer 1991). Additionally it requires these spacings to be of a minimum width of 10^{-4} meters (Groves and Howard 1994). For the epigenic caves used in this study, there is also the additional requirement of transition from laminar to turbulent flow (breakthrough).

The simplest answer to how old a cave can be is that it is no older than the rock in which it develops (Myroie and Carew 1987). Myroie and Carew (1987) showed that karstification could happen soon after rock deposition and diagenesis, especially in young, eogenetic limestones. For telogenetic limestones (such as those in glaciated regions) pore spaces exist, though they are smaller, and thus require a longer time to enlarge to a size for initial breakthrough for turbulent flow and karstification (A. Palmer 1991). Epigenic voids in these telogenetic limestones begin after their uplift from the mesogenetic realm.

To definitively answer the question of when a void starts there is a need to establish what the void cuts across, which can just be the karstified rock. To determine that a void is post-glacial requires that the void crosscuts some glacial feature, or is controlled by glacial features. A. Palmer (1972) suggested that the caves would reflect post-glacial drainage patterns. Myroie and Carew (1987) elaborated on this hypothesis,

and gave a possible schematic representation (Fig. 2.12) to determine post-glacial origins, though no further studies have been conducted representing this approach in the field. Additionally these caves should be small in cross-section in agreement with wall-retreat rates and the time since the last glacial maximum.

These criteria can be compared to pre-glacial and sub-glacial caves, with respect to current post-glacial conditions. This comparison is detailed in Table 2.2.

Table 2.2 Comparisons of caves of different time origins in a post-glacial landscape.

Criterion	Pre-glacial	Sub-glacial	Post-glacial
Cross-sectional Area	Large with some small passages.	Depends on time length of exposure to sub-glacial waters.	Small
Connection to Drainage	Major passages are not connected to deranged drainage, though small active tributaries are.	Relict in post-glacial drainage.	All passages are controlled through deranged drainage, such as ponded water in depressions or flow off of glacial deposits.
Connection to Base Level	Trunk passages aligned with pre-glacial base level.	Passages aligned to base level during glaciation.	Passages are aligned to current base level, or align with downcutting of post-glacial channels.
Glacially Derived Sediment	Present, can exist as sequences.	Present and contemporaneous with speleogenesis.	Allogenicly transported, no sequences.
Speleothem Dating	Range of age dates from post-glacial to pre-glacial.	Not present or post-glacial.	Will not have age dates older than the glacial retreat.

Note that there can be small passages in pre-glacial caves, but the entire cave is not small. Also note that pre-glacial caves can have post-glacial speleothem dates. Age dates do not definitively show that a cave is post-glacial, and the presence of age dates older automatically invalidates post-glacial origin.

Maze caves

One type of cave that exists in both glaciated and non-glaciated areas is a maze cave. Maze caves differ from typical cave branchwork caves (Fig. 2.1) in that they consist of many closed loops with passages all having the same or similar dimensions (A. Palmer 1975). The simplest manner for this development to occur is that passages are enlarged at the same time, and the same rate, with little to no competition of flow paths.

In order to remove competition, maze caves require large amounts of recharge (Q), and/or a short flow length in the soluble rock (L), and in particular the ratio between these variables (Q/L) should be large. This ratio allows a smaller value to Q to be effective if the value of L is *very* small (A. Palmer 1991). A. Palmer (1975) initially gave three speleogenetic methods that satisfy this high Q/L ratio: recharge through floodwater, recharge through diffuse infiltration, and potentially “artesian” flow. Maze caves with recharge connected to the surface (floodwater and diffuse origin) tend to form in the shallow subsurface (A. Palmer 2001). A. Palmer (1975) also outlined the patterns formed by these recharge routes (Fig. 2.1) which are related to type of recharge, and the dominant type of porosity of the rock (Fig. 1.1, A. Palmer 1991). As hypogene speleogenesis theories were developed, hypogenic recharge was added to the speleogenetic origins of maze caves, essentially replacing the “artesian” model (A. Palmer 1991).

Maze caves have been mentioned in the glaciated karst literature, and maze cave literature refers to the glaciated geographic provenances (A. Palmer 1972, 1975, Mylroie 1977). A. Palmer’s (1972) paper on the Onesquethaw Cave System (Fig. 2.10) discussed both directly, by giving this cave system a speleogenetic origin of floodwater from a sinking stream, and by postulating that it is post-glacial in origin due to the small passage cross-section and agreement with deranged drainage. A. Palmer (1975) further identified the network pattern as the dominant pattern in glaciated regions. While both glaciated karst and maze caves have been discussed in the other’s literature, little has been done to connect them. While A. Palmer (1975) noted the dominant pattern in glaciated regions, he did not identify a dominant speleogenetic origin. While some maze caves in glaciated

areas have been hypothesized to be of post-glacial origins (A. Palmer 1972), no work completely discussed whether maze caves are dominantly pre-, post- or sub-glacial in origin.

Cave patterns

The majority of *known* caves in the world are of a branchwork pattern (Fig. 1.1), with an arrangement much like a dendritic stream (A. Palmer 1975). These form with differing discharges and flow paths in stream-like tributary passages (A. Palmer 1975, 1991). Maze caves do not have differing sized passages, and instead have passages that are of the same, or close to the same, cross-sectional areas. These passages form closed loops, and are arranged into different patterns depending on the dominant type of porosity, and the dominant type of recharge (Fig. 1.1, A. Palmer 1991). All the recharge patterns for these maze caves have a high discharge to flow length ratio (Q/L) to enlarge passages at the same rate. This large Q/L ratio does not allow passages to form preferentially, and instead enlarges all available voids at the same rate, as a result of no competition for flow paths. The cave patterns produced by this large Q/L ratio are network pattern, anastomotic pattern, and spongework pattern (Fig. 2.1).

Network pattern

Network patterns are regular patterns of closed-loop passages (Fig. 2.1). They usually are joint controlled, with approximately equal spacing between joint sets (A. Palmer 1991). These joint sets are often orthogonal, or near orthogonal. Joints are typically in a near-vertical, or vertical orientation (A. Palmer 1975).

Anastomotic pattern

Anastomotic pattern maze caves are similar in geometry to braided streams (Fig. 2.1). They typically have circular or elliptical cross-sections (A. Palmer 1975). The dominant type of porosity for forming an anastomotic pattern is bedding-plane partings (A. Palmer 1975, 1991). This pattern, along with network pattern, is typical of telogenetic rock, as joints and bedding planes are often the only available pore space.

Spongework pattern

Spongework pattern is a globular, seemingly chaotic pattern (Fig. 2.1, A. Palmer 1975). This pattern is constructed of interconnected, dissolutionally enlarged intergranular porosity (A. Palmer 1991). This intergranular porosity is typically seen in young, eogenetic rocks, and therefore is mostly limited to young coastal karst, carbonate island karst, and hypogenic caves such as Carlsbad Caverns.

Branchwork cave speleogenetic origins

Branchwork caves are formed due to competition of aggressive waters to find the most efficient flow path (A. Palmer 1991). The branchwork pattern arises due to the intersection of single, non-contemporaneous passages of differing discharges (Q). This discharge is produced by recharge of point sources such as dolines (sinkholes).

These intersections are due to chance, structural controls, and difference in hydraulic head. These structures include jointing and bedding planes, which under high Q/L conditions will produce maze caves (A. Palmer 1975, 1991). These structures under lower Q/L conditions however, will produce a branchwork pattern as there is not enough discharge to equally enlarge passages. Flow will instead follow only certain passages that

are more efficient, and therefore some passages out-compete their neighbors. This pattern can have long flow paths (high L) and thus be located fairly deeply in the subsurface, as compared to maze caves (A. Palmer 2001).

Floodwaters also modify branchwork caves. Floodwaters can arise from intense recharge, internal cave blockage, or from resurgence blockage (A. Palmer 1975, 1984, 1991, 2001). In branchwork caves these floodwaters modify passages of the cave system to form maze-like sections, from the periodic high Q/L conditions (e.g. Fig. 2.11). These maze-like sections are similar to maze caves, and produce the same patterns depending on the dominant structural and lithologic controls.

Maze cave speleogenetic origins

Maze caves have several speleogenetic origins. These origins are: 1) recharge through diffuse infiltration either directly into a soluble rock, or through a permeable, insoluble cap-rock; 2) recharge through floodwaters by stream piracy or dammed lake overflow; and 3) recharge by hypogenic waters, initially called “artesian” recharge, by A. Palmer (1975) but subsequently modified (A. Palmer 1991, 2007). All of these recharge methods produce a high Q/L ratio required to equally enlarge cave passages and form the maze patterns. This Q/L ratio must be greater than 0.001-cms^{-1} (also taking into account the passage radius), and thus will produce wall-retreat rates of 0.1-cma^{-1} (Fig. 2.2, A. Palmer 1991, 1999). Note that these values are instantaneous values, and can vary depending on the length of time the passage is at conduit-full condition.

Maze caves of diffuse infiltration origin

A. Palmer (1975) originally hypothesized two epigene maze cave origins, and one artesian origin (later to be replaced by hypogene). The first of these speleogenetic origins is diffuse infiltration, whether directly onto soluble rock, or through a permeable, insoluble cap-rock. This diffuse origin allows the Q/L ratio to be satisfied by adding aggressive water that is channeled uniformly into fissures, thus eliminating competition and having a short flow path in the soluble rock. This uniformity allows all passages to be recharged at the same rate (A. Palmer 1975, 1991, 2000, 2007).

Diffuse infiltration on soluble rock

Diffuse recharge on soluble rock tends to produce denudation and surficial features, however some maze cave development is possible (A. Palmer 1991). Maze caves in non-capped soluble rocks are enigmatic and produce rudimentary networks, and spongework patterns depending on structural control (A. Palmer 1975, 1991). A. Palmer (1975) originally hypothesized this origin in isolated hills of limestone, however does not give much evidence or an origin of aggressive water, as most dissolutional potential is expected to be lost at the surface due to saturation of dissolved surface material. As development of hyogenic (and in particular mixing water) speleogenesis theories were developed, A. Palmer (1991) revisited these caves and associated these origins coupled with diffuse flow from the surface as the recharge method. Such caves in isolated hills were relict features.

A. Palmer (1991) detailed this speleogenetic origin as having aggressive water from mixing with saltwater, or H₂S-rich water. This approach moves onward from his earlier paper (A. Palmer 1975) on continental, telogenetic karst, and instead focuses on

porous island carbonates (A. Palmer, 1991). These processes produce patterns similar to patterns as seen on continental karst, but are more directly observable evidence for this type of speleogenesis on islands.

Diffuse infiltration on a permeable, insoluble cap-rock

The other surface coupled diffuse flow origin for speleogenesis is through a permeable, insoluble cap-rock, typically sandstone (A. Palmer 1975, 1991). This cap-rock is typically thin, less than 10 meters. Thicker or less permeable cap-rocks produce isolated recharge to specific points in the limestone, creating a typical branchwork pattern (A. Palmer 1975). With a thinner cap-rock the diffuse water flows through the permeable rock, primarily along joints, and penetrates to the soluble rock. This water follows the structural control in the cap-rock, and imprints this pattern on the soluble rock. This can produce maze patterns that do not line up with the jointing in the soluble rock, but instead line up with jointing in the cap-rock, as can be seen in Crossroads Cave (Fig. 2.13). This type of speleogenesis does not require the high discharge required of floodwater origin, as the water is recharged uniformly (providing a very low L , and thus a high Q/L even with a low Q) and remains aggressive uniformly allowing the development of extensive maze caves such as Anvil Cave (Fig. 2.14). Evidence for this speleogenetic origin is downward fluting, which removes upward or laterally flowing water as a possible cause (A. Palmer 1975, 1991, 2000). Additional evidence includes termination or the changeover to branchwork pattern when the cap-rock becomes thicker or less permeable, and the distance to contact of passage to the cap-rock, which can often act as the cave ceiling in these types of caves (A. Palmer 2000).

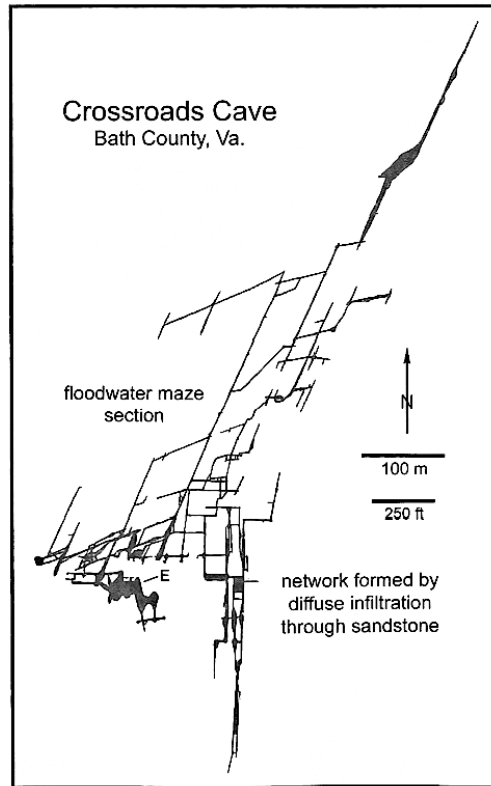


Figure 2.13 Map of Crossroads Cave, Bath County, Virginia.

This cave shows two distinct network mazes. The maze section in the southern portion of the cave is of diffuse origin and follows the fracture pattern of the overlying sandstone. The midsection of the cave is of floodwater origin and shows the fracture pattern within the limestone. Map from A. Palmer (2007).

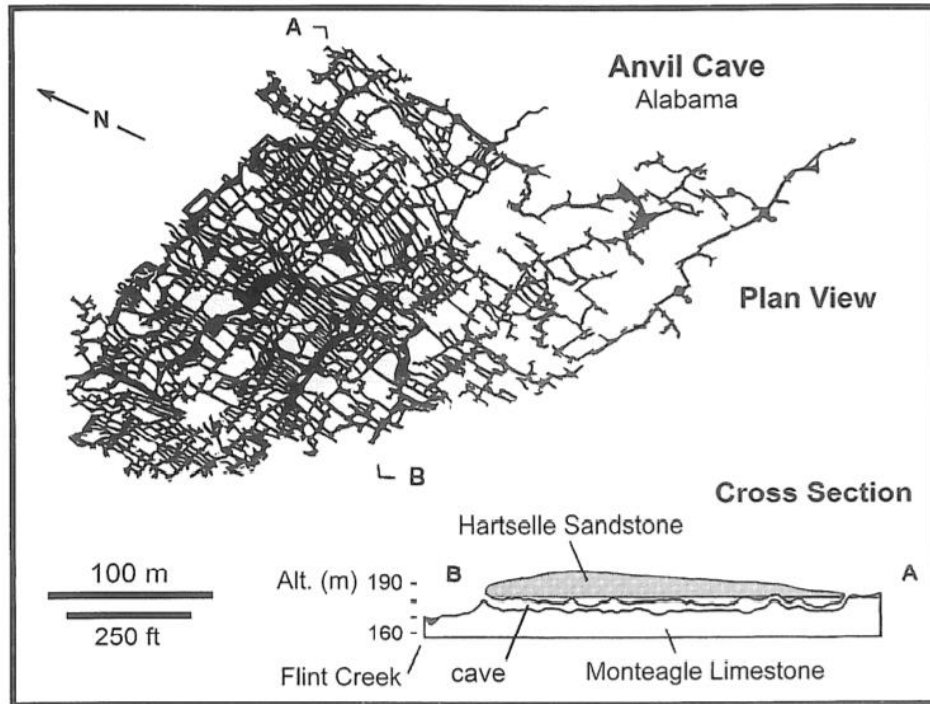


Figure 2.14 Cave map of Anvil Cave, Alabama.

This cave is of diffuse flow origin through an insoluble cap-rock. This cave is extensive, though passage is only contained within a small (~150 meters by ~250 meters) area. Map from A. Palmer (2007).

Maze caves of this origin have a distinct evolution (A. Palmer 1975, 2000). Originally the permeable rock has a higher hydraulic conductivity (K) than the soluble rock, allowing higher discharge, and a higher head in the cap-rock. As passage is formed, the hydraulic conductivity of the soluble rock becomes larger. Eventually the hydraulic conductivity of the soluble rock will be greater than that of the cap-rock, allowing water to preferentially flow through the conduits more efficiently than through the cap-rock (A. Palmer 2000). Preferential flow through the cave allows it to enlarge at a higher rate, as well as gives it the ability to host flood pulses at a later time. The control of recharge by the cap-rock removes competition between passages, so they all enlarge equally.

Like the diffuse infiltration on soluble rock, diffuse flow through a cap-rock can also produce mixed water origins. Caves such as those in the Black Hills, South Dakota have an origin of diffuse flow through a permeable cap-rock, in combination with existing waters in the soluble rock to create mixing chemistries, producing some of the maze caves seen there (A. Palmer 2000).

Maze caves of floodwater origin

The second type of epigenic maze cave is of floodwater origin. This origin is similar to the formation of the maze-like patterns seen in larger branchwork caves, though instead of only partial maze sections, the entire cave is a maze (A. Palmer 1975, 1991). The development of this type of caves satisfies a large Q/L ratio through flood pulses. These flood pulses can happen due to sinking stream piracy, which A. Palmer (1972) gave as the speleogenetic origin for Onesquethaw Cave, and to flood stages of dammed lakes and streams (A. Palmer 1975, 1991, 2001, 2007). He further related this type of recharge to “bank flow”, or “bank storage” (A. Palmer 1975, 1991, 2007), similar to that in clastic rocks or unconsolidated materials along the margins of streams and other bodies of water. These flood pulses remove competition for more efficient flow routes through complete inundation of the carbonate rock with aggressive water, therefore allowing passages to equally enlarge.

The geometries of floodwater maze caves vary with the dominant type of porosity and create the most distinct end-members of the maze cave patterns. Network mazes arise from fracture networks such as jointing; anastomotic mazes arise from bedding plane parting flow paths; and spongework mazes arise from intergranular pores (Fig. 1.1, A. Palmer 1991). Other recharge methods produce these types of patterns, but are not as

distinct. For instance, maze caves of diffuse flow through permeable, insoluble cap-rock can follow bedding planes, but the descending water to these bedding planes follow typical vertical shafting to reach the bed (Fig. 1.1, A. Palmer 1991).

Maze caves of hypogenic origin

A. Palmer's (1975) seminal maze cave paper does not directly discuss maze caves of hypogenic origin, as hypogenic karst theories had not been developed yet. He instead suggested "artesian" flow as a possible maze origin, as hypothesized by White (1969), though this approach requires a skeptical view due to lack of water aggressiveness. As hypogenic origins were developed, such as rising hydrothermal water, H₂S-freshwater mixing, and saltwater-freshwater mixing, they were applied to the formation of maze caves at depth (A. Palmer 1991).

These waters are not surface-coupled. Though meteoric waters do recharge these sources, it is not the ultimate driver of speleogenesis, but rather the mixing of this water with the deep-seated source. This mixing, or the rising of thermal waters provides a large Q/L ratio (by uniform inundation of soluble rock) that can then make use of any available porosity and form maze caves (A. Palmer 1991). In addition to the large Q/L ratio these waters tend to be highly aggressive due to their chemistry (A. Palmer 1991).

Unlike maze caves of epigenic origin, hypogenic maze caves can exist at greater depths (A. Palmer 2001). These caves are not connected to surface hydrology, and therefore cannot show the effects of glaciation on karst as well as epigene maze caves. While not useful for the scope of this study, hypogene speleogenesis is important to mention in any discussion of maze caves, and it is possible that glacial quarrying and/or glacio-isostasy has placed such maze caves into the surface environment as relict forms.

Maze caves in glaciated karst

Glaciated karst studies (Mylroie 1977) mentioned maze caves, and maze cave studies (A. Palmer 1972, 1975, 2001, Ryder 1975) discussed some glacial effects on maze caves. More recent work conducted by Lauritzen (2001), and Skoglund et. al. (2005, 2010, 2011) has directly related maze cave speleogenesis to glaciation, though only in the stripe karst of Norway.

Mention of glaciation in maze cave literature

Onesquethaw Cave

Early researchers who mentioned glaciation and maze caves include A. Palmer (1972), who discussed the formation of a cave with anastomotic pattern imposed on it, Onesquethaw Cave. He gave the origin of this cave as due to floodwater recharge from a sinking stream. In addition, he discussed its possible time period of development, which he stated as post-glacial. He hypothesized this origin due to small cross-sectional area, and the concordance of the cave to the post-glacial drainage (A. Palmer 1972). Age dates obtained by U/Th dating of speleothems provided a minimum age of 8.96 ± 2.1 ka (Lauritzen and Mylroie 2000). As there are no pre-glacial dates of speleothems in this cave, the possibility remains that it is post-glacial in origin.

Glaciated lowlands geographic province

A. Palmer (1975) mentioned the glaciated central lowlands geographic (of the Midwest to New York) provenance with respect to maze caves. He listed geographic provinces and assigned a typical geometric pattern for them. For the glaciated central lowlands, he stated the dominant pattern was network mazes. While he mentioned the

dominant patterns for these provinces, he did not mention the dominant speleogenetic origin of them.

Possible effects of glaciation

A. Palmer (1975) detailed several effects on maze development due to glaciation. The primary effect is the development of maze-like sections due to damming with glacial debris. Other effects may be due to glacial unloading (A. Palmer 1975, 2001). Glacial unloading can cause mechanical enlargement of jointing (Harland 1957, A. Palmer 1975, Baker 1976). As jointing is one of the dominant porosity types for maze cave development (A. Palmer 1975, 1991), this effect could cause the initiation of maze cave development in glaciated regions, without initial chemical breakthrough times (Faulkner 2006a). If, due to this unloading, these joints are mechanically enlarged enough to allow the beginnings of speleogenesis, then the maze caves developed within these joints can be said to be post-glacial. These effects can also work together; such as within Skull Cave of the Helderberg Plateau, where water backfloods from glacial damming and enlarges glacially unloaded joints (Fig. 2.11), superimposed on a branchwork, pre-glacial cave.

Sub-glacial origins of network maze caves in the stripe karst of Norway

The most comprehensive work done so far on glaciation and maze cave development has been done in the stripe karst of Norway. Stripe karst is a form of karst where the soluble rock lays between two insoluble, impermeable rocks (Lauritzen 2001). Bands of stripe karst are thin, and are typically at high dip angles. The karst formed within these soluble layers represents an end-member of the contact karst phenomena, where karstification happens along the contact of soluble and insoluble rocks (Lauritzen

2001). The type representation of stripe karst is from Norway, in which maze caves can be found (Skoglund and Lauritzen 2005).

These maze caves have been used in several studies by Skoglund et. al. (2005, 2010, 2011). They have been used to model the effects of glacial ice-contact and glacial chemistry on maze cave development (Skoglund et. al. 2010), as well as in the studies of their speleogenetic origins (Skoglund and Lauritzen 2011). These studies concluded that due to the relict nature of the caves, their structural character, and their development time, that the caves are sub-glacial in origin (Skoglund and Lauritzen 2011).

While these caves show an effect of glaciation and the relation to maze cave development, these effects cannot be extrapolated to other glaciated karst areas. The stripe karst represents only one type of karst, and the thin and dipping nature (Lauritzen 2001) generally restricts its exposure. In addition, the caves are relict (not connected to current hydrology), in rock of low lateral extent, and in between insoluble and resistant layers (Lauritzen 2001, Skoglund and Lauritzen 2005). These characteristics make them fairly resistant and able to survive glaciations, and do not reflect the character of maze caves in other glaciated areas such as New York. While marbles, layered between schist, exist in New York associated with the Grenville Orogeny, they are not at high enough dip angles to produce stripe karst (Faulkner 2009).

Hypothesized effects of glaciation on maze caves

Removal of existing maze caves

In addition to the effects of glaciation on maze caves that were hypothesized in the literature (e.g. A. Palmer 1975), further effects can be considered. Epigenic maze caves, due to their speleogenetic origins requiring a large Q/L ratio involving surface

waters, are typically located in shallow rock (A. Palmer 2001). The addition of porosity by karstification weakens otherwise resistant carbonates to the effects of ice advance, erosion, and crushing (Myroie 1977). Maze caves, due to their geometric character, represent large porosity, and this porosity along with their shallow natures makes them susceptible to removal by glaciation. From this nature it can be hypothesized that maze caves in glaciated areas may be predominantly post-glacial in origin.

Controls on speleogenetic origins

An additional effect comes from the preferential removal of weaker clastic sedimentary rocks (Myroie 1977). These clastic rocks include shale, and sandstone (the typical cap-rock for permeable, insoluble cap-rock maze cave origin by diffuse flow) (A. Palmer 1975). The removal of these clastics make it possible that the primary mode of speleogenesis for maze caves in glaciated areas is floodwater, though this removal can also expose more sandstone by removing overlying shale.

Initiation of caves

Tectonic events produced by isostatic rebound may have a substantial influence on the development of post-glacial caves (Faulkner 2006a, 2009). These tectonic events can produce jointing, and enlarge existing jointing enough to greatly lessen or eliminate, chemical breakthrough times. The minimizing of this breakthrough time and the enlargement of jointing remove initial competition for flow paths. Additionally, as jointing is one of the dominant porosity types for maze caves, these tectonic events can directly allow the formation of maze caves.

New York geology

New York has been a study area in many branches of geology including paleontology, stratigraphy, glacial geomorphology, and karst geomorphology and hydrology (Isacshen et. al. 2000). In particular, studies connected glacial geomorphology and the geomorphology and hydrology of karst in New York within the Helderberg Plateau (Baker 1973, 1976, Kastning 1975, M. Palmer 1976, Mylroie 1977, Mylroie and Carew 1987, Dumont 1995, Mylroie and Mylroie 2004). In addition to the glaciated karst studies, maze cave studies were conducted in New York with caves in the Helderberg Plateau, as well as elsewhere in the state (A. Palmer 1972, 1975, 1991, 2001). The combination of studies on glaciated karst, and on maze caves makes New York a productive study area for the effects of glaciation on maze caves, and the determination of the speleogenetic origins of these caves.

New York glaciation and glacial landforms

Timing of glaciation

New York has been repeatedly glaciated through the Pleistocene (Ridge 2004), with the most recent being the Wisconsinan glaciation. Much of the pre-Wisconsinan glacial material has been overprinted by the subsequent Wisconsinan glaciation (Muller and Calkin 1993, Ridge 2004). The timing of this glaciation has been determined through techniques such as pollen stratigraphy (e.g. Muller and Calkin 1993); dating and position of end moraines (Muller and Calking 1993, Ridge 2004), and dating of lake core sediment (Rayburn et. al. 2011), which indicate the timing of last glacial maximum at 28–24 ka BP. These methods show complete retreat within New York by 12–13 ka BP

(Muller and Calking 1993, Ridge 2004, Rayburn et. al. 2011). A complete mapping of ice retreat and re-advances (Fig. 2.15) can be found in Ridge (2004).

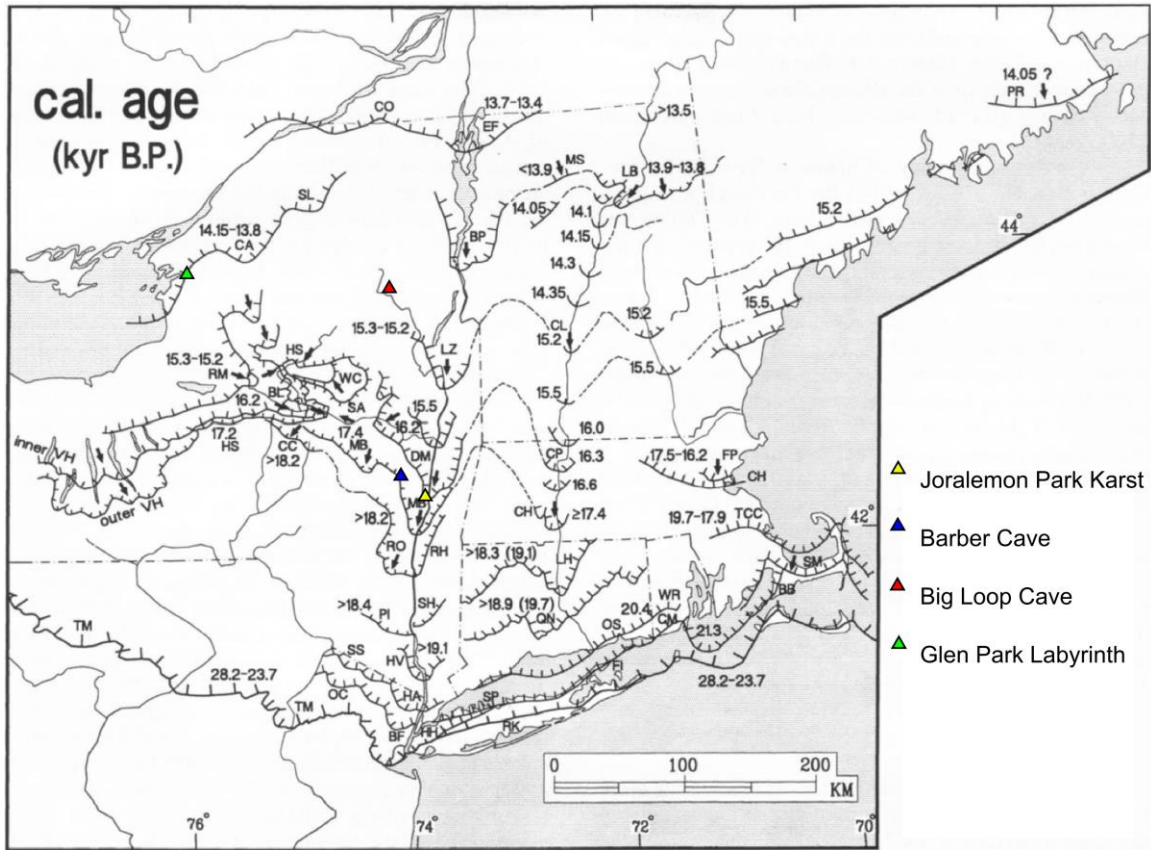


Figure 2.15 Map indicating time of glacial retreat in calibrated years before present (in ka BP).

Cave locations are plotted for the caves used in this study. Modified from Ridge (2004).

Glacial landforms

New York contains many erosional and depositional landforms, as well as landforms left over from glacial lakes. The largest of these features are large-scale depressions that are now lakes, such as the Finger Lakes in the central part of the state. Large-scale depositional features include end and terminal moraines, such as Long

Island. Landforms directly influencing karst development include the infilling of pre-glacial valleys with sediment, and filling in of insurgences and resurgences (Baker 1973, 1976, Kastning 1975, M. Palmer 1976, Mylroie 1977).

Smaller scale depositional features include drumlin and kame fields, which are visible on topographic maps (Goldring 1943, Isacshen et. al. 2000) and indicate ice flow directions. Smaller scale erosional features include local depressions in which swamps and small lakes formed, and glacial striations (Fig 2.5). These features align with ice-flow direction, and show a general north-south orientation along the Hudson Valley (Fig. 2.6).

Deranged drainage of New York

The smaller scale depositional and erosional features contribute to deranged drainage patterns seen in the state. This derangement includes ponded water in swamps and lakes dammed by glacial sediments, with interconnecting streams. This deranged pattern is seen on many topographic and geologic maps of New York quadrangles (e.g. the Ravena quadrangle, Fig. 2.6). With respect to New York karst this derangement modified pre-glacial caves with waters coming from drumlins, till sheets, and moraines (Mylroie and Carew 1987).

New York karst areas

New York has several distinct karst regions (Fig. 2.16). These include the Cambro-Ordovician carbonates in the northern part of the state, the Siluro-Devonian carbonates in the western and central region of the state, and several bands of marbles such as those in the Adirondacks and Taconic metamorphic provinces (Engel 2009). These units are shown in the stratigraphic column for New York (Fig. 2.17). The red

units on this stratigraphic column represent karst forming units, of which maze caves can be found in the Cambro-Ordovician strata, the Siluro-Devonian strata, and the marbles of the Adirondacks.

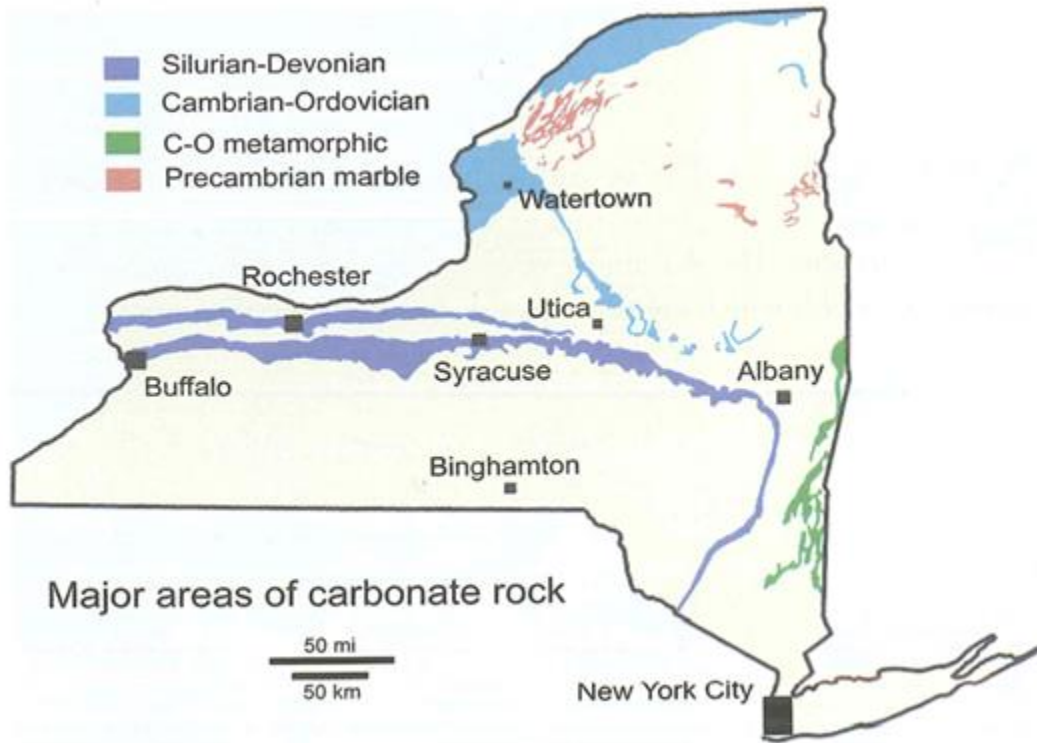


Figure 2.16 Map areas in which carbonates are exposed in New York State. From Engel (2009).

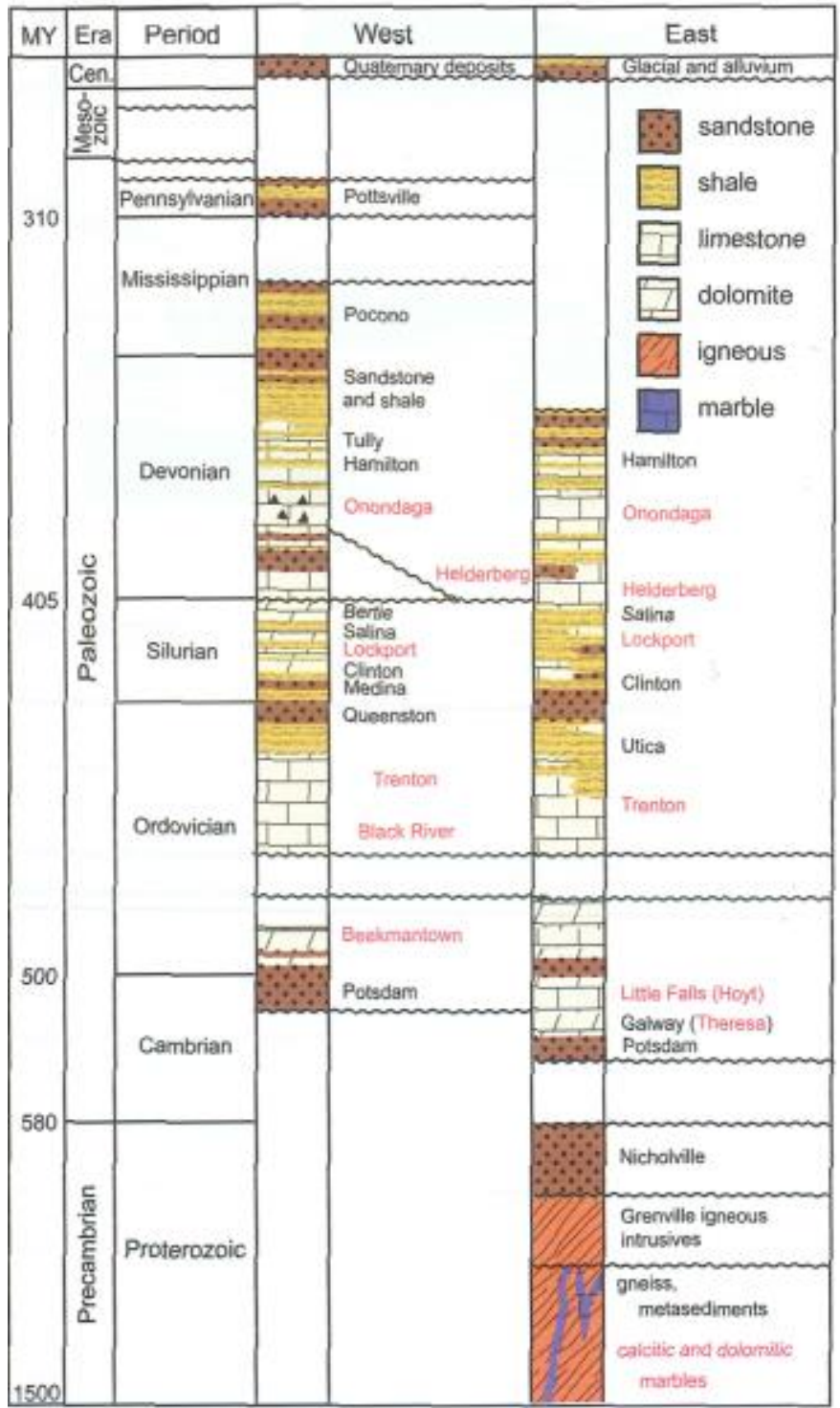


Figure 2.17 Stratigraphic column of New York State geologic units. Karst forming units are in red. From Engel (2009).

Grenville Marble

The Grenville Marble is a group of highly deformed marbles. These marbles are the metamorphosed limestones that were deposited on proto-North America before the formation of the Grenville Supercontinent (Isachsen et. al. 2000). These marbles have been dated to 1.1–1.3 Ga in age.

The Grenville Marble as well as other metamorphic rocks crop out in the Adirondack Mountains, and other parts of northern New York (Cushing et. al 1910, Isachsen et. al. 2000) due to the recent uplift and erosion of these areas. In other areas to south these metamorphic rocks act as the basement rock (Isachsen et. al. 2000).

Cambro-Ordovician strata of the Ontario Lowlands

The carbonate strata of the Cambro-Ordovician time in New York contain several caves, including maze caves such as the Glen Park Labyrinth at Watertown, New York, which is mentioned in A. Palmer's (1975) original maze cave paper. These caves are located in the Black River Group, and Trenton Group carbonates (A. Palmer 1975, Engel 2009).

Black River Group

The Black River Group is a group of Middle Ordovician strata. It includes several carbonate formations: the Lowville Formation, and the Watertown Limestone. The formations from oldest to youngest are the Pamela Formation of dolostones and sandstones, the Lowville Formation of micrites and grainstones, and the Watertown Limestone (Isachsen et. al. 2000). Both limestone formations contain abundant fossils, and are karstic, with the Watertown Limestone being more soluble (Cushing et. al. 1910,

Carroll 1969a). The total thickness of these units in the Ontario Lowlands region is 90 meters.

Trenton Group

The Trenton Group consists mainly of carbonates interbedded with thin black shales. This group is more extensive than the Black River Group, and extends down into the Mohawk valley with outcrops in the Canajoharie Creek where it has a thickness of 4.5 meters. Other outcrops are in the Ontario Lowlands near Watertown with a 160-meter thickness, and near Trenton Falls with a 130-meter thickness (Isachsen et. al. 2000). The limestone beds are between 0.05 meters and 0.30 meters in thickness.

Siluro-Devonian strata of the Appalachian Plateaus

Most of the glaciated karst studies in New York have taken place in the karst within Siluro-Devonian strata in the Appalachian Plateaus, particularly the Helderberg Plateau west of Albany (Fig 2.16). The stratigraphy of these plateaus includes the upper Silurian Rondout Formation, the formations of the Siluro-Devonian Helderberg Group, the Devonian Tristates group, Onondaga Formation, and Hamilton Group (Kastning 1975, Baker 1976, Mylroie 1977, Isachsen et. al. 2000).

The main karst forming units are the carbonates of the Helderberg Group, particularly the Manlius Formation, and the Onondaga Formation. The stratigraphic units of most interest are the Rondout Formation, the formations within the Helderberg Group (the Manlius Formation, the Coeymans Formation, the Kalkberg Formation, the New Scotland Formation, the Becraft Formation, the Alsen Formation, and the Port Ewen Formation) (Isachsen et. al. 2000), the Oriskany Formation, and the Onondaga Formation

with its underlying formation, the Esopus Formation. These units make up the karstic rock of the Appalachian Plateau, or provide controls for karst formation. The stratigraphy described here is that of the north-south oriented band of the Appalachian Plateau (Fig. 2.16), parallel to the Hudson River, and its relation laterally to the historically studied Helderberg Plateau to the west (Engel 2009).

Rondout Formation

The Rondout Formation has several members of limestone and dolomite (Isacshen et. al 2000). In the north-south band of the Appalachian Plateaus the members include the Rosendale Waterlime, the Glasco Dolomite, and the Whiteport Waterlime. To the west the Rondout Formation is represented by the Chrysler Member (a dolomite). The Rondout Formation has some sparse karstification (Mylroie 1977).

Helderberg Group

Manlius Formation

The Manlius Formation is a carbonate unit of mainly finely bedded carbonate mudstone. It is sparse in fossils, though it does contain stromatolites, stromatoporoids, ostracodes, brachiopods, and other fauna. It is composed of two members: the Lower Manlius and the Upper Manlius. The Manlius has been interpreted to represent a near-shore facies (Isacshen et. al. 2000).

The Manlius Formation is the main karst-forming unit within the Helderberg Group. It contains many of the large caves within the Helderberg Plateau including Howe Caverns, and McFail's Cave (Kastning 1975, Mylroie 1977, Engel 2009).

Coeymans Formation

The Coeymans Formation is the unit above the Manlius Formation in the Helderberg Group. It represents a transition to shallow carbonate shelf facies, with thicker layers of fossiliferous pack-to-wackestone, and contains isolated chert nodules (Mylroie 1977, Isacshen et. al. 2000). A thick, massive unit, it provides a protective cap to the Manlius, and is a major cliff former in the Helderbergs.

Kalkberg Formation

The Kalkberg Formation is another limestone, and lies above the Coeymans Formation. It is richer in chert than the Coeymans Formation, and contains prominent banding of this chert (Mylroie 1977, Isacshen et. al. 2000). It has a similar biofacies to the Coeymans, though it has more fossils than the Coeymans. The Kalkberg is a packstone that represents a deeper water environment than the Coeymans Formation (Isacshen et. al. 2000).

New Scotland Formation

The New Scotland Formation represents the deepest water facies of the Helderberg Group. It is also the most fossiliferous, and is considered a grainstone (Isacshen et. al. 2000). It contains numerous shale beds and shaly limestones, and acts as an aquitard. This grainstone is in beds of medium thickness. Within outcrops of the north-south band this unit is well exposed. Moving westward however, this unit interfingers the Kalkberg Formation, and disappears, such as within the Helderberg Plateau (Mylroie 1977).

Becraft, Alsen, and Port Ewen Formations

The Becraft, Alsen, and Port Ewen formations represent a repetition of the Coeymans, Kalkberg, and New Scotland type facies. The Becraft contains some caves, of which there are some maze caves of diffuse flow origin where it directly underlies the Oriskany Sandstone (A. Palmer 2000). In the north-south band all of these formations crop out, however going westward from this band the Alsen and Port Ewen are not present, and the Becraft is unconformably overlain by the Oriskany Formation.

Oriskany Formation

The Oriskany Formation unconformably overlies the Becraft in the west of the Appalachian Plateaus, and the Alsen in the eastern portion (Myroie 1977, Isacshen et. al. 2000). To the south in Virginia it overlies the equivalent of the Coeymans Formation (A. Palmer 2000). The Oriskany Formation is quartz and carbonate sandstone that can act as the cap-rock for maze cave development as it is only a meter or two thick in the Helderberg Plateau region, but erosionally very resistant and has well-developed orthogonal joints (A. Palmer 1975, 2000).

Esopus Formation

The Esopus Formation is a shale formation. This formation overlies the Oriskany Formation, and underlies a variety of formations both conformably and unconformably. In different areas it underlies the Carlisle Shale, the Schoharie grit, or the Onondaga Limestone (Goldring 1943, Myroie 1977). When the Esopus Shale underlies the Onondaga Limestone it acts as base level for cave development in that unit.

Onondaga Formation

The Onondaga Formation is a limestone formation with several members. These members are fossiliferous, and the lower members contain abundant chert (Isacshen et. al. 2000). These members are the Edgecliff Member, the Nedrow Member, the Moorehouse Member, and the Seneca Member. The Onondaga is a major karst-forming limestone and extends karst further to the west in New York than the formations within the Helderberg Group (Engel 2009).

Structural geology of New York karst areas

The best-exposed karst areas of the Appalachian Plateaus, as well as the Ontario Lowlands are fairly simple in structure (Cushing et. al. 1910, Mylroie 1977, Engel 2009). The well-studied Helderberg Plateau in the Appalachian Plateaus is only slightly dipping at 1°- 3° SSW (Mylroie 1977, Engel 2009). These contain few other structures, but there is the presence of some folding and faulting that provides controls on some caves in this area (Mylroie 1977). Eastward towards the Hudson River Valley from the Helderberg Plateau structural deformation increases, with folds controlling caves, such as Onesquethaw Cave (Fig. 2.10, A. Palmer 1972), and faulting in Clarksville Cave (Kastning 1975) (both of which are within the Onondaga Limestone). Deformation becomes more pronounced along the Hudson River Valley, with intense folding and faulting being present. The general trend of structures such as folds is north-south.

The most important structures for the purpose of this study are joints. Joints are one of the primary controls for maze cave development, particularly for network maze caves (Fig 1.1, A. Palmer 1975, 1991). The dominant joint sets in the Helderberg Plateau are oriented between 2° a 30° azimuth (Kastning 1975), with an orthogonal set at 120° to

135° (Fig. 2.5, A. Palmer 2007). Joints in the Onondaga Limestone are oriented between 31° and 32°, and 292° (Goldring 1935). Jointing in the eastern, folded region can be more complex.

CHAPTER III

STUDY AREAS AND CAVE DESCRIPTIONS

Introduction

This thesis has several study areas, with the primary being within and near Joralemon Park, in Ravena, New York. Other study areas include maze caves within the Helderberg Plateau, as well as in the Ontario Lowlands and Adirondack Mountains (Fig. 1.2). Each of these locations has differing stratigraphy, structural geology, drainage, and glacial history. The New York caves visited in this study include several in Joralemon Park in Albany County; Barber Cave in the Helderberg Plateau, Schoharie County; Big Loop Cave in the Adirondack Park, Essex County; and Glen Park Labyrinth near Watertown, Jefferson County, New York. Cave descriptions herein discuss the geometry of the caves, hydrology, presence of sediments, and depth. These descriptions are based partially on available literature, and on fieldwork performed in this study. These descriptions are further discussed in the results as to their significance to pre-glacial or post-glacial origins.

Joralemon Park karst area

The Joralemon Park karst area is located near Ravena, New York, within the 15-minute Cocksackie Quadrangle, and the 7.5-minute Ravena Quadrangle (Fig. 1.2). The geology and hydrology of the area has been described by Goldring (1943), and through

several amateur publications in the journal *The Northeastern Caver* (e.g. Nardacci 1994), in a guidebook for the National Speological Society convention (A. Palmer et. al. 1991), and in a field trip guidebook for the New York State Geological Association (NYSGA) (Rubin et. al. 1995). This area contains several caves, including a relict cave, several swamps, streams, and glacial depositional landforms (Goldring 1943). A map of the area is shown in Fig. 3.1 with the locations of active caves (Hannacroix Maze, Merritts Cave, Skip's Sewer, Tetanus Shot Cave, and Minicroix Cave), relict caves (Joralemons Cave and Joralemons Backdoor), karst features, and surface hydrology.

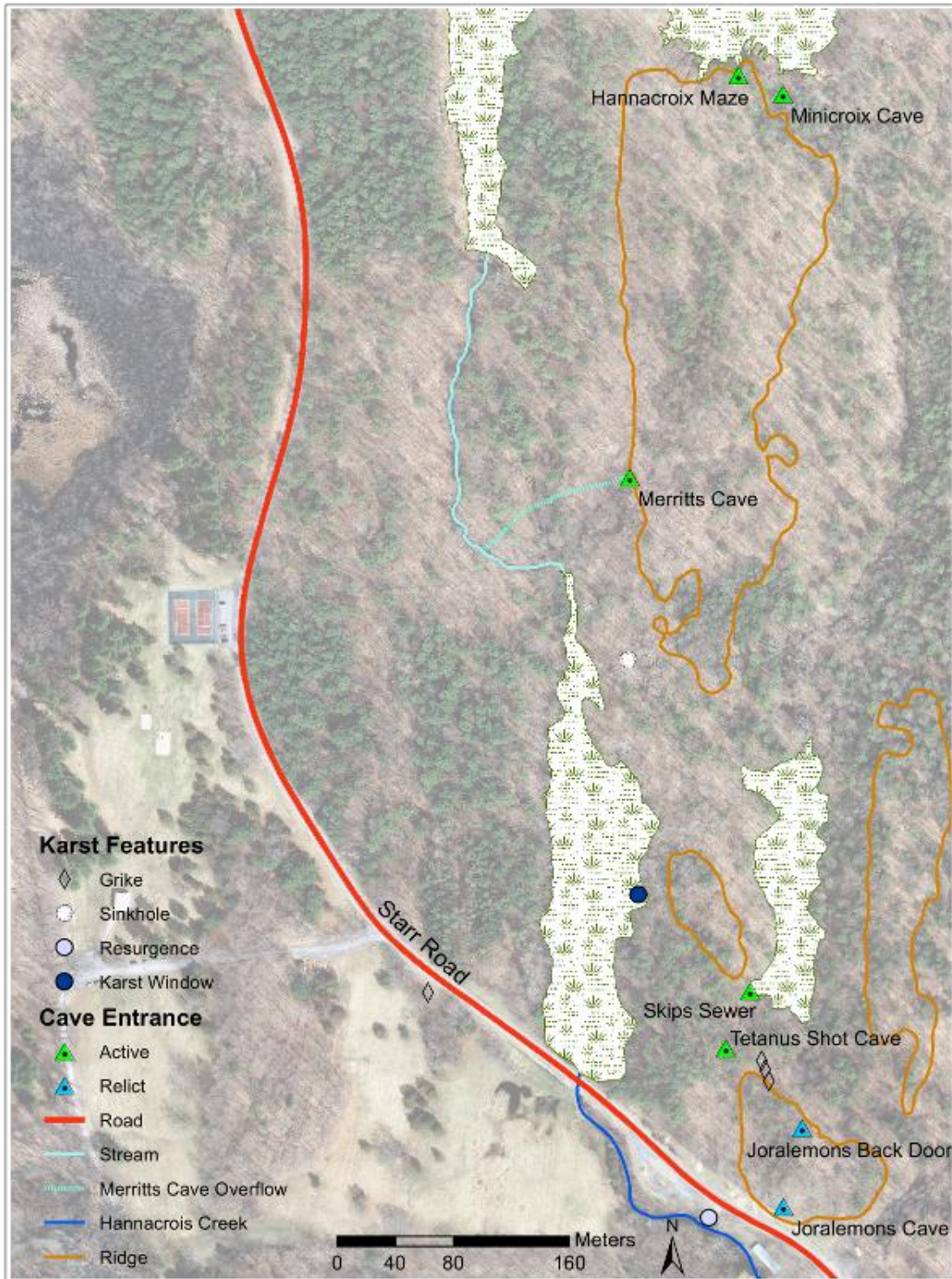


Figure 3.1 Map generated from the GIS results of the study area.

This map shows the active caves, relict caves, karst features, ice-aligned ridges and surface hydrology. The relict caves exist at a higher elevation than active caves, showing a different, lower base level.

Geology of Joralemon Park

The geology of this park has been described by Goldring (1943), and by Rubin et. al. (1995). The stratigraphy of this area consists of the Onondaga Limestone, underlain by the Schoharie Formation (also termed as the Schoharie grit in the literature, e.g., Goldring 1943, Mylroie 1977) and the Esopus Shale, which acts as the local solutional and hydrological base level for cave development. The Onondaga in this area consists of the upper three members, including the chert-rich Nedrow Member (Isacshen et. al. 2000).

Structural features include a fault near Joralemons Cave, and prominent jointing in the Onondaga Limestone (Nardacci 1994). The jointing in the Onondaga provides the structural control for Hannacroix Maze (Fig. 3.2), Merritts Cave (Fig. 3.3), and Skips Sewers (Fig. 3.4). Grikes also exist on the surface as epikarst.

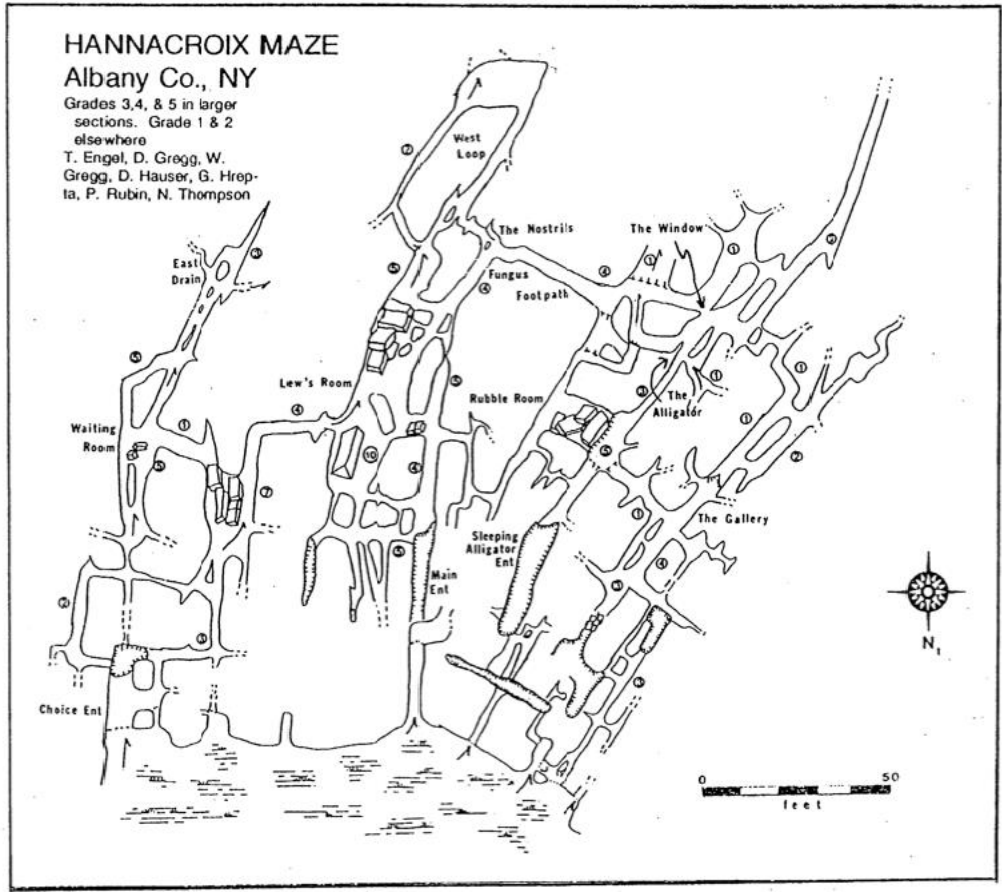


Figure 3.2 Cave map of Hannacroix Maze, Albany County, New York.

This cave is of a network pattern, and seems to align with post-glacial deranged drainage. From Rubin et. al. (1995).

Merritts Cave
Albany Co., New York
May 30, 2013
Max Cooper

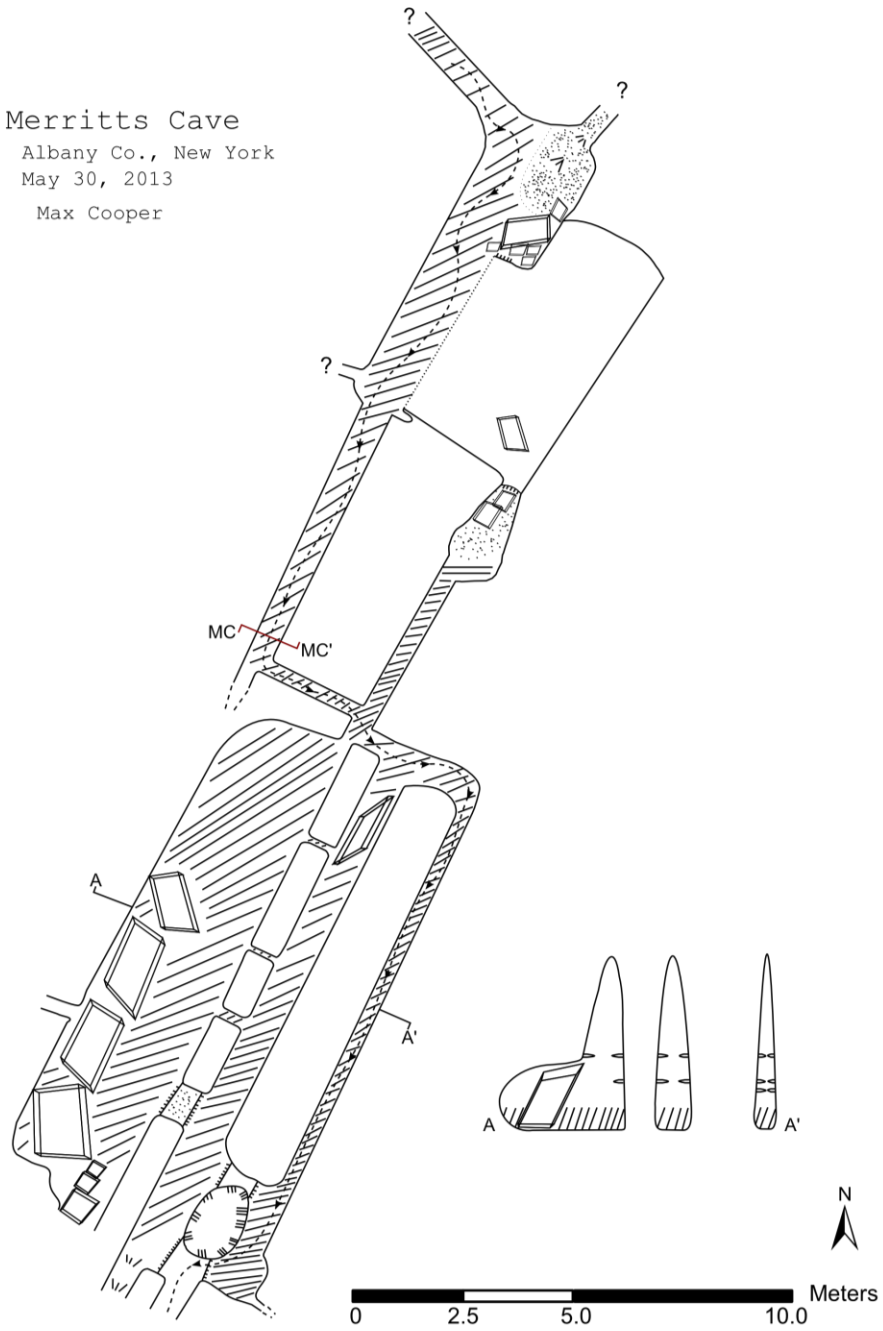


Figure 3.3 Map of the previously unmapped Merritts Cave.

The methods used to produce this map are located in the Methods section of this paper. Cross-section MC-MC' is illustrated in the results section of this paper.

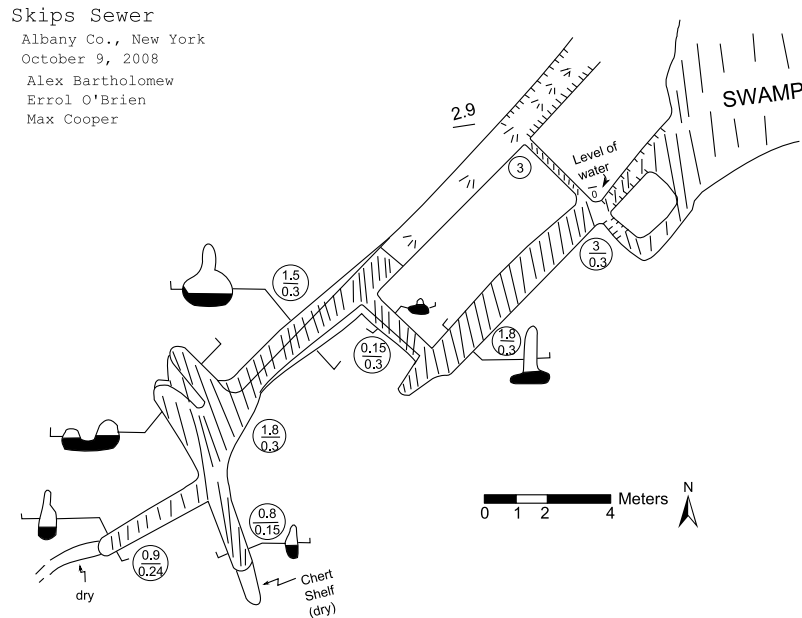


Figure 3.4 Map of Skips Sewer, a floodwater maze cave of network pattern located in Joralemon Park.

The entrance to this cave is currently occluded by organic debris. Redrawn from map by Dr. A.J. Bartholomew (unpublished map).

Glacial landforms also exist in this area, both erosional and depositional.

Depositional features include several large erratics, as well as tills. These tills cap ridges above the Esopus Shale on the outskirts of the park (Goldring 1943, Fig 3.5). These form controls for drainage into the swamps, and demonstrate agreement of cave formation with post-glacial landforms. Erosional landforms include several depressions that have been filled with water as seen in Figures 2.3 and 3.1 (Goldring 1943, Rubin et. al 1995), as well as glacial striations aligned north-south to the south of the park (Goldring 1943). In the vicinity of the park are additional ridges, aligned with the ice flow direction of the

previous glaciation (Fig 3.5), which control the drainage of the area. This area was deglaciated 16.2 ka BP (Ridge 2004, Fig 2.15).

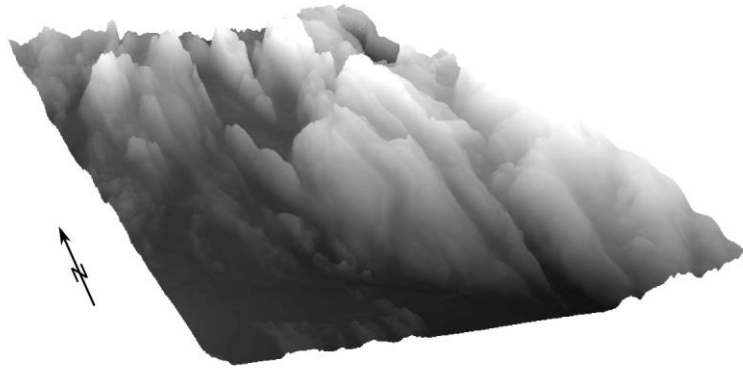


Figure 3.5 Exaggerated DEM (6.5x) of the area around Joralemon Park showing ice-aligned (north-south in this area) ridges and swamps.

The lighter shading indicates higher elevations. This DEM was generated from 2-ft LiDAR contours provided by the NY State GIS Clearinghouse.

Hydrology of Joralemon Park

This area also includes several surficial hydrologic features (Fig. 3.1). These features are streams, and several swamps in glacial depressions (Goldring 1943, Nardacci 1994, Rubin et. al. 1995). One of the larger swamps (Fig. 3.6) in this area is drained by an intermittent surface stream perched on the Esopus Shale, while the other large swamp is drained through a cave where it is adjacent to an outcrop of the Onondaga Limestone (Fig. 3.7). A further larger swamp exists upstream from the northern swamp in Figure 3.7 that drains into this northern swamp. During higher water levels after glacial retreat it was likely that a lake existed connecting these swamps (Rubin et. al. 1995) before draining through the surface streams and the caves. The hydrology of this area has been

described by Nardacci (1994) and Rubin et al. (1995) and is further elaborated within the results section of this thesis.



Figure 3.6 Photograph taken from looking upstream of surface stream at swamp adjacent to Hannacroix Maze in Fig. 3.1.

A surface stream flowing over the Esopus Shale drains this swamp.



Figure 3.7 Photograph of limestone ridge containing Hannacroix Maze, which drains the swamp it is located in.

This ridge is oriented in a north-south direction (Figs. 2.6, 3.5), in alignment with ice flow direction. This swamp is directly adjacent to the swamp that is drained by a surface stream (Fig. 3.6). Here however water enters the Onondaga Limestone, which outcrops in the right of the photo.

The hydrology described and observed is complex and represents a post-glacial deranged drainage system (Fig. 3.1) with a karst drainage system superimposed upon it. Water from karst springs enters the intermittent stream, which connects to another resurgence (Fig. 3.8, Nardacci 1994). Merritts Cave also contributes to this stream during high water conditions. During these conditions water will exit the entrance, pond at the

entrance, and then flow over a waterfall into the stream (Fig. 3.9). Additional complexity is added through damming by organic matter (Rubin et. al 1995).



Figure 3.8 Photograph of the resurgence labeled in Fig. 3.1.

Water bubbles through this resurgence, which remains unfrozen during winter. This resurgence appears to be the furthest from insurgence points (Nardacci 1994, Rubin et. al. 1995). Photo credit Dr. A.J. Bartholomew.

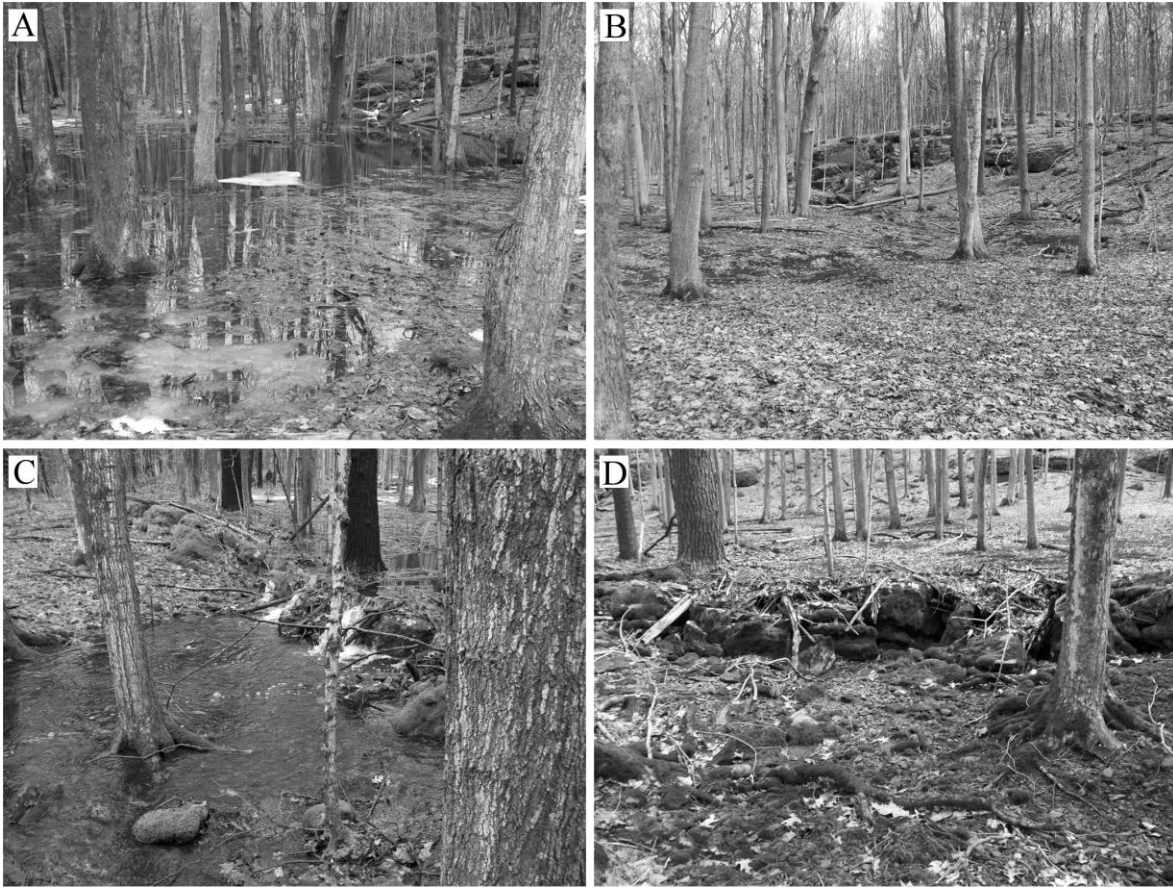


Figure 3.9 Photographs showing flow out of the entrance to Merritts Cave (Merritts Cave Overflow in Fig. 3.1).

A and B show the ridge where Hannacroix Maze and Merritts Cave are located, along with ponded water from high flow conditions in A. C and D show the waterfall where ponded water flows into the surface streams connecting swamps, in high and low flow regimes respectively (Fig. 3.1).

While the hydrology has been described in fine detail for this area, no flow routes have been proven through dye traces through Hannacroix Maze and other caves (Fig. 3.1). The possibility of connection of Hannacroix Maze and Merritts Cave (if not explorable, hydrologically) is high, as there is little catchment of water besides from diffuse flow. As distinct flooding is apparent from fieldwork and the presence of organic debris in the roof of Merritts Cave, combined with no evidence of downward water

speleogenetic features, it is likely that Merritts Cave is of floodwater origin with waters originating from Hannacroix Maze. Dye tracing would be useful to demonstrate this connection if there is no humanly explorable link, and would also be useful in connecting other karst features such as the sinkhole and karst window of the area.

Caves of Joralemon Park

Joralemons Cave and Joralemons Backdoor

Joralemon Park consists of several caves, at different elevations. Joralemons Cave and Joralemons Backdoor (Fig. 3.10) are relict, truncated, and at a higher elevation not connected to current hydrology, suggesting that these caves are pre-glacial in origin and were abandoned after glacial retreat (Rubin et. al. 1995). Additionally, paleontological remains from the late Pleistocene exist within this cave, suggesting it was already at a size for habitation by animals (e.g., *Ursus americanus*) (Steadman et. al. 1993).

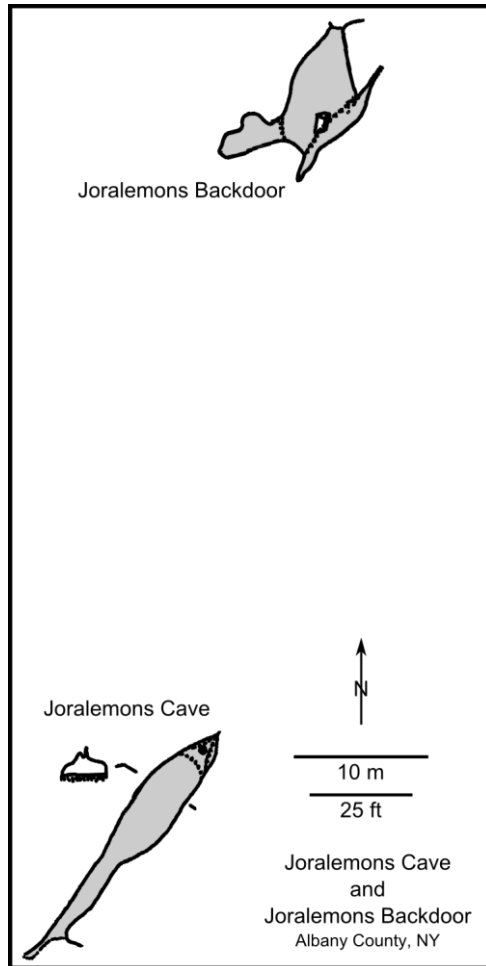


Figure 3.10 Map of Joralemons Cave and Joralemons Backdoor.

Cross-sections indicate burial of the floor with sediments, as well as occlusion of the back of the passages. Alignment of the two caves makes it possible that these were formerly connected. Redrawn from Rubin et. al. (1995).

Unlike other caves in the area, these are non-maze caves, and are likely master passage from an old branchwork cave truncated during glaciation. The passage shape for these caves resembles a phreatic tube; however the bottom is occluded with an unknown amount of glacial sediment (Fig. 3.10).

Active Caves

Other caves in this area are thought to be post-glacial, though this had not been proven in the literature (Rubin et. al 1995). These caves include Hannacroix Maze (Fig. 3.2), Merritts Cave (Fig. 3.3), and Skips Sewer (Fig. 3.4). Hannacroix Maze and Merritts cave exist in the same limestone ridge (interpreted to be a roche moutonnée), and are connected hydrologically.

These caves appear to exist within the post-glacial deranged drainage system (Fig. 3.1). Agreement with this drainage strongly suggests that they are post-glacial in origin from the model hypothesized by Mylroie and Carew (1987), and thus will be examined in this study to test their hypothesis.

Hannacroix Maze

Hannacroix Maze (Fig. 3.2) is a floodwater maze cave with a network pattern, adjacent to a swamp and active in the current hydrology. It contains much organic debris, including nests of mammals. The cave exists in the Onondoga Limestone, and contains chert in several areas.

Hydrology

This cave is active in the current hydrology with parts of the cave containing water constantly throughout the year, though not entirely to the ceiling. During spring snowmelt this cave experiences conduit-full conditions, and floods to the ceiling. This cave drains a swamp to its north, and water flows through the passages to the south, through Merritts Cave (Fig. 3.3), and ultimately returns to the deranged drainage of the area.

Paleohydrologic conditions are indicated by scallops. An additional paleohydrologic consideration for this cave was the covering of the outcrop this cave exists in by a lake after glacial retreat (Rubin et. al. 1995). This lake subjected the outcrop in which the cave is located to water through the entire year, thus subjecting any passage to conduit-full conditions throughout the year.

Depth of the cave

Depth indicators in the cave include roots growing through the joints located in the ceiling. These roots are covered in organic muds, indicating recent high water conditions. This cave exists beneath a till cap (Fig. 3.11), exposed in at least one place in the cave (Fig. 3.12a). The proximity to the surface allows such sediments to come through and become emplaced within the cave. The till cap is no more than several meters deep, and the cave is contained entirely within a ridge with a total relief of less than six meters.



Figure 3.11 Photograph of till cap.

This picture was taken standing in the Sleeping Alligator entrance of Hannacroix Maze.

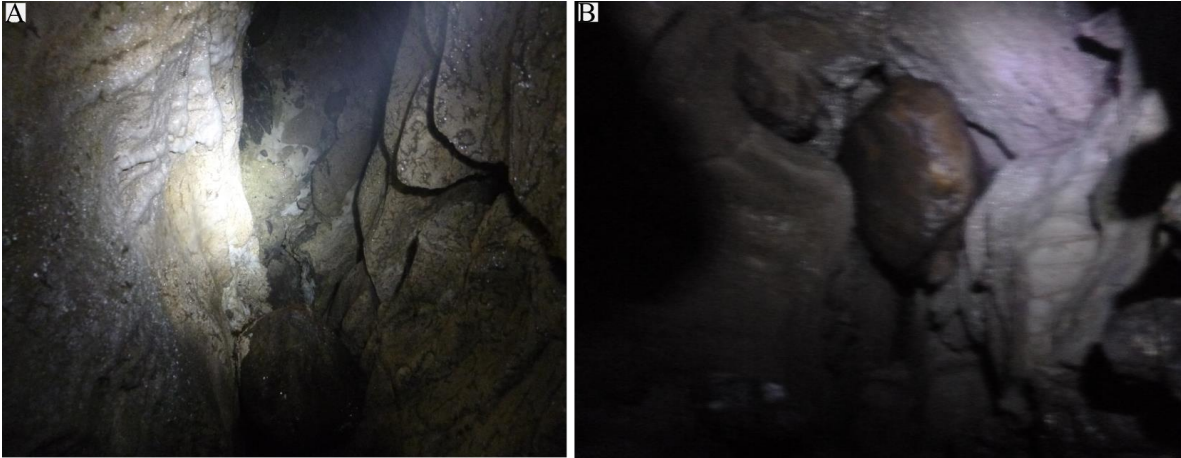


Figure 3.12 (a) Photograph of consolidated till cap in Hannacroix Maze that acts as the roof of passage near the Sleeping Alligator entrance. (b) Emplaced glacial cobble located within Hannacroix Maze.

This large cobble could have been moved post-glacially by large flooding or rafting on organic debris.

Presence of sediments

Glacial cobbles and pebbles exist within Hannacroix Cave (Figs. 3.12a, b). While one parameter for post-glacial caves is the lack of glacial sediment (Table 2.2), these cobbles and pebbles could be emplaced from the till cap overlying the cave. The large cobble in Fig. 4.6b may have been placed during a flood of the swamp, or may have been rafted into the cave on organic debris. The presence of this sediment does not negate post-glacial origins of this cave.

Cave geometry and passage shape

The shape of most passages within Hannacroix Maze is a tube, with a canyon cut into the tube (Fig. 3.2). These passages follow local jointing in the roche moutennée in which they exist. The tubes are interpreted to be of phreatic conditions during flooding,

which can occur several times a year. The canyon is interpreted to be vadose downcutting of the tube passage when not at flood conditions.

Merritts Cave

Merritts Cave (Fig 3.3) is an active floodwater maze cave with a network pattern, downstream from Hannacroix Maze. It contains less large organic debris, but does contain much organic mud. Like Hannacroix Maze, Merritts Cave exists in the Onondoga Limestone; however this cave is richer in chert nodules. Unlike Hannacroix Maze, no glacially derived sediments were found within the cave.

Depth of the cave

This cave is located within the same ridge as Hannacroix Maze, and exists within six meters of the surface. It contains many roots growing through the joints in the ceiling of the cave. These roots have organic mud coverings indicating high water conditions.

Hydrology

This cave shares a direct hydrologic connection with Hannacroix Maze, and is thus within the deranged drainage. No additional catchment spots exist for waters to enter Merritts Cave directly, and aquatic animals have been seen within the cave. Flooding to the ceiling occurs regularly in this cave, and these floods can occur even when Hannacroix Maze is not flooded. Flooding occurs after snowmelt for multiple days, and after large rain events for multiple days. This cave supports water most of the year and the water can flow out either directly through the entrance (Fig. 3.9a), or through small passage trending towards the karst window (Figs., 3.1, 3.3).

Cave geometry and passage shape

The passage shape for Merritts Cave is entirely fissure shaped passage (Fig. 4.9), except for where breakdown is present. Throughout all these passages are prominent chert bands along beds within the Onondaga Limestone. The orientation of these passages follows the jointing within the roche moutonnée, with the ceilings of passage containing a clear lineation at the joint.

Skips Sewer

Skips Sewer (Fig. 3.4) is a floodwater maze cave with a network pattern, adjacent to a swamp of which it drains. It is occluded with organic debris, including large logs, and thus makes a poor drain for this swamp. This cave was mapped prior to near complete occlusion of the entrance by this material. Like the other caves in the Joralemon Park karst area, it exists within the Onondaga Limestone, and contains chert banding. Like Merritts Cave, this cave contains no known glacial sediments.

Depth of the cave

This cave exists within four meters of the surface, and includes unroofed portions. In roofed portions of the cave roots grow down indicating proximity to the surface.

Hydrology

This cave experiences flooding to the ceiling, with the tube shaped portion of the passages regularly experiencing full water conditions. This cave exists in a swamp, and always has water in the bottom portion of passage. Drainage of this cave is occluded, though water may pass through the occlusion and continue to a resurgence located in

Hannacrois Creek (Fig. 3.1). The spelling difference from Hannacroix Maze is due to different interpretation of the original Dutch word (Nardacci 1994).

Cave geometry and passage shape

The shape of the passage in Skips Sewer is a tube, with canyons cut into the bottom of the tube (Fig. 3.4). These passages follow the jointing that exists in the Onondaga Limestone, and joints are visible in the ceiling. Additional complexity is added to the passage shape by chert banding within the bedrock.

Helderberg Plateau, Barber Cave

Helderberg Plateau geology

The stratigraphy of the Helderberg Plateau (Fig. 2.17) is covered in the literature review of this paper. The cave forming units in this area are the Manlius Limestone (which contains several of the largest caves in New York), the Coeymans Limestone, and the Onondaga Limestone. This area has many caves, including the maze caves Barber Cave, and the Pygmy Caves.

This area has less structural features compared to the main study area, though there are several folds and faults. The dip of the area is 1-2° to the south (Myroie 1977). The most important structural features for this study are the jointing that controls the formation of maze caves.

The hydrology of this area includes several large streams: the Cobleskill Creek, and Fox Creek. It also includes several smaller streams such as King Creek, which runs near several caves (Myroie 1977). The deranged drainage pattern of the area reflects the recent glaciation, with retreat occurring 17.4 ka BP in this area (Fig. 2.15) (Ridge 2004).

Barber Cave

Barber Cave is a floodwater network maze cave within the Manlius Limestone. It is located in Schoharie County, New York in the Gallupville Quadrangle (Fig. 3.13). The hydrology and geology of Barber Cave is described in Mylroie (1977). This cave appears relict in the current topography (Fig. 3.13), but sees conduit-full conditions during high flows.

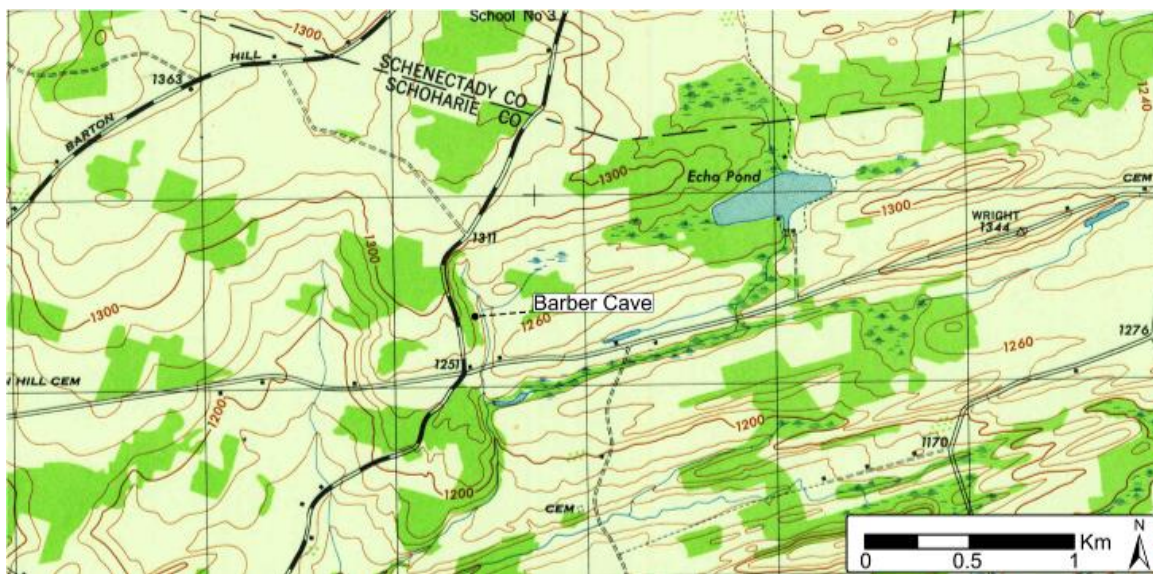


Figure 3.13 Location map of Barber Cave, Schoharie County, New York.

This map shows that the cave is currently located above the deranged drainage, though water may enter during times of high flow. Modified from USGS topographic map of the Gallupville 7.5 minute quadrangle (1946).

Surface geology and depth of the cave

The surface geology of the area includes a limestone pavement, with many grikes and clints. This limestone pavement indicates the recent glaciation and removal of material. This surface also includes a gully, in the side of which is the cave entrance.

The distance of the limestone pavement at the surface to the floor of the cave is less than ten meters. Depth of this cave is several meters deeper than other caves in this study, and its presence in close proximity to the southern face of a hill may protect it from future glaciation, or may have protected it from previous glaciation.

Hydrology

Barber Cave appears relict in the current hydrology, as it is at a higher elevation than other caves in the area. Though it appears relict on a topographic map (Fig. 3.13), it receives water during intense flooding of nearby cave systems (Myroie 1977). This flooding typically happens during spring snowmelt, and when the nearby resurgence (Paradise Lost Resurgence) backs up, causing backflooding of upstream caves (Myroie 1977). These conditions may only occur one or two days per year in the current drainage. The surrounding hydrology is deranged in nature, with ponded waters in glacial depressions as swamps and lakes, connected by small streams (Fig. 3.13). The gully in which Barber Cave resides channels water into this deranged drainage and the position of this cave can be explained by changing base levels as the stream downcut the topography (Fig. 3.13).

Cave geometry and passage shape

Barber Cave is a maze cave of network pattern (Fig. 3.14). The passage shape for this cave is a simple fissure formed by flooding to the ceiling. The dimensions of the passage for this cave are very small, as evidenced by the scale on the map. Larger passages in this cave exist, but are mechanically enlarged rather than dissolutionally.

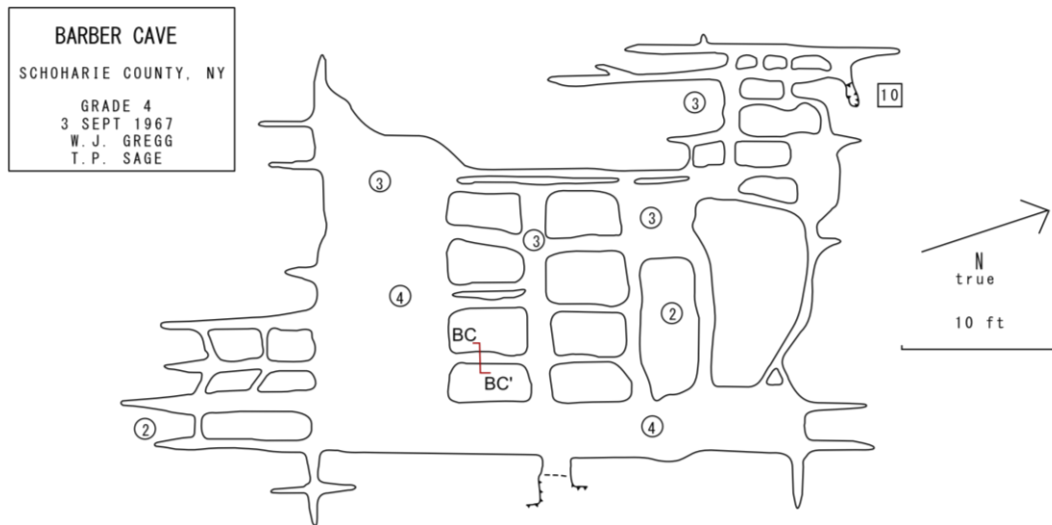


Figure 3.14 Map of Barber Cave.

Cross-section BC-BC' is presented in the results section of this paper. Redrawn and modified from Mylroie (1977).

Adirondacks region, Big Loop Cave

The Adirondacks region is highly deformed and includes metamorphic basement rocks (from 1.1 Ga, Isacshen et. al. 2000) that have been uplifted. These rocks include marble, typically bounded by schist units. These marbles can contain caves, including several maze caves such as X Cave (a network maze cave), and Big Loop Cave (examined for this study) (Engel 1989).

This area has been glaciated, as evidenced by extreme derangement of the drainage (Fig. 3.15), and by tills located to the south containing cobbles of Adirondack units (including at the primary study site). This glaciation has disrupted the drainage, which includes the Hudson River, a major river draining eastern New York. Deglaciation has occurred in this area as early as 15.2 ka BP (including near X and Big Loop caves) (Ridge 2004).

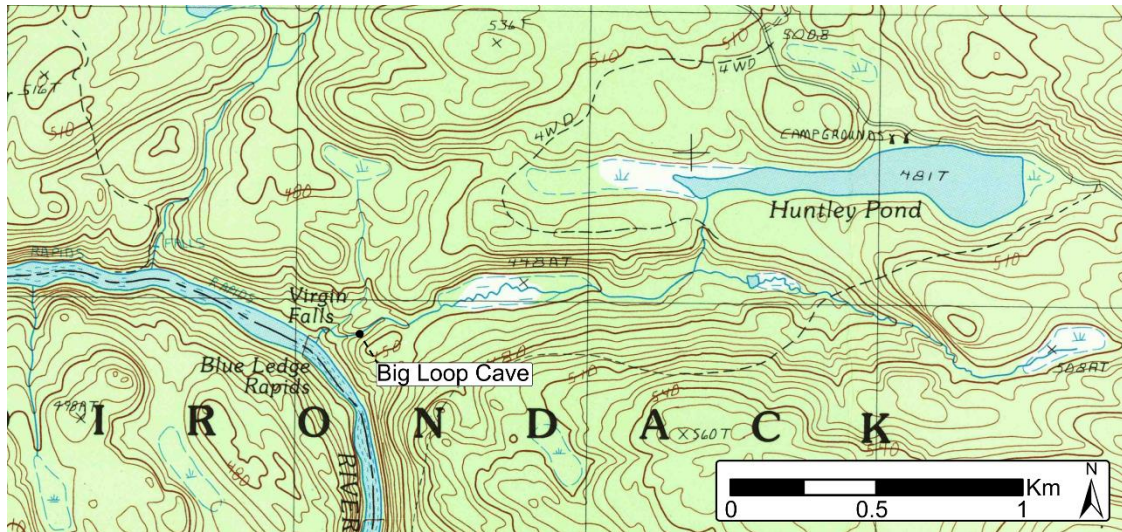


Figure 3.15 Location map of Big Loop Cave showing its location within the deranged drainage.

This cave accepts a sinking stream and fits well into the current drainage. Modified from USGS topographic map of the Dutton Mountain 7.5 minute quadrangle (1997).

Big Loop Cave

Big Loop Cave has been described by Engel (1989), with attention paid to the relationship of the cave to the geology and topography. It is an anastomotic maze cave accepting a sinking stream (Fig. 3.16). This cave exists in the Grenville Marble, bound by schist within the Dutton Mountain Quadrangle (Fig. 3.15). The marble and schist dip at 15° , with the cave following this dip (Engel 1989). The conditions this cave exists in are similar to the stripe karst of Norway (Lauritzen 2001); however the dip is not steep enough to produce stripe karst (Faulkner 2009).

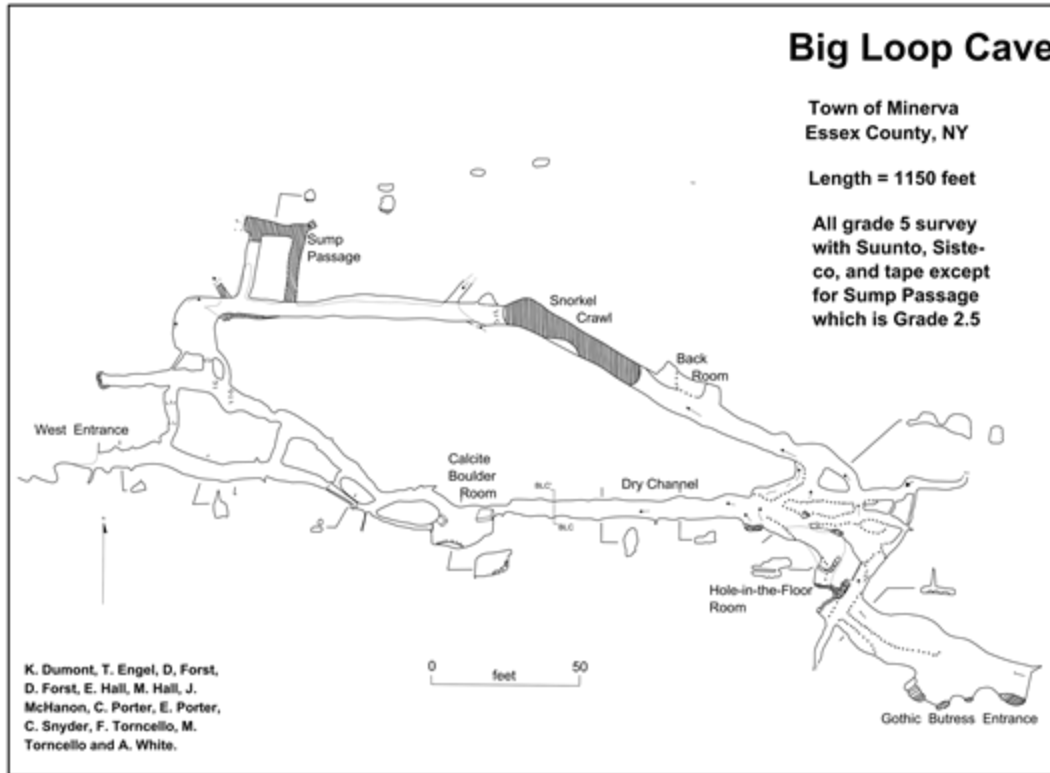


Figure 3.16 Map of Big Loop Cave.

This cave exhibits an anastomotic maze cave pattern. Cross-section BLC-BLC' is shown in the results section of this paper. Redrawn and modified from Engel (1989).

Depth of the cave

Big Loop Cave has been described by Engel (1989), with careful attention to the relationship of the surface to the cave. The cave exists in dipping marbles, and the cave itself follows this dip. This marble has a greatest thickness over the cave at 15 feet (five meters) (Engel 1989). The greatest height of passage in this cave is up to two meters, making the cave within three meters of the surface.

Presence of sediments

This cave contains sediments that occlude several parts of the cave, diverting water by making an inefficient path (Engel 1989). These sediments are glacial in origin, but may be transported post-glacially, as this cave receives a sinking stream that can produce high flow velocities during snowmelt. If these were transported in post-glacially, it is possible this cave is post-glacial.

Hydrology

This cave receives input from a stream, directly connected to deranged drainage (Fig. 3.15). This stream drains Huntley Pond, which exists in a glacial depression. Additional deranged drainage of this area includes several swamps in glacial depressions, with streams connecting these to other swamps and lakes. Water from this deranged drainage occupies this cave to the ceiling during high flows, and can fill the cave after large rain events and snowmelt.

The velocity of the sinking stream is enough to transport large logs into the cave, and enough to wedge these to the ceiling. This cave is nearly water filled year round in the Snorkel Crawl and the Sump Passage, but is mostly dry in the Dry Channel (Fig. 3.16). Regular flooding in the dry channel is indicated however, as organic debris can be found wedged in the ceiling. During this flooding Dry Channel fills and diverts water out the southern passages of this cave, and eventually out West Entrance (Fig. 3.16).

Cave geometry and passage shape

Big Loop Cave is a maze cave with an anastomotic pattern (Fig. 3.16), following the dip of the marble. Most passage in Big Loop Cave is either partially water filled, or

has sediment obscuring true passage shape and dimensions. The general shape of passage exists on the continuum between a tube and a fissure, and in some places a canyon has cut in the floor. The tube and fissure portion of the passage dimensions is shaped during conduit-full conditions, and the canyon shaped during non-full conditions.

Ontario Lowlands, the Black River, and the Glen Park Labyrinth

The stratigraphy of the Ontario Lowlands includes the Cambro-Ordovician stratigraphy described within the literature review, as well as Precambrian units (Cushing et. al. 1910). Soluble units include formations within the Black River and Trenton groups of carbonates.

Structurally this area has an overall low dip angle of 5° to the southwest, though there are many folds in Precambrian strata. Folds also exist in the Cambro-Ordovician strata, with folds in the Black River Group and Trenton Group controlling incision of the Black River (Cushing et. al 1910). Brittle features include jointing and faulting, with jointing causing the control of the several maze caves in the area including the Glen Park Labyrinth, Three Falls Complex, and Kronos Maze (along the Black River) (Carroll 1969a, 1969b, Zimmerman 1992), as well as SCAG Maze and others which accept the entire Perch River during lower discharges (Zimmerman 1992).

Glaciation has profound impacts on this area. These impacts include not only glacial landforms as drumlins and kames, but also sediments and landforms associated with lakes at higher elevations than current lake level (Stewart 1958). After the retreat of the glaciers in this area (around 13.8 ka BP) (Ridge 2004), an ice-dammed lake was present (Glacial Lake Iroquois) until 10,900 C¹⁴ years before present (12.9 calibrated ka BP) (Rayburn et. al. 2011). Glaciation of this area also produced deranged drainage, and

has entirely changed the pre-glacial drainage pattern of the region, including that of the Black River (Cushing et. al. 1910).

Black River

The Black River contains a drainage area of nearly 5000 km² (USGS 2013). This river drains the western side of the Adirondacks into Lake Ontario (Cushing et. al. 1910). The current path travels directly through the previous pre-glacial drainage divide for the St. Lawrence River, and Lake Ontario (Cushing et. al. 1910, Stewart 1958). The location of this crossing is near Great Bend, New York, with a post-glacial channel to the west of this bend. The Black River west of this bend passes through Watertown, New York, the location of the Glen Park Labyrinth and other maze caves. These caves therefore exist in a post-glacial channel.

Data on this river from the USGS include stream gage data, with stage heights and related discharges. This stream gage has measured floods producing discharges of 55,000 cfs (1550 m³/s), producing a gage height of 16 ft (4.9 m). Records of these previous large discharge events are present in the maze caves located next to the Black River at higher elevations, such as Glen Park Labyrinth (A. Palmer 1975). Current measurements of discharge are impacted by the damming of lakes to create reservoirs along the river (USGS 2013), and therefore this needs to be accounted for when using these data in extrapolating into the past.

Glen Park Labyrinth

The Glen Park Labyrinth is an extensive maze cave of over 12,500-ft (3810-m) of passage including 1800-m length at one level (Fig. 3.17). This cave has been discussed in

the caving periodical *The Northeastern Caver* (e.g., Carroll 1969a, 1969b); as well as in A. Palmer's seminal maze cave paper (1975). This cave is a floodwater maze cave of network pattern. It is located adjacent to the Black River; at a higher elevation (18 m above the current river position) than current flood events can reach even at record discharges. While it is located near the Black River, an exact location is not provided, as to protect landowners.

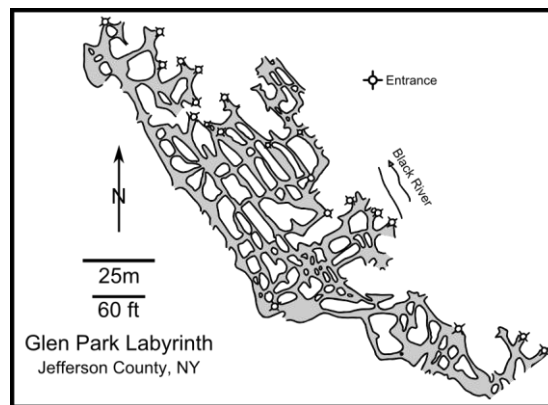


Figure 3.17 Map of the “Old Labyrinth” section of Glen Park Labyrinth.

This section represents the main level of the cave, and contains 1800-m of passage. Map adapted from Carroll (1972).

Large paleo-discharge is evidenced by small scallops (Fig. 3.18), indicating velocities up to and greater than 3 m/s (A. Palmer 1975). For this cave it is likely that the floodwaters are not from A. Palmer's (2007) “bank storage” analogy, but from accepting the entire Black River prior to downcutting to the current position. This is evidenced by the maze caves located in the nearby Perch River, which accept the entire river during low flow events, with water only flowing over the surface during large discharge events (Cushing et. al. 1910).



Figure 3.18 Photograph showing the small scallops in Glen Park Labyrinth.

These scallops are located through the entire cave (even along the ceiling), and have a median length of 1.9cm. Photograph by Dr. A.J. Bartholomew.

Surface geology and depth of the cave

The surficial geology around this cave is limestone pavement, with many grikes and clints. This cave has many entrances located within grikes of this limestone pavement.

Depth indicators of this cave exist in the form of roots growing down from the surface. This cave has many entrances, all of which are enterable within outcrops of the Black River Group limestone. These entrances exist within three meters of the surface,

and for most of the cave the floor of the cave is two to three meters below the entrances (with some depths up to 10 m on other levels).

Presence of sediment

This cave contains several glacial cobbles, though no large deposits of these. These cobbles are located near entrances, and have not been moved far from them. The location of these cobbles can be suggestive of transport by rolling over the surface and into the entrances. Additionally, floodwaters in this cave are of high discharges as evidenced by scallop sizes and could move such cobbles post-glacially.

Hydrology

This cave is formed by paleo-baseflow and paleo-floodwaters of the Black River prior to downcutting to current position. Appearances based on topographic maps, without additional geologic information does not completely show deranged drainage. While the Black River itself does not appear deranged, the current arrangement of this river is a result of glacial diversion (Cushing et. al. 1910, Stewart 1958). As the hydrologic control of this cave is flooding from the Black River, and the Black River is post-glacial in this area, a post-glacial origin of this cave is required.

Paleohydrologic data exist in this cave in the form of scallops (Fig. 3.18). These scallops were measured during the course of this study, with the majority of scallops measuring 1.9 cm. Also measured were lengths between 1.4 cm and 2.1 cm. These scallops indicate mean flow velocities up to three ms^{-1} .

Additional considerations for the paleohydrologic conditions of this cave include the placement of glacial Lake Iroquois, with a lake level that would have covered the

current position of the cave (Cushing et. al. 1910). This glacial lake would produce stagnant conduit-full conditions in this cave.

Cave geometry and passage shape

The shape of the passage in this cave is mostly within the continuum between tube and fissure shape. In various locations within the cave there are small canyons cut into the floor. The joints controlling these passages are visible in the ceiling throughout the cave.

CHAPTER IV

METHODS

Introduction

The methods that have been used previously for research in karst and glaciated karst in particular are cave surveying, dye tracing, and age dating of sediment and speleothems. These methods have been used in glaciated karst studies to determine the pre-glacial origin of caves, such as those in the Helderberg Plateau. Pre-glacial origin was verified through the observation of large caves, dye traces revealing pre-glacial dendritic patterns in contrast to post-glacial deranged drainage (Baker 1973, 1976, Kastning 1975, Mylroie 1977, Dumont 1995, Fig. 2.8), the presence of glacial sediments in caves (Fig 2.6) (Mylroie 1984, Dumont 1995), and ultimately U/Th absolute dating of speleothems up to the maximum date obtainable through this method, 350 ka (Dumont 1995, Lauritzen and Mylroie 2000) (Table 2.1).

Arguments on finding post-glacial origins of caves include congruence of caves to the deranged drainage (Fig. 2.12), and small passage character (A. Palmer 1972, Mylroie and Carew 1987). While these had been hypothesized, they have not been previously demonstrated in the field and proven through methods such as dye tracing. As this hypothesis has not been studied, the goal of this research is to demonstrate this.

In order to demonstrate post-glacial origins, one type of cave was used: epigenic maze caves. Epigenic maze caves are typically shallow (A. Palmer 2001), and thus

should not survive repeated glaciations due to weakening of the rock. These caves should then line up with the post-glacial deranged drainage.

To demonstrate congruence with deranged drainage, water flow analysis was performed in ArcGIS for the primary study area (the Joralemon Park karst area). As previously discussed this area includes two large, connected caves, Hannacroix Maze, Merritts Cave, which drain the upper drainage for the area, and other smaller caves, including Skips Sewer and the relict Joralemons Cave and Joralemons Backdoor. Cave positions on topographic maps were analyzed for additional caves not in the primary study area. Additionally in the primary study area a GIS database and map were created showing pre-glacial karst features, current active hydrologic and karst features, and glacial landforms.

Additional parameters for determining post-glacial origins are shown in Table 2.2, and include small passage cross-sectional areas. To demonstrate the hypothesis that most maze caves in glaciated areas are post-glacial, these parameters were directly examined by cave exploration and description, cave map analysis, and measurement of cross-sectional areas.

Wall-retreat rates allowing maze cave formation combined with passage dimensions allow calculation of cave formation times after initial breakthrough (A. Palmer 1991). As these caves are located in a glaciated area, glacial unloading and tectonism may have caused the initiation of the caves (Faulkner 2006a), eliminating chemical breakthrough times or dramatically shortening them. These formation times will then be compared with glacial retreat in their respective location (as determined by Fig. 2.15) (Ridge 2004) and verified by boundary conditions.

GIS Analysis

Creating the initial GIS Description

A GIS database and map were created through the mapping of surface features at the primary study location. These features include glacial landforms, surface streams and lakes, insurgences of water, resurgences of water, and cave entrances. These features and their position were obtained from fieldwork using GPS (global positioning system), and from aerial photographs and LiDAR contours (contours generated by laser ranging).

Field work

Fieldwork was performed in the primary study location to record hydrologic features, karst features (active and non-active), stratigraphic information including that of the Paleozoic rocks and glacially derived sediment. The areas in and around Joralemon Park were walked in detail looking for these features, and were recorded in point feature shapefile using ArcPad.

Karst features were recorded as point data in ArcPad from GPS. These coordinates were collected in the WGS84 datum (the datum used for GPS). Karst features recorded include sinkholes, water insurgences and resurgences, dissolutionally enlarged joints, and cave entrances of relict and active caves. For cave entrances attribute table data included the cave name, the cave entrance name (if more than one exists), the altitude in meters above seal level, and whether the cave was active or relict. For karst features the attribute table includes type of feature, and elevation.

Stratigraphic information was recorded to verify the literature of the area. This information includes the presence of units of the Paleozoic stratigraphy and their elevations, positions, and what units act as base level for streams and karst formation.

Additional stratigraphic information includes glacial material and its relationship to cave entrances.

Data from aerial imagery and LiDAR contours

The karst feature data were added to a GIS using ArcGIS. This GIS contains 0.5-ft (0.15-m) resolution aerial imagery, and 2-ft (0.6-m) contour lines derived from LiDAR data. These datasets were downloaded from the New York State GIS Clearinghouse and use the NY State Plane coordinate system in the NAD1983 datum with US feet as the linear unit. Data obtained from fieldwork were re-projected into this system.

From aerial imagery, hydrologic data were derived. Hydrologic data were obtained by tracing swamps as polygon features, and streams as polyline features. These are projected in the NY State Plane coordinate system with the NAD1983 datum.

From the LiDAR data, a DEM (digital elevation model) raster was generated in ArcGIS using the TopoToRaster tool. The cellsize set for this DEM is 2ft by 2ft (0.6 by 0.6 m). This DEM is used to show the orientation of till capped ridges, depressions caused by glaciation and to support water flow analysis related to these features and their relation to cave positions and elevations.

Water flow analysis

Water flow analysis was performed to show the features controlling the hydrology of the caves in the primary study area. Water flow analysis was performed using the DEM generated from 2-ft (0.6-m) contours of LiDAR data obtained from the New York State GIS Clearinghouse.

To show flow into the caves, the flow direction and flow accumulation generated by ArcGIS were used. Sinks (artifacts generated in the process of DEM creation that are below the natural topography and thus divert water during analysis) were not filled in this analysis, as the karst terrain produces natural sinks in the raster. Flow direction was obtained using the Flow Direction tool, and flow accumulation was obtained using the Flow Accumulation tool, in ArcGIS. The flow direction analysis calculates slopes based off of the DEM raster to show the direction water will take at any point on the raster. Flow accumulation analysis shows the path water will take on the surface. If the analysis shows control of caves by glacial landforms, the caves can be said to be post-glacial in origin by the model proposed by Mylroie and Carew (1987).

A new GIS map was created with the DEM raster, flow accumulation raster, the swamp and stream vectors, and positions of relict and active cave entrances. These are all projected in the NY State Plane system with the NAD1983 datum. This new map shows the flow of water through these caves, and demonstrates whether glacial features control the caves, and fit into the deranged drainage.

Additional information added to this new GIS includes the flow of water through Hannacroix Maze, and Merritts Cave, to show the connection of these caves to the deranged drainage, as determined by exploration and analysis of the map of Hannacroix Maze, and survey of Merritts Cave.

Cave description, and surveying

For each cave visited, both within the primary study area and at other study areas, descriptions carefully recorded to describe the size and shape of passage, presence of allogenic sediments, presence of indicators of the depth of the cave (such as roots

penetrating the ceiling), and whether the caves were active or relict. These parameters are important in determining the time origins of a cave (Table 2.2), and are discussed in Chapter III. Position of cave entrances was also noted, along with the controlling hydrologic features for analyzing whether pre-glacial or post-glacial features controlled the cave. Additionally, any information pertaining to calculation of wall-retreat rates was recorded, such as scallop length. The caves visited as previously described were Hannacroix Maze, Merritts Cave, Skips Sewer, Joralemons Cave, Big Loop Cave, Glen Park Labyrinth, and Barber Cave. These caves were selected for access reasons, as well as their end-member positions in size, relict or active nature, and locations within varying representative strata (including Grenville marble, Cambro-Ordovician limestone, and Siluro-Devonian limestone).

For the unmapped caves of this study, a cave survey was performed to record features that determined the hydrologic controls and speleogenesis of the cave, in both sketches and on the final maps. In addition, accurate cross-sectional data were obtained for all caves visited.

Cave Survey

For caves without prior survey, cave maps were produced through the standard surveying methods described in *On Station* (Dasher 1994). In addition to a typical azimuth, inclination, LRUD (left, right, up, and down distances perpendicular to azimuth at each station), and sketch data, finer data on passage cross-section were taken, as well as hydrological and geological data. Hydrological data include the direction of flow, and paleo-flow indicators such as scallops. Geologic data include the trend of jointing, presence of speleothems, and breakdown. Azimuth, inclination, and LRUD data were

entered into the COMPASS program to produce a wall and line plot in SVG (scalable vector graphics) format, and then the sketch overlain using a vector-image editing program, Inkscape. Sketches were transferred to the map by following sketched walls with the vector tools available in the program. All measurements were taken in the MKS (meters, kilograms, seconds) system. Maps created for this study are: Merritts Cave, and Minicroix Cave (a small, previously unmapped cave within Joralemon Park). The created maps use the standard NSS (National Speleological Society) symbology (e.g. Dasher, 1994).

Passage cross-sectional data

Measuring cross-sections

Measurements

In addition to the typical LRUD passage dimensions, a more accurate means of measuring cross-sectional area must be used, due to the calculations to be performed on these data. In order to obtain this more accurate data a Leica Disto™ laser rangefinder was used, and swept through a radial pattern perpendicular to the cave walls as shown in Figure 4.1 and described by Sasowsky and Bishop (2006). This rangefinder was mounted to a tripod with ratcheting adjustments through angles in increments of 22.5° (Fig 4.2). Due to equipment failure during fieldwork, further measurements were taken using the same tripod; however the measuring device was a Keson™ fiberglass tape. As the tape was not directly mountable to the tripod, bubble levels and a plumb bob were used to maintain measured angles. Measurements taken with the rangefinder provide values in 1-mm increments, while the fiberglass tape has increments of 2-mm. Caves where cross-sections were measured by rangefinder are Big Loop Cave, Merritts Cave, and

Hannacroix Maze. Caves where cross-sections were measured by tape are Barber Cave, and Glen Park Labyrinth.

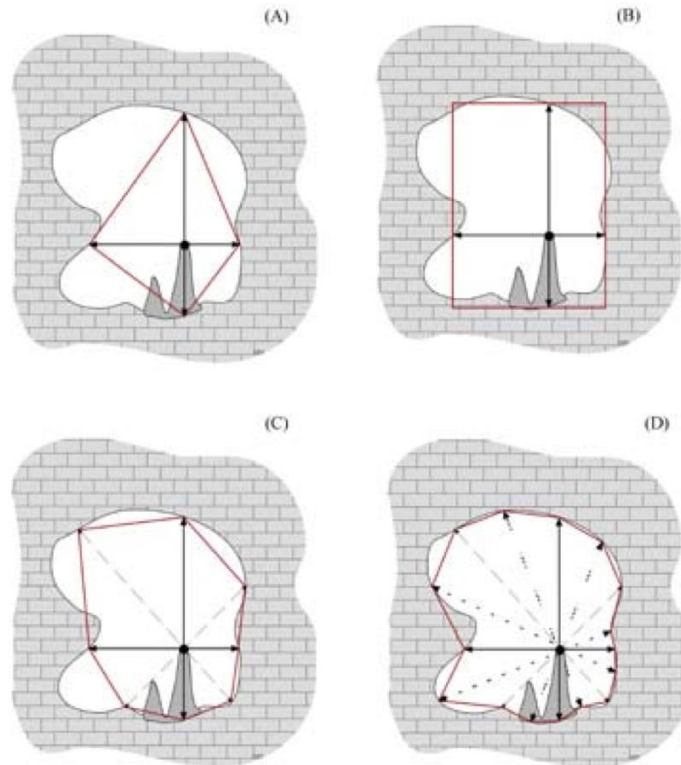


Figure 4.1 Different methods of deriving cross-sectional area approximations.

Shapes A and B use standard LRUD data to construct shapes. C and D show additional shots that can be made for a better approximation of passage geometry, and area. From Sasowsky and Bishop (2006).

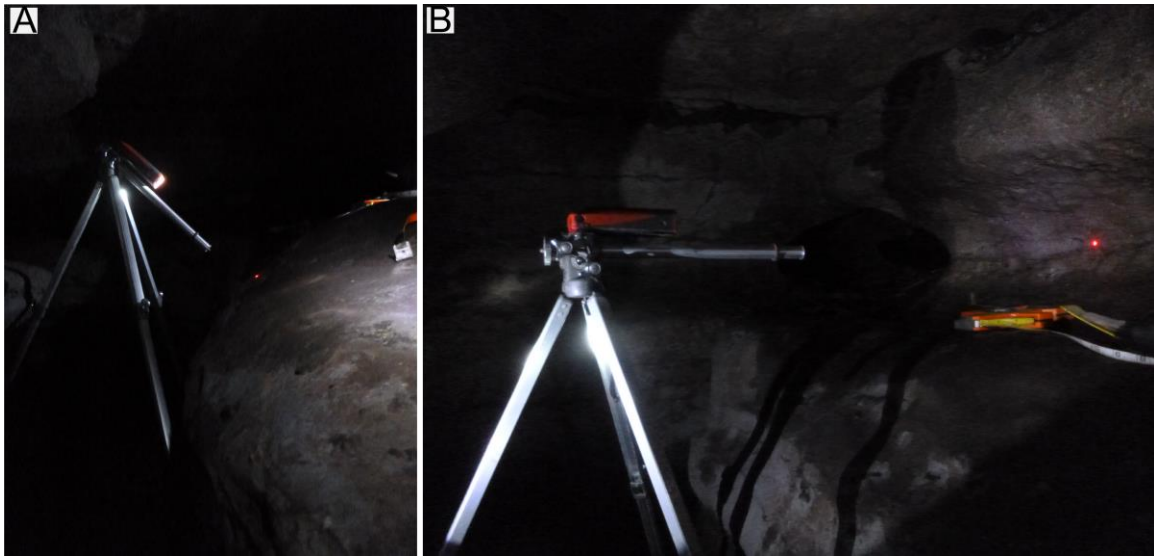


Figure 4.2 Picture of tripod and Disto used for measurements.

This tripod can be ratcheted in increments of 22.5° . The tape seen in B was used for measurements after equipment failure of the Disto.

Sampling

Differing amounts of data points were collected depending on the complexity of the passage, and on equipment (ranging from four in Barber Cave to 16 in Merritts Cave). Measurements were taken in areas in the cave with the largest apparent dissolutional passage cross-section. Passages with clear evidence of breakdown were not selected, as wall-retreat rates cannot be applied to these to obtain a date. In addition to these data, sketches were produced of these cross-sections. A sketch was taken for each cave cross-section.

Calculation of possible times of formation by wall-retreat rate

Calculations of the time required to form a passage in its current condition can be performed based on wall-retreat rates given by A. Palmer (1991, 1999) for maze caves

(the area bounded by brackets in Figure 3.3), and by values specifically for cold water (up to $0.2\text{-cm}\cdot\text{a}^{-1}$) (Faulkner 2006b), as conditions during glacial retreat produced cold waters. Times were calculated and plots were generated based on the wall-retreat rate given by A. Palmer (1999) for maze caves, and days in conduit-full condition per annum. Conduit-full days per annum were then chosen based off known field observations extrapolated to greater times during glacial retreat. Additional analyses were performed to find potential days in conduit-full conditions per annum, and to model potential growth pathways these caves could have taken.

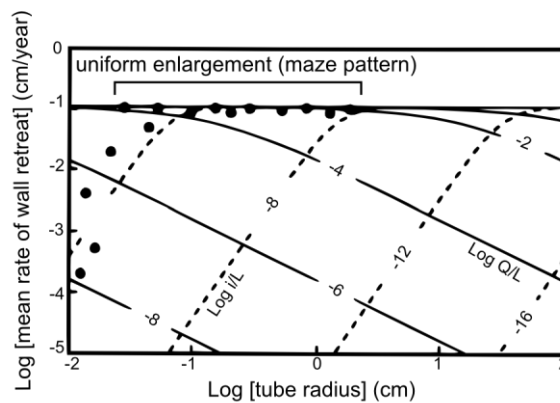


Figure 4.3 Graph of wall-retreat rates allowing uniform enlargement of passages and the formation of a maze cave.

Dots in the bracket represent a Q/rL ratio that is greater than 0.001 cm , allowing the formation of a maze cave. Dots not within the bracket indicate uniform enlargement of only small tubes undergoing laminar flow, and not to the maximum enlargement rate. For the purposes of this study the wall-retreat rate used is that of turbulent flow, as calculations assume breakthrough by tectonics rather than chemical processes. Redrawn from A. Palmer (1999).

Calculations of cross-sectional areas

Cross-sectional areas were calculated in two different ways: from area calculations on triangles created by rays connecting adjacent data points, and from image analysis of sketches fitted to cross-sectional measurements.

The overall cross-sectional areas can be calculated by summing the areas of triangles created by the length measurement and their angles. From these measurements and known angle increments, two sides of a triangle are known, as well as an angle. From these measurements the third side can be computed using the law of cosines. Area can then be computed using the three sides and Heron's formula:

$$T = \sqrt{s(s-a)(s-b)(s-c)} \quad (4.1)$$

$$s = \frac{a+b+c}{2}$$

where T is the area, s is the semi-perimeter, and a, b, and c are the sides of a triangle. This calculation only calculates the area of these triangles, and does not compute the entire area if the area deviates from the triangles.

Cross-sectional areas can also be calculated through image analysis in the program ImageJ. Transformed sketches were loaded into ImageJ with a scale bar. These were then analyzed with the measurement tool for area. To obtain the transformed sketch, the initial sketch was scanned and traced as a vector path in the Inkscape vector image-editing program. This traced path was then added to a plot of the distances at their respective angles and adjusted to keep the shape of the sketched cross-section, but to match the measurements.

These two methods produce close values, and are both useful. The method used for analyzing sketches can be used for additional caves not visited, by sketching cross-sections in existing maps, and setting the scale based on scale bars.

Calculation of possible formation times

Calculation of the time required to enlarge to current conditions can be performed based on the width, or the height of the passage, depending on how it grew (growth based on perimeter, or downwards). Fissure passages grow along a perimeter, and thus the width of the passage controls the time. Tube shaped passages grow along the perimeter, and grow in a circular or elliptical pattern; thus the radius controls the time. Canyon-shaped passages grow downward; thus height controls the time (A. Palmer 1984). For the purposes of the calculations, breakthrough times are ignored, as inception can occur through rebound and tectonically in glaciated regions for joint controlled caves (Faulkner 2006a), which are the majority of the caves in this study.

To calculate based on widths, first the widths are divided in half, as the passage grows as separating planes (for fissure passage) or by radius (for tube passages). These half-widths can then be divided by wall-retreat rates and plotted. Additional consideration for these time plots are the period of conduit-full condition, as wall-retreat rates given by A. Palmer (1991, 1991), and Faulkner (2006b) are for phreatic passage filled by water for the entire year. The equation used to plot these possible times of formation is given in Equation 4.2:

$$T = \frac{w}{2 * S * 1000} * \frac{365.25}{d} \quad (4.2)$$

where T is the time required (in ka) to form a passage of width w ; 2 converts width to a half-width; S is the wall-retreat rate; 1000 converts a to ka; and d is the days per year in conduit-full conditions. For these plots S was held constant at 0.1 cma^{-1} , the wall-retreat rate for maze caves at 10°C and $0.01\text{-atm } P_{\text{CO}_2}$ (A. Palmer 1991, 1999).

These plots have several caveats:

- (1) They are simplistic representations of actual conditions, as frequency and length of flood events has changed through time, especially during the time after glacial retreat with melt-waters. Another simplistic assumption is a wall-retreat rate of 0.1-cma^{-1} , as at colder temperatures wall-retreat rates can be double this value (Faulkner 2006a). Retreat rates also change depending on the radius or half-width of passage, though evaluation of paleodischarge indicators can show Q/L ratios that support 0.1-cma^{-1} growth even at larger radii.
- (2) The plots only determine the length of time to form a particular cross-section, and do not give a time of origin. Time windows less than the time since glacial retreat only lends evidence, and are not complete evidence of post-glacial origins (especially if the cave is in a relict position).
- (3) These plots ignore the length of time required to form a vadose canyon cut into the phreatic passage, if such exists. This caveat is only minor however, as these canyons can form during times where the passage is not in conduit-full conditions.

The time to form the passage, depending on passage width and days per year in conduit-full conditions, can be solved by Equation 4.2. These calculated dates are then

compared to the date of glacial retreat in the area. These dates can be obtained from Figure 2.15, and are in calibrated ka BP (Ridge 2004). Dates calculated that are less than the date of glacial retreat for the area lend some evidence to post-glacial origins of these caves.

Evaluation of time in conduit-full conditions

The plots holding days in conduit-full condition per annum constant are a simplistic representation of actual conditions. These assume constant conditions, which may not be the case. To determine actual time in conduit-full conditions several methods can be used, including direct observation for some caves. Methods used are comparing the discharge a cave can support based on scallop data and comparing these values to recorded discharge, and modeling of passage growth based on varying times in conduit-full conditions extrapolating back in time from current conditions and assumptions of past conditions.

Comparison of recorded discharges to supported discharge

As caves can only support a certain amount of discharge before flooding on the surface occurs (Fig. 4.4) (White 1988), a comparison of this discharge to available discharge data can be used to estimate a number of days in conduit-full condition per annum.

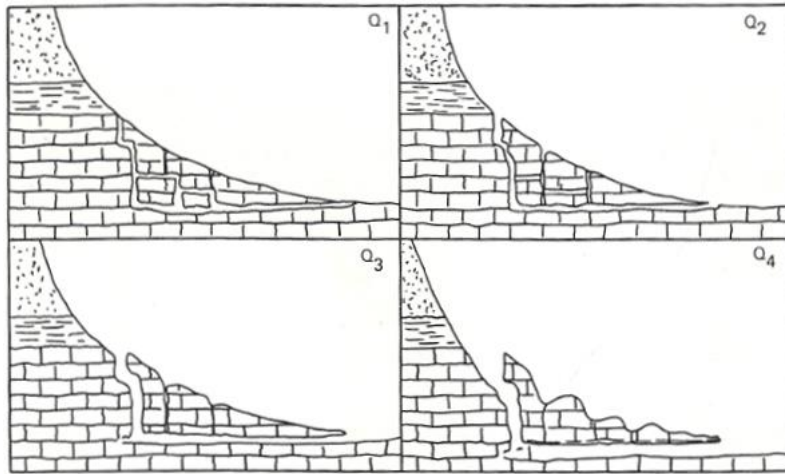


Figure 4.4 Diagram showing different conditions of conduit-full conditions at varying discharges.

At Q_1 the discharge is handled entirely by the cave, though the cave does not experience conduit full conditions. At Q_2 the discharge is handled entirely by the cave in conduit full conditions. At Q_3 the cave is in conduit full conditions, with discharge flowing over the surface and incising the channel. From White (1988).

Maximum supported discharges can be calculated by paleoflow indicators in the form of scallops. Figure 2.4 gives a velocity based on scallop data, which multiplied by the cross-sectional area measured provides a discharge. As the caves in this study are maze caves, the discharge is split along each parallel passage. To obtain the total discharge supported by the cave, the discharge calculated is multiplied by the number of conduits.

For some caves the number of conduits can be counted from the cave map, and for others extrapolation is needed due to downcutting of channels by the stream. To extrapolate, the number of passages per meter is used by measuring the current number of passages and dividing that number by the distance perpendicular through the parallel

passages (Fig. 4.5). This number can then be multiplied by the map distance that the cave previously covered. As this is an extrapolation, the number of passages may not be the exact number, but does provide a maximum number of passages, and thus an end-member condition.

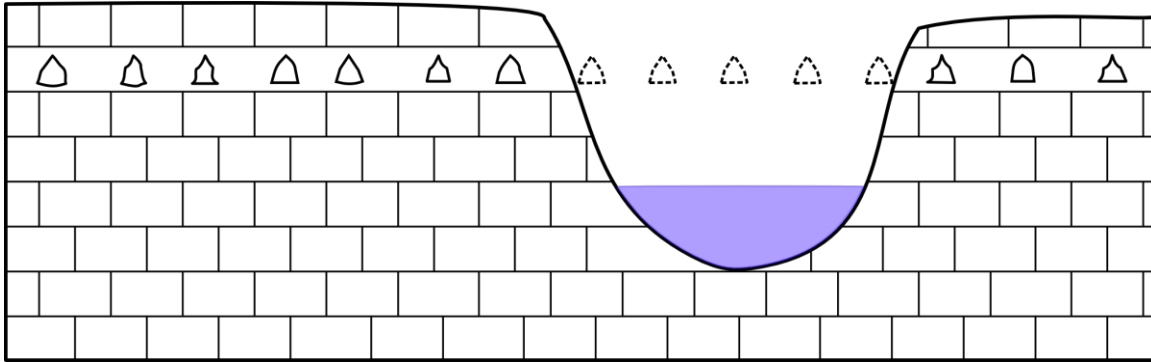


Figure 4.5 Joint spacing can be further extrapolated after downcutting of a channel.

Solid line chambers indicate current passages. From the number of current passages per unit distance previous passages can be extrapolated.

From this discharge a comparison can be made to the median daily discharges, available from the USGS water data website. The data provided are statistical data of discharges for each day of the year in cubic feet per second (converted to cubic meters per second for this study). If the median discharge for a single day is greater than the discharge capable of being handled by the cave, the cave can be said to be in conduit-full condition for this day. These days can then be summed for the total days in conduit-full condition per annum.

Limitations of this method include lesser ability to handle large discharges when cross-sectional area is smaller.

Modeling of passage growth

Passage cross-sectional area growth can be modeled based on varying conduit-full conditions from glacial retreat to present day. Unlike the time windows generated, these assume growth beginning at glaciation. If the path of growth from these models creates a passage size similar to those seen for each cave, the cave can be said to be post-glacial in origin.

Growth is modeled at a starting condition of high conduit-full conditions per year for several thousand years (for caves with an ice-dammed lake or post-glacial lake). These conditions can include up to the entire year of conduit-full conditions. For caves that receive few conduit-full days per annum, a higher than current value will be used, congruent with discharges seen in other maze caves in the study. For increasing years close to the present, decreasing conduit-full days per annum are used. For each year passage half-width is incremented by 0.1 cm (the growth of a maze cave per year if subjected to conduit-full conditions for the entire year), multiplied by a ratio of days in conduit-full conditions. Days in conduit-full conditions per annum are randomized within a range of values that can be currently observed. This generates a pair of values of current radius/width and the years since the start of the model. These pairs can then be plotted, with the last radius/width value being the passage size possible to grow in this time. A brief Python code listing can be found in Appendix A for the generation of these pairs.

CHAPTER V

RESULTS

Results of Fieldwork and GIS Analysis

The products of the fieldwork and GIS analysis performed in this study include a map of the hydrological, geological, and karst features (Fig. 3.1), a description of the karst of the study area, in particular base level of the current active caves and their relationship to the previous base levels, and a map of flow accumulations showing the connection of active caves to the deranged drainage, with their relationship on the model proposed by Mylroie and Carew (1987). These results only pertain to the main study area, the karst of Joralemon Park, in Albany County, New York.

Description of the study area

This area is well described in the literature by Goldring (1943), A. Palmer et. al. (1991), Nardacci (1994), Rubin et. al. (1995), and others. The fieldwork verified the descriptions in this literature, adds information to the description, and creates an accurate GIS for this study (Fig. 3.1). This GIS allows for an understanding of this study area in terms of relationship of active and relict caves, and their respective base level.

As the description of this study area exists in the literature (and within Chapter III), this description includes only additional information pertinent to the study.

Topography

This area contains topographic features as the result of structural deformation, glaciation, and karst. The main features are several ridges aligned with the ice flow direction of the Wisconsinan glaciation (north-south in this area), and glacial depressions currently occupied by swamps (Fig. 3.1). Karst features such as surficial features and caves exist on ridges where the Onondoga Limestone crops out.

The ridges of importance for this study are the ridge containing Hannacroix Maze and Merritts Cave, the ridge containing Skips Sewer, and the ridge containing Joralemons Cave and Joralemons Back Door (all of which are composed of the Onondoga Limestone). Also important are the ice flow aligned ridges surrounding the park, which channelize water into the swamps of this area. These ridges are composed of varying insoluble formations depending on position, and include the Esopus shale to the north and east, and the Backoven shale to the west (Goldring 1943).

The ridge containing Hannacroix Maze and Merritts Cave is a *roche moutonnée*, with the stoss side existing near Hannacroix Maze, and the lee side near Merritts Cave. The ridge containing Skips Sewer trends the same as the *roche moutonnée*, however is separated topographically (though the Onondoga Limestone is continuous under the intervening low topographic point). Upon this ridge are several large blocks of Onondoga Limestone, perhaps plucked during the formation of the *roche moutonnée*. The ridge containing Joralemons Cave and Joralemons Back Door is of similar orientation, but reaches a higher elevation.

The topographic depressions of importance hold the several swamps in the area. The large swamp to the north of the study area drains into the smaller swamp adjacent to

the ridge containing Hannacroix Maze. The depressions containing swamps adjacent to Hannacroix Maze and to Skips Sewer are important, as if these depressions did not exist, they would not fill with water as swamps, and as thus the caves would not have formed as they are. These depressions aligned with ice flow direction are one piece of the evidence of the post-glacial nature of these caves.

Surficial karst

Surficial karst of the Joralemon Park karst area includes the interface features of cave entrances, dissolutionally enlarged joints, sinkholes and a karst window. The terminology applied to dissolutionally enlarged joints is a grike, or a cutter (with a clint or pinnacle as the bedrock between them, respectively). The term grike will be used here, as the origin is from the British glaciated karst, versus the non-glaciated, and typically mantled by soil, cutter of the American Midwest, where the term originated.

Grikes in this area exist at higher parts of the relative topography, where the Onondoga Limestone crops out. These exist in the ridge containing Hannacroix Maze and Merritts Cave (as well as its continuation point past the caves), the ridge containing Joralemons Cave and Joralemons Back Door, and the ridge containing Skips Sewer (including grikes forming the entrances to this cave). Additionally they exist in other parts of the park with no located caves. Several large grikes exist directly north of Hannacroix Maze, and serve as entrances to the cave.

The karst window of this area serves a resurgence point for water flowing through the ridges composed of Onondoga Limestone. This karst window is active year round; even at very low flow, draining Hannacroix Maze and Merritts Cave. The karst window is located in another swamp, also in a glacial depression.

Cave positions, hydrologic activity and base levels

There exist several caves in the Joralemon Park karst area. Several have been named in the previous literature, several were discovered during fieldwork, and one was mapped during this fieldwork. The caves from the literature are Hannacroix Maze, Merritts Cave, Skips Sewer, Joralemons Cave, and Joralemons Back Door. Caves found and named include Tetanus Shot Cave, which is currently occluded by organic material and unmapped, and Minicroix Cave, which was mapped during this study (Fig. 5.1). Detailed descriptions were taken of these caves (Chapter III); however for the purpose of this section only their positions and hydrologic activity are discussed for the relation of base level through time.

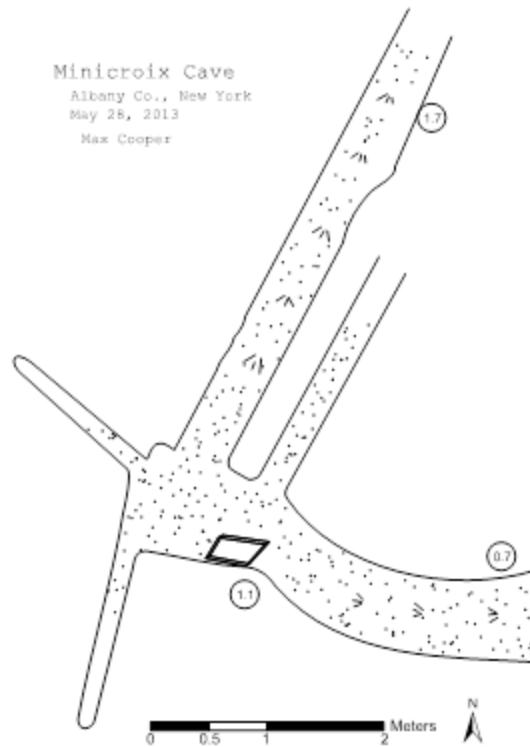


Figure 5.1 Map of Minicroix Cave, a previously undescribed and unmapped cave in the Joralemon Park karst area.

This cave is located in a small outcropping of the Onondaga Limestone adjacent to Hannacroix Maze and is completely joint controlled.

The current active caves are Hannacroix Maze, Merritts Cave, and Skips Sewer. Hannacroix Maze and Skips Sewer are both directly adjacent to swamps located in glacial depressions, and are controlled by flooding of these swamps. These swamps are underlain by the Esopus Shale, which acts as the local base level for streams and swamps, as well as the solutional base level for cave development. The entrance for Hannacroix Maze that receives water year round (and thus the lowest entrance) is located at 340-ft

(104-m) elevation. The entrances for Skips Sewer are located at 326-ft (99-m) elevation, and the ultimate resurgence for this system at a lower elevation..

Relict caves are Joralemons Cave and Joralemons Back Door. These two caves were at one point connected, but are currently occluded by sediments. The entrance for Joralemons Cave is at 358-ft (109-m) elevation.

Joralemons Cave and Joralemons Back Door have been demonstrated to be pre-glacial in origin due to the presence of paleontological remains (Steadman et. al. 1993), and thus are indicators of a pre-glacial base level. These caves exist at least 5-meters above current base level development for caves. This change in base level and the presence of current active caves at the new base level support the post-glacial origins of the maze caves in this area.

Tills and their position relative to cave entrances

The area in and around Joralemon Park contains glacial till and erratics. These tills exist on the tops of the ridges surrounding the park, as well as within the park itself. The ridge containing Hannacroix Cave and Merritts Cave is covered with this till, in close proximity to the cave entrances (Fig. 3.11). Tills also exist in lower topographies within the park, mantling most bedrock.

These tills (and in particular their positions) are important in understanding the time formation of these caves, as the existence of glacially derived particles within caves may support pre-glacial origins for caves (Table 2.2). If tills are local, and in close proximity to the cave entrances however, high flow conditions can move these sediments into post-glacial caves. Additionally, if tills cap a cave and the passage forms up to this till cap, the cave can still be considered post-glacial. Tills capping the ridge containing

Hannacroix Maze and Merritts Cave are located directly near the cave entrance (Fig. 3.11). Thus, tills within these caves will not be conclusive evidence to pre-glacial origins of these caves.

Results of GIS water flow analysis

The flow accumulation map produced from the 2-ft (0.6-m) resolution DEM (Fig. 5.2) shows the flow of water into the active caves of Joralemon Park. This map shows the till capped ridges surrounding the park as the controls for the waters in the swamps located in and around Joralemon Park. This water flows into the large swamp to the north of the park, which then follows a surface stream into the swamp (swamp A in Fig. 5.2) where Hannacroix Maze is located. Additional water channelized by these ridges travels into the swamp, bypassing the larger swamp to the north. Ridges to the west of the park channelize water into other local depressions containing swamps, but are not drained by any caves as they are not adjacent to any soluble bedrock.

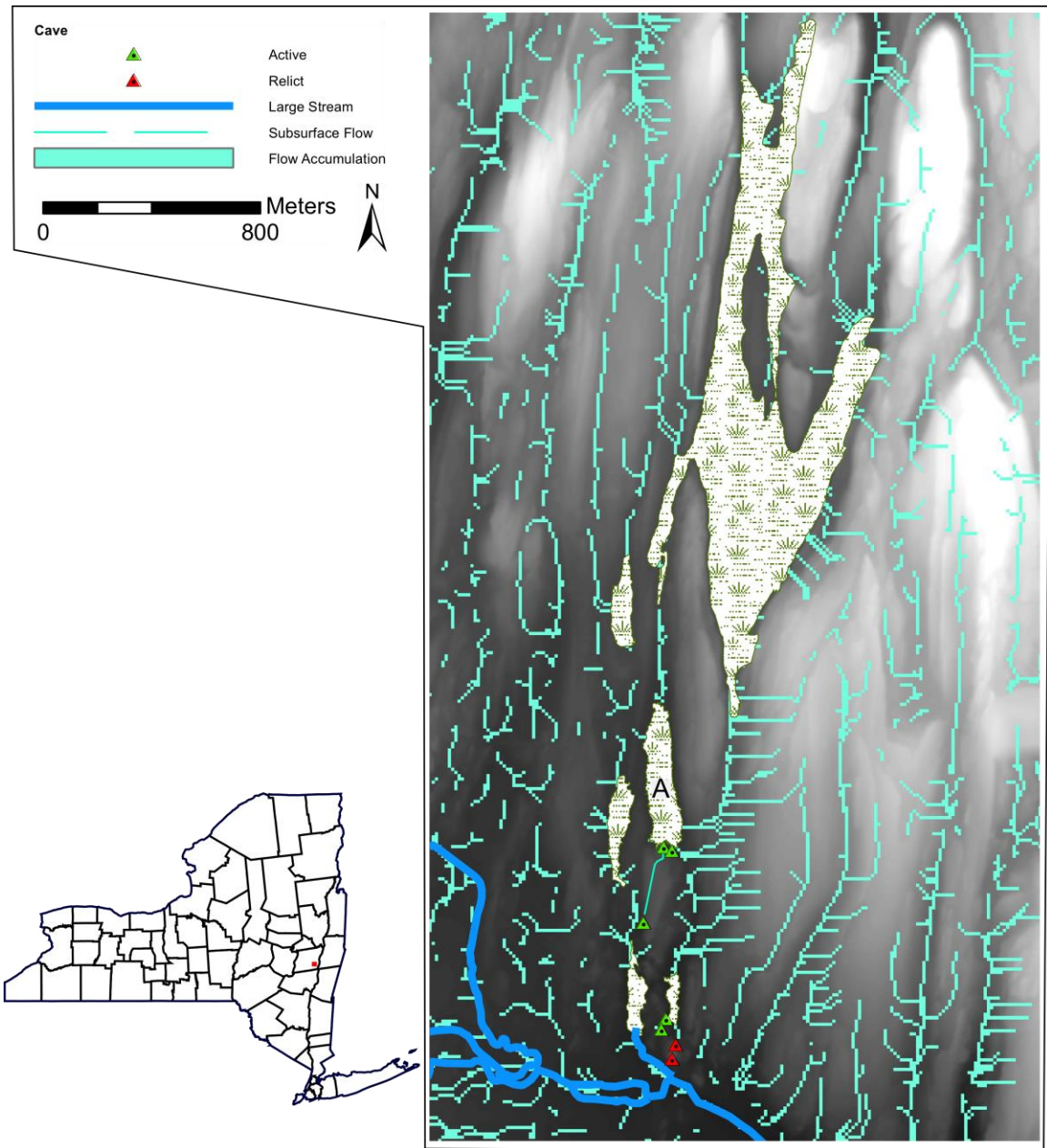


Figure 5.2 Flow map produced from flow accumulation tool.

Flow accumulation raster was generated based off of a DEM created from 2-ft (0.6-m) LiDAR contours of Albany County, New York. This map shows water being channelized from the ice-aligned ridges, into ice-aligned swamps. Additionally it shows the subsurface flow route through Hannacroix Maze and Merritts Cave, resurging at the Merritts Cave entrance. This flow map shows congruence with glacial landforms, and fits the model created by Mylroie and Carew (1987).

The waters entering Hannacroix Maze drain through the cave, and then into Merritts Cave. These waters then either directly exit through the entrance of Merritts Cave (Fig. 3.9a), or continue through bedrock other resurgences. These waters ultimately end up in the same surface stream, which then contributes to Hannacroix Creek.

This flow map shows the connection of Hannacroix Maze, Merritts Cave, and Skips Sewer to the drainage of the area. It reveals an exact connection to the post-glacial deranged drainage, with Hannacroix Maze being directly influenced by floodwaters from a swamp located in a glacial depression. As Merritts Cave drains Hannacroix Maze downstream, Merritts Cave can also be said to be post-glacial in origin.

These results do not directly line up with the model proposed by Mylroie and Carew (1987), but instead show caves on the periphery of features in the model. Instead of waters entering sinkholes, with the waters being controlled by glacial landforms, the waters are entering swamps controlled by ice-flow aligned ridges. This places the caves along the bank of swamps. The placement of these caves in the model is shown in Figure 5.3.

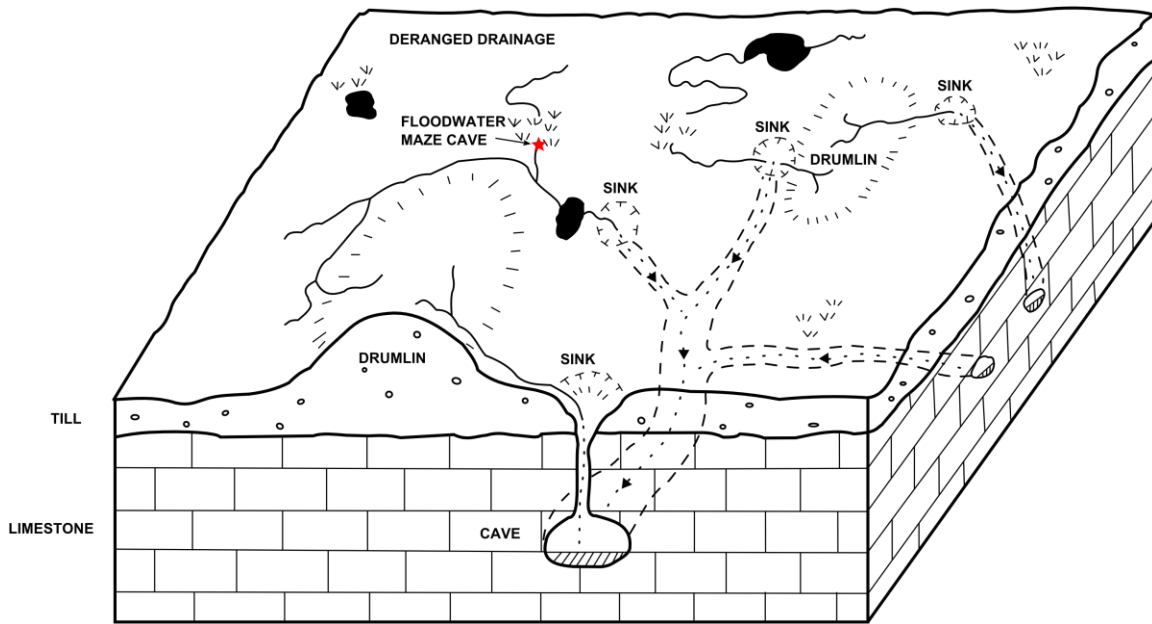


Figure 5.3 Schematic map showing the position of Hannacroix Maze, Merritts Cave, and Skips

Sewer in the original model proposed by Mylroie and Carew (1987).

Possible times of passage formation

For each cave in this study a passage cross-section was sketched and measured, and a cross-sectional area was computed. In cave sketch and measurement data can be found in Appendix B along with computations of cross-sectional area. Table 5.1 lists areas measured and calculated for each cave visited, as well as their times of formation.

Table 5.1 Time of glacial retreat and cross-sectional areas for each cave measured in this study.

Cave	Time Since Glacial Retreat (ka)	Width (cm)	Height (cm)	A - Calculated (cm ²)	A - Box (cm ²)	A - Measured (cm ²)
Hannacroix Maze	16.2	177	137	11472	24249	15246
Merritts Cave	16.2	92	373	24913	34316	25217
Big Loop Cave	15.2	136	244	22374	33184	21141
Barber Cave	17.4	37	149	2607	5513	4774
Glen Park Labyrinth	13.8	200	287	35689	57400	44227

Calculated cross-sectional areas are based on Equation 4.1. Box cross-sectional areas are obtained by multiplying width and height. Measured cross-sectional areas are measured with the image analysis program ImageJ by setting a scale and using the measurement tool on the area.

Using the widths and Equation 4.2 a series of plots and calculations were performed for comparison with the time of retreat for each area. If these times calculated are less than the time since glacial retreat, it is a possibility that these caves have formed entirely since this glaciation.

Hannacroix Maze

The phreatic tube in Hannacroix Maze (Fig. 5.4) has a maximum observed width of 177 cm, and a time since glacial retreat of 16.2 ka (Fig. 2.15) (Ridge 2004).

Calculations based on Equation 4.2 produce the plot in Figure 5.5, and the calculated times in Table 5.2.

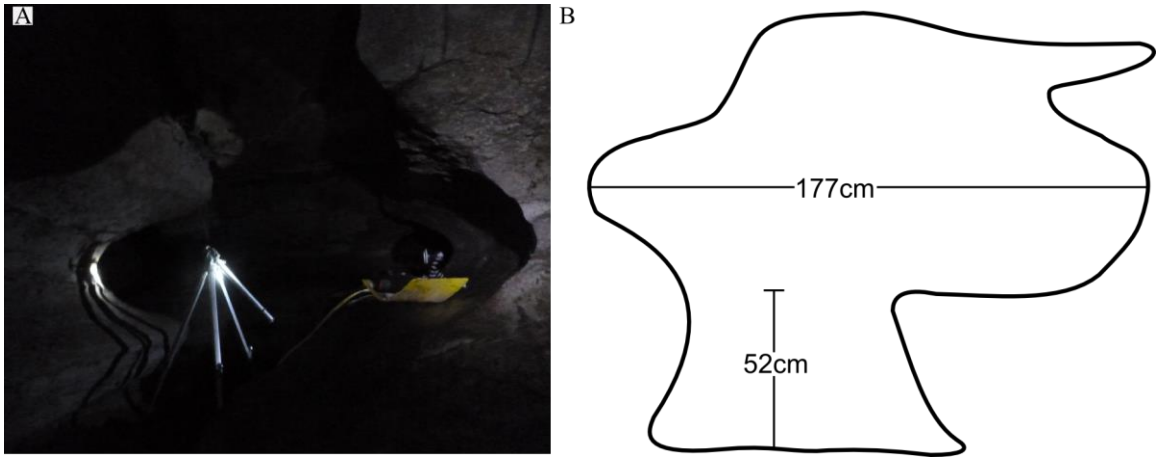


Figure 5.4 (a) Photograph of the cross-section of Fungus Footpath of Hannacroix Maze. (b) Transformed cross-section of Fungus Footpath from sketch and measurement data.

Original sketch and measurement data is located in Appendix B.

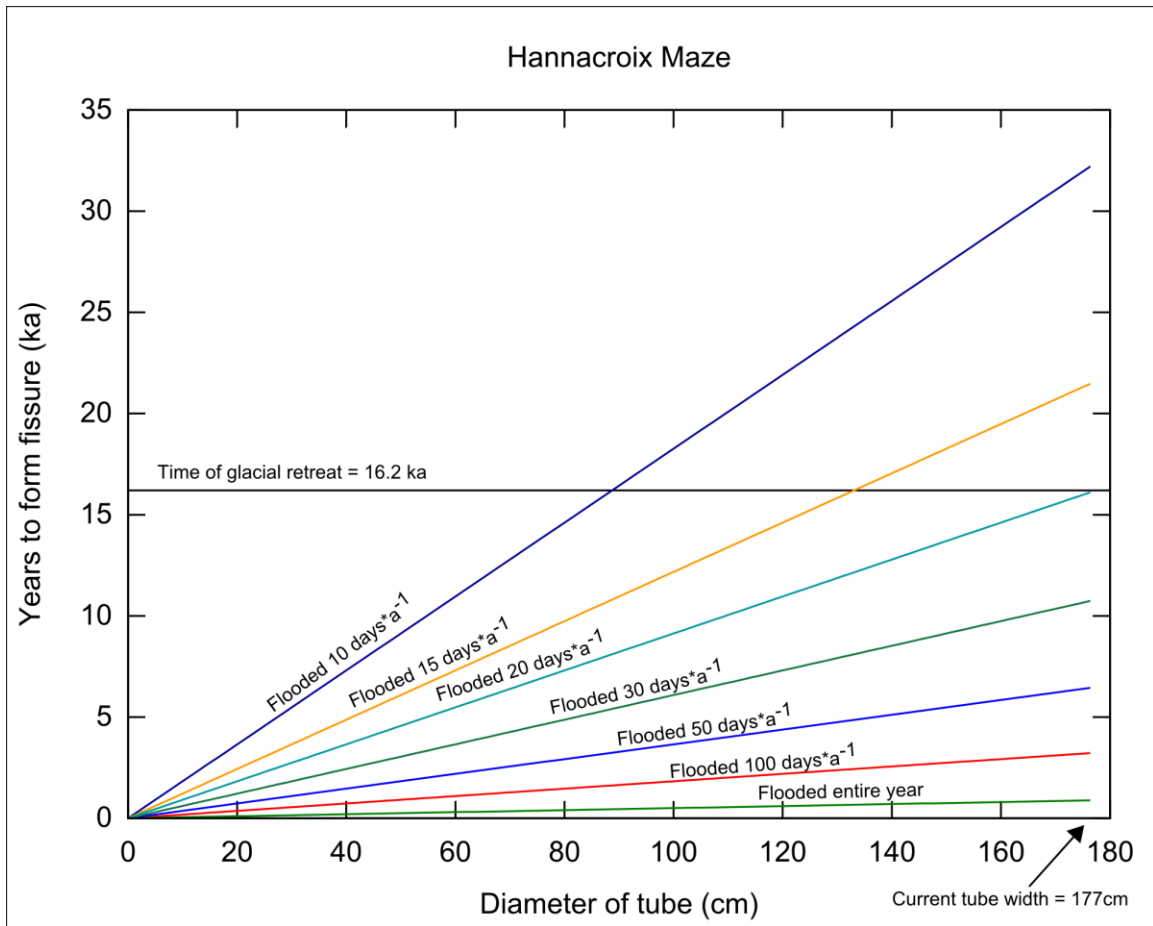


Figure 5.5 Plot of diameter of tube versus time to form at varying conduit-full days per annum for Hannacroix Maze.

Note that 20 conduit full days per year produces nearly exactly 16.2 ka, indicating a possible mean time per annum spent in conduit full conditions.

Table 5.2 Calculated times to form the current passage width in Hannacroix Maze depending on days in conduit full conditions.

Days in Conduit Full Condition	Time to form Passage
365.25	0.89
100	3.23
50	6.46
30	10.77
20	16.16
15	21.55
10	32.32

The results from these calculations show that at 20 conduit-full days per annum Hannacroix Maze could form to its current dimensions in 16.2 ka, less than the time since glacial retreat. While this cave may see this amount of conduit-full days per year on some years, the higher discharges during glacial retreat could produce an average over this time span of 20 conduit-full days per annum, giving a time window for this cave to form in less than the time since glacial retreat. To show a possible path of growth for this cave, the modeling method was used generating a plot shown in Figure 5.6. Factors for this model include the time a larger lake than the current swamps inundated the outcrop, and larger times in conduit-full conditions during draining of this lake, with full conditions of the lake for 400 years, and 600 years of 30 to 50 conduit-full days per annum. The remaining conduit-full days per annum reflect current conditions of 5 to 15 days. The width generated with the parameters of this model is 176.3 cm. This model only represents possible conditions, and leaves out any mechanical processes.

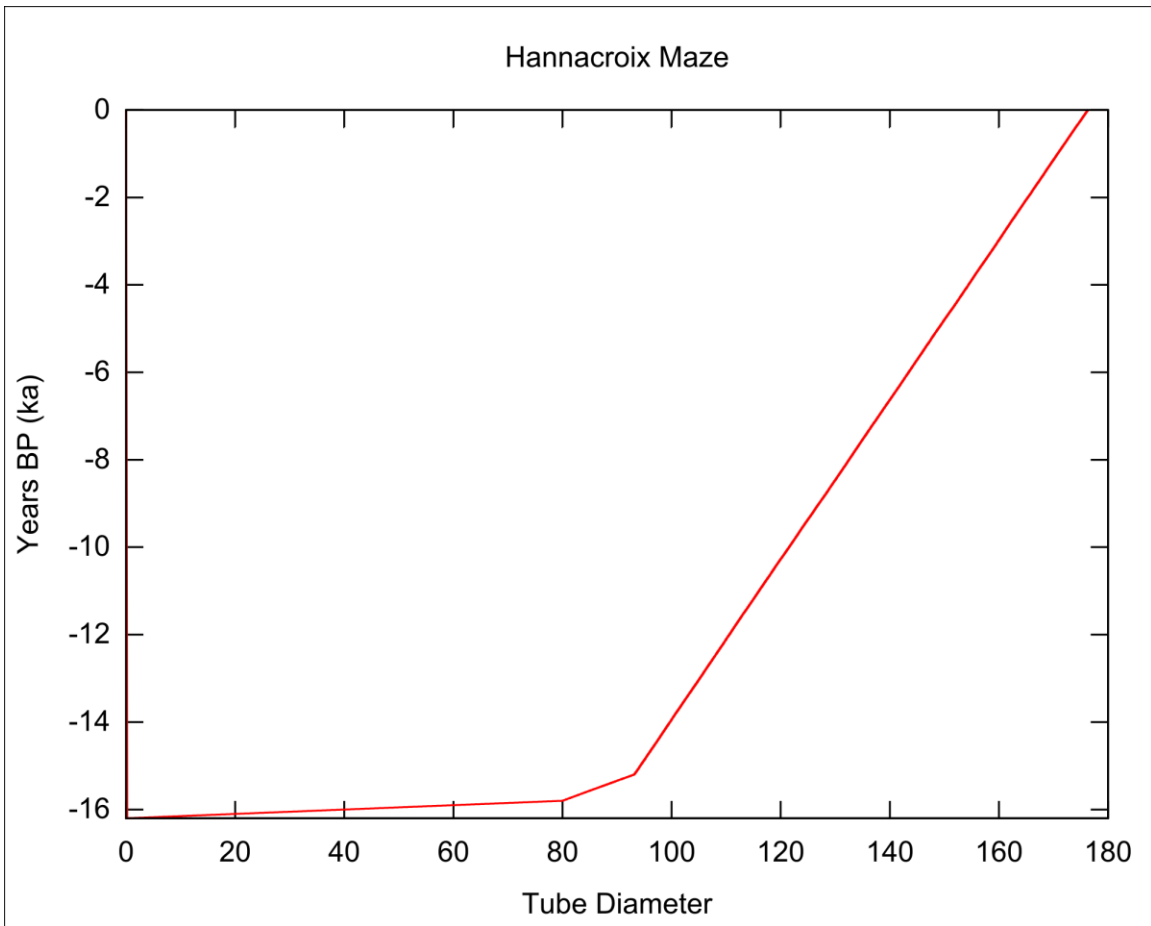


Figure 5.6 A model of possible growth path for Hannacroix Maze.

The first slope is rapid growth due to inundation by a lake. The next slope represents wetter climate (30—50 days in conduit-full conditions per annum). The final slope represents current conditions of 5—15 conduit-full days per annum. This path produces a passage width of 176.3 cm.

Merritts Cave

The maximum observed fissure width for Merritts Cave is 72 cm (Fig. 5.7), and the time since the glaciers retreated in this area is 16.2 ka (Fig 2.15) (Ridge 2004).

Calculations give the plot in Figure 5.8, and the calculated times in Table 5.3.

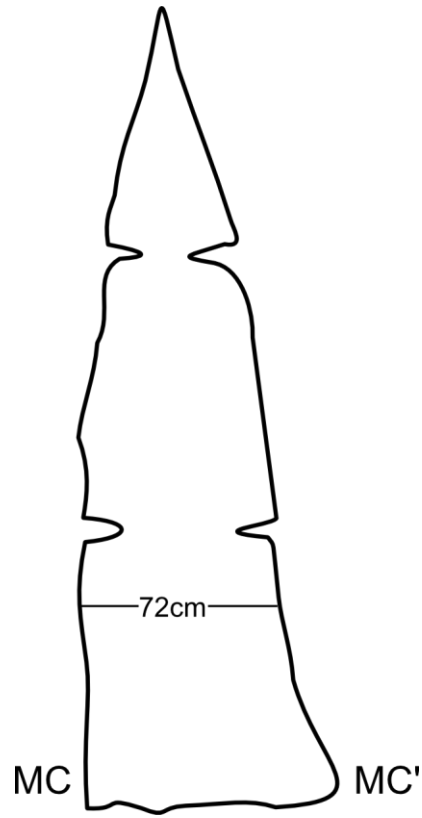


Figure 5.7 Transformed cross-section MC-MC' (Fig. 4.8) in Merritts Cave.

Intrusions of bedrock into the passage are non-soluble chert. Original sketch and measurement data is available in Appendix B.

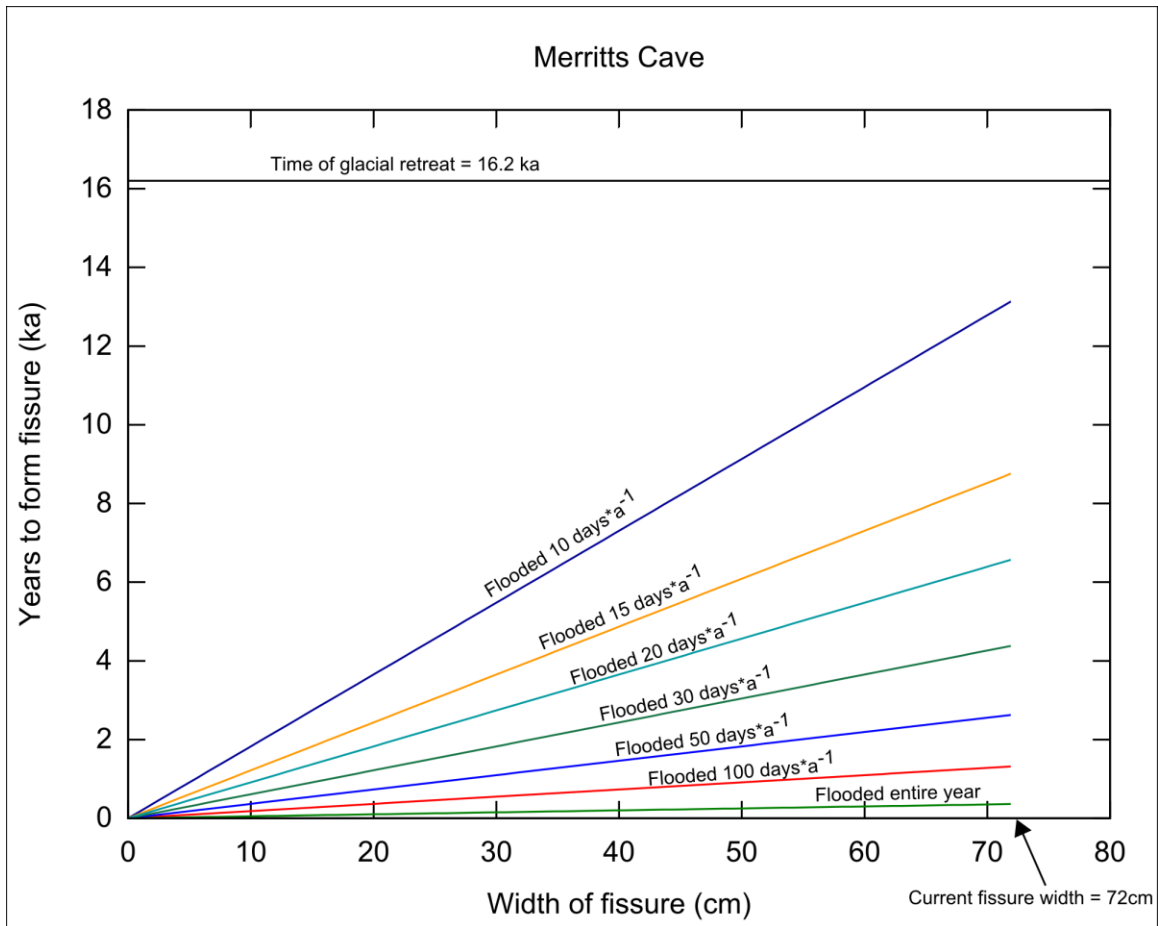


Figure 5.8 Plot of width of fissure versus time to form at various conduit full days per annum for Merritts Cave.

All conduit full days per annum ratios plotted produce the current fissure size in under the amount of time since glacial retreat. The current activity of this cave, its position in the deranged drainage, and the time to form are all evidence of post-glacial origins.

Table 5.3 Calculated times to form the current passage width in Merritts Cave depending on days in conduit full conditions.

Days in Conduit Full Condition	Time to form Passage
365.25	0.36
100	1.31
50	2.63
30	4.38
20	6.57
15	8.77
10	13.15

Note that these times are less than that of Hannacroix Maze, even though the two caves are connected hydrologically.

From calculations in Table 5.3 Merritts Cave could form to its current size in 13.2 ka with 10 conduit-full days per year. This amount of conduit-full days has been observed directly in the field, including with waters to a depth of 30 cm outside the entrance of the cave (Fig. 3.9). After snowmelt this cave experiences several days of conduit-full conditions, and after large rain events this cave can also experience a day or more of conduit-full conditions. Field observation of current show 15 to 20 conduit-full days per annum shows a probable path of this cave growing in the time since glacial retreat.

Barber Cave

The observed fissure width for Barber Cave is 37 cm (Fig. 5.9), and the time since glacial retreat in this area is 17.4 ka (Fig. 2.15) (Ridge 2004). Equation 4.2 gives the plot in Figure 5.10 and calculated times in Table 5.4.

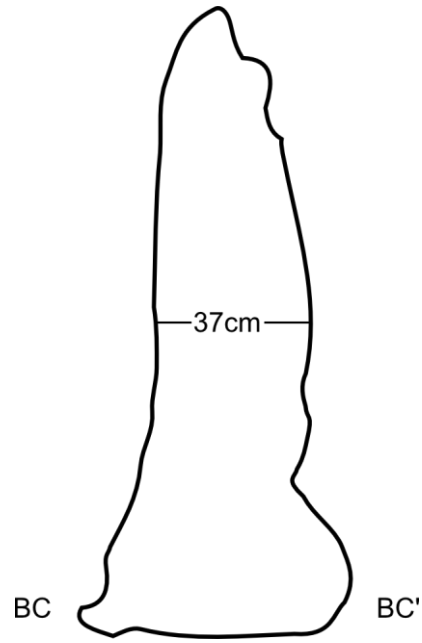


Figure 5.9 Transformed cross-section along BC-BC' in Barber Cave showing fissure shaped passage.

Original sketch and measurement data are available in Appendix B.

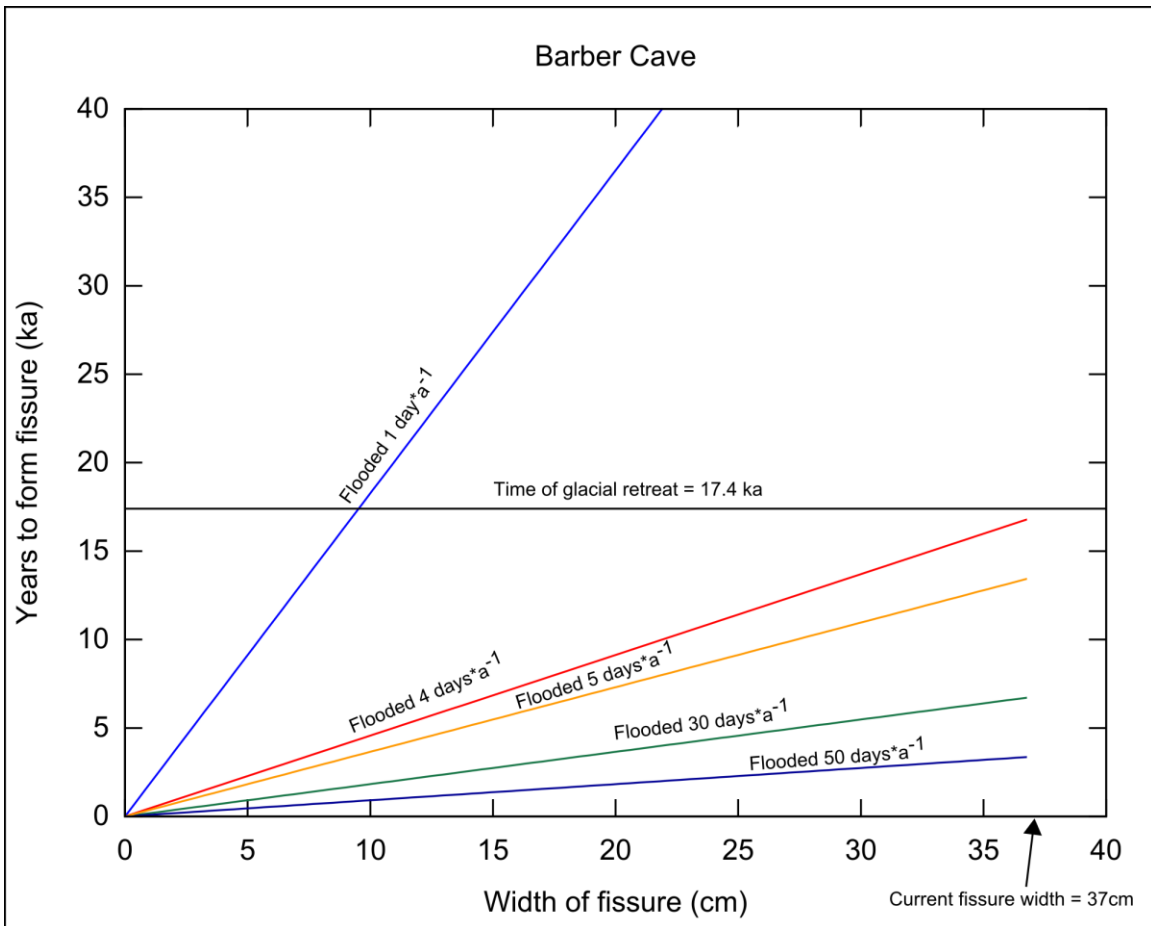


Figure 5.10 Plot of width of fissure versus time at various conduit-full days per annum for Barber Cave.

This cave rarely experiences conduit-full conditions; however during past conditions it may have experienced a greater amount of conduit full days.

Table 5.4 Calculated times to form the current passage width in Barber Cave depending on days in conduit full conditions.

Days in Conduit Full Condition	Time to form Passage
50	1.35
30	2.25
5	13.51
4	16.89
3	22.52
1	67.57

Calculations in Table 4.4 show the passage in this cave could have formed in less than 17.4 ka with mean conduit-full days per annum of four. Under current conditions this cave experiences four conduit-full days per annum rarely, with the usual occurrence of one day. While this is the case, this cave likely received more conduit-full days per annum prior to the downcutting of the gully it is located near, and during the time after glacial retreat. Extrapolating longer conduit-full days per annum is modeled in Figure 5.11.

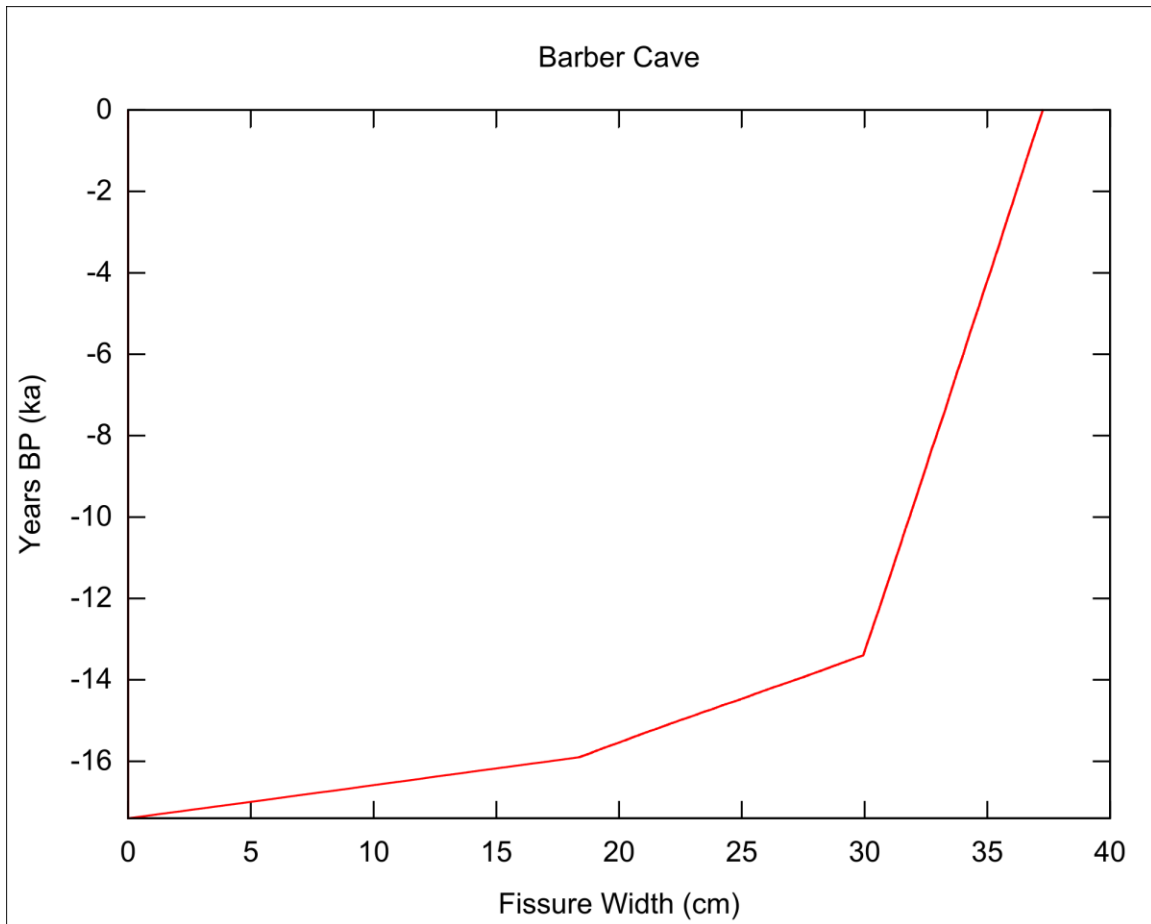


Figure 5.11 Model for one path of Barber Cave growth.

This model uses 15—30 days (similar to other maze caves in this study that are completely congruent with current drainage) for initial conduit-full days per annum, 2—15 days (when lower flood stages would inundate the cave) for the second slope, and 0—2 days (current conditions) for the third. This projects growth of 37.2 cm in the time since retreat.

Big Loop Cave

Big Loop Cave has a fissure width of 136 cm (Fig. 5.12), and a time since glacial retreat of 15.2 ka (Fig. 2.15) (Ridge 2004). Equation 4.2 gives the plot in Figure 5.13 and calculated times in Table 5.5.

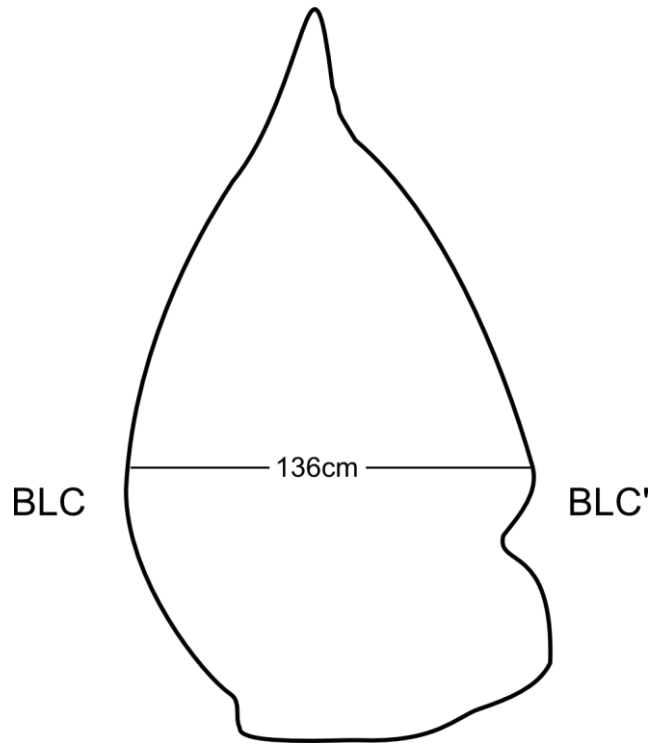


Figure 5.12 Transformed cross-section of Big Loop Cave along BLC-BLC'.

This cross-section shows the shape of the passage of this cave being within the continuum of phreatic tube and fissure passage. Original sketch and measurement data are available in Appendix B.

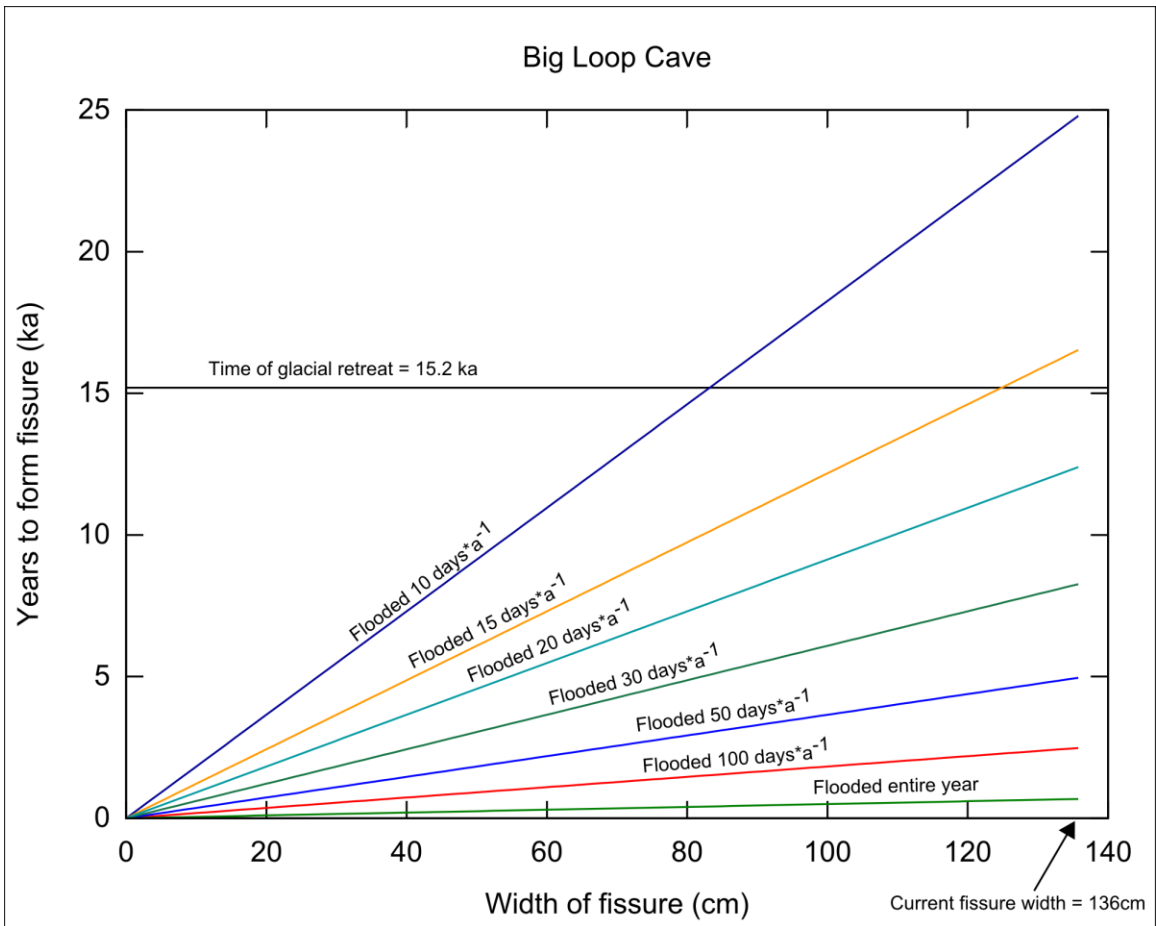


Figure 5.13 Plot of width of fissure versus time at various conduit-full days per annum for Big Loop Cave.

Table 5.5 Calculated times to form the current passage width in Big Loop Cave depending on days in conduit full conditions.

Days in Conduit Full Condition	Time to form Passage
365.25	0.68
100	2.48
50	4.97
30	8.28
20	12.42
15	16.56
10	24.84

The calculations in Table 5.5 show that the passage within Big Loop Cave could form in less than 15.2 ka with 20 conduit-full days per annum. This ratio is current observed, and occurs during snowmelt and large rainfall events. The sinking stream entering this cave regularly fills to the ceiling during these events, emplacing organic debris within the cave.

Glen Park Labyrinth

Glen Park Labyrinth has the largest cross-sectional area of any of the maze caves in this study (Table 5.1), and is the most extensive maze cave known in New York. The fissure width is 201 cm for this cave (Fig. 5.14), and glacial retreat in this area occurred between 14.15–13.8 ka BP (Fig. 2.15) (Ridge 2004). Additional limits to the time of formation are due the caves current relict position at 18-meters above the current position of the Black River. As the Black River is post-glacial in this area the incision rate is between 0.127–0.130 cm a^{-1} . Equation 4.2 gives the plot in Figure 5.15 and the calculated times in Table 5.6.

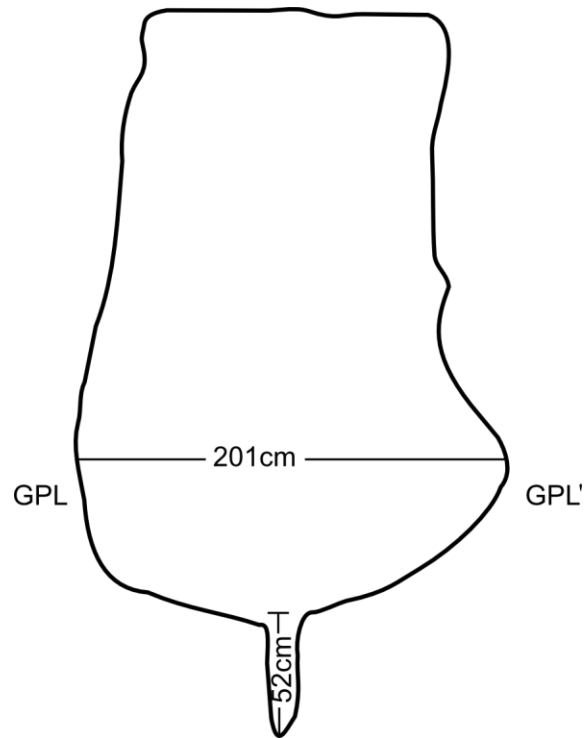


Figure 5.14 Transformed cross-section along GPL-GPL' in Glen Park Labyrinth.

This cross-section shows a phreatic fissure with a vadose canyon downcut into it. Original sketch and measurement data are available in Appendix B. This cross-section was taken near an entrance, and thus had a short flow length (L), allowing it to enlarge more rapidly than the rest of the cave, which has smaller passage cross-sectional areas. Mechanical processes such as breakdown and abrasion also contribute to the larger cross-section.

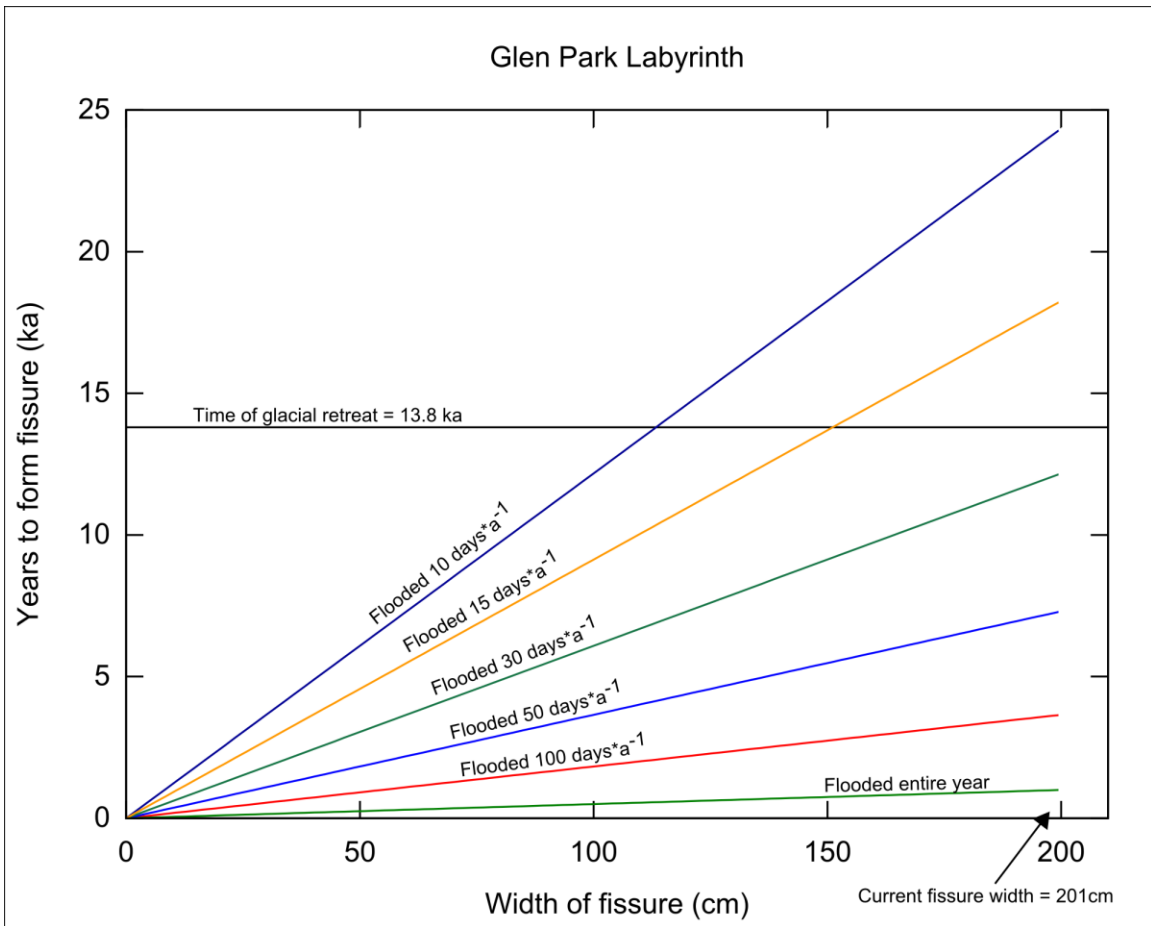


Figure 5.15 Plot of width of fissure versus time at various conduit-full days per annum for Glen Park Labyrinth.

This cave no longer experiences conduit full conditions, but at one point accepted the Black River for large parts of the year prior to incision of the river to its current level.

Table 5.6 Calculated times to form the current passage width in Glen Park Labyrinth depending on days in conduit full conditions.

Days in Conduit Full Condition	Time to form Passage (ka)
365.25	1.01
200	1.84
100	3.67
50	7.34
45	8.16
30	12.24
20	18.35
15	24.47
10	36.71

Highlighted row uses the days in conduit full conditions computed based on current discharge measurements of the Black River compared to the total discharge Glen Park Labyrinth can handle.

From Table 5.6 this cave could have reached its current size with the limitations imposed if exposed to conduit-full conditions at 30 days per annum. Potential time in conduit-full conditions can be extrapolated by comparing current discharges and maximum discharges supported by the conduits.

Using the method to find total discharge, a measurement perpendicular to the passage of Glen Park Labyrinth (Fig. 5.16) shows eight passages per 44 meters (a ratio of 0.182 passages per meter). Measurement on the topographic map shows a total possible range at the elevation of the current cave of 102 meters (where it is bound by the furthest extent of mapped passage and extrapolated across the current river channel at 106-m amsl, or above mean sea level). From this the greatest number of parallel passages is 18 (multiplication of the ratio to 102 meters produces 18.55 passages, but partial passage is nonsensical). As the cross-section in Figure 5.4 is the maximum observed cross-section, a different cross-section is computed based on the mean passage width measured along the

traverse in Figure 5.16 (1.49 m) and passage shape of the majority of passage (Fig. 5.17) as 2.95m^2 . Scallops indicating flow velocities up to three meters per second and thus 18 passages of 2.95m^2 can handle 159.3 cubic meters per second. Comparing this number to available USGS stream data (USGS 2013) provides that under the current discharges of the Black River, the cave would be in conduit-full conditions at a minimum of 45 days per year and be formed in 8.16 ka if this was the case. This number is a minimum as 45 days is actually the number where water exceeds what the passage can handle, with extra days possible. Additionally, damming of upstream lakes for reservoirs, and canals impacts the compared data (USGS 2013). A change of even one day in conduit-full conditions per annum can reduce the time of formation of this cave by hundreds of years.

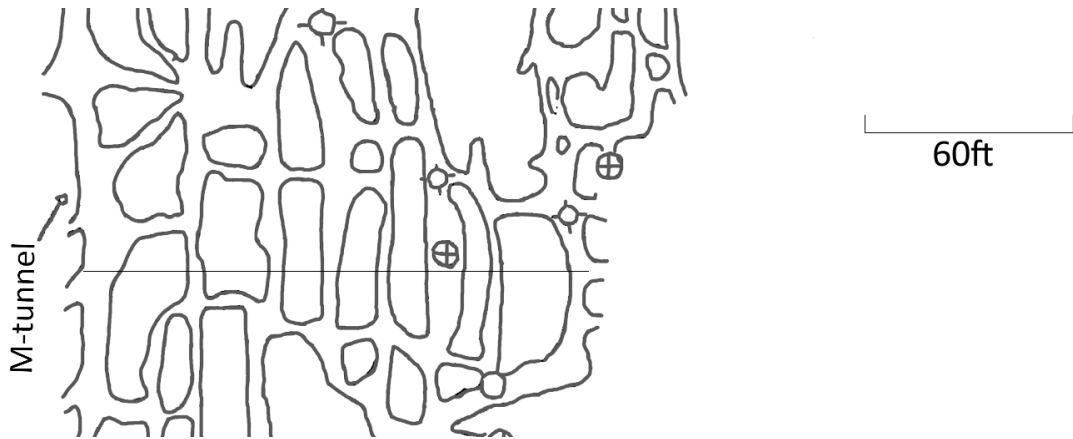


Figure 5.16 Map section of Glen Park Labyrinth with line indicating where passages were counted and measured for extrapolation across the channel.

Modified from Carroll (1972).

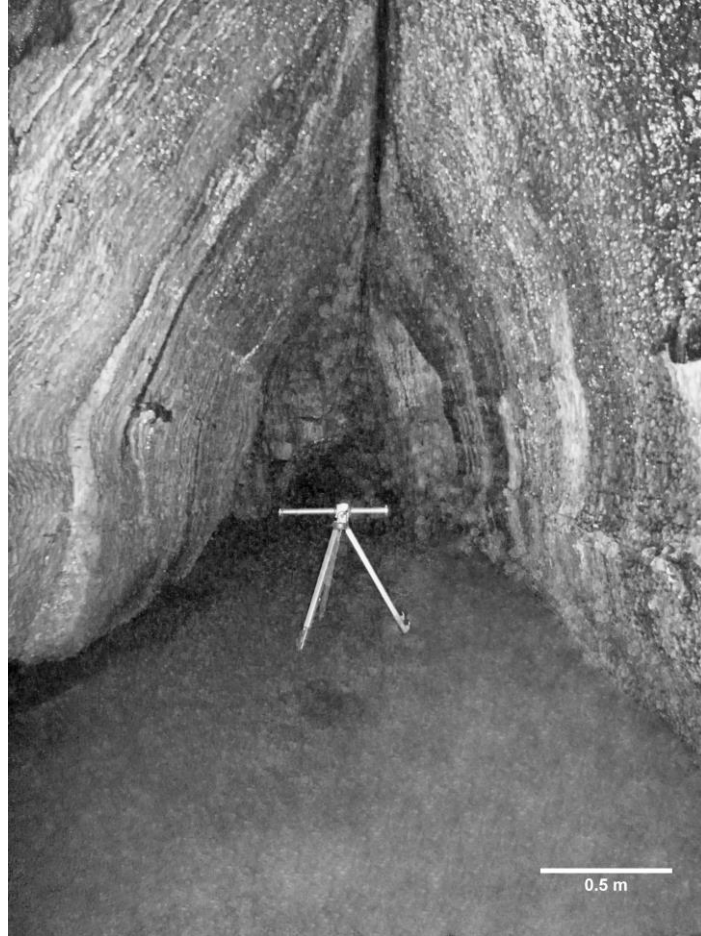


Figure 5.17 Photograph showing typical passage cross-section in Glen Park Labyrinth. The scale bar in this photograph represents scale along the depth at the tripod crossbar.

The relict condition of this cave imposes further boundaries, as floodwaters even at the highest discharges of the Black River cannot reach Glen Park Labyrinth. The largest discharge recorded by the USGS stream gage produced a stage height of 4.9m. As the floor of the main level of the cave is within 6 meters of the surface, with a ceiling height of 2.1 m for most passages (Fig. 5.17), the cave could only experience conduit-full conditions until the Black River incised to 8.5 meters. This limits a time window to around 6500 ka of formation; requiring 56.5 conduit-full days per annum to form (by

solving Eq. 3.2). This cannot occur with current conditions, but by modeling previous conditions such as inundation by Lake Iroquois, and higher rates of discharge associated with draining of the lake and prior to damming lakes for reservoirs (Fig. 5.18). This model gives the path for the mean widths of cave passages, and not for the maximum seen in Fig. 5.16.

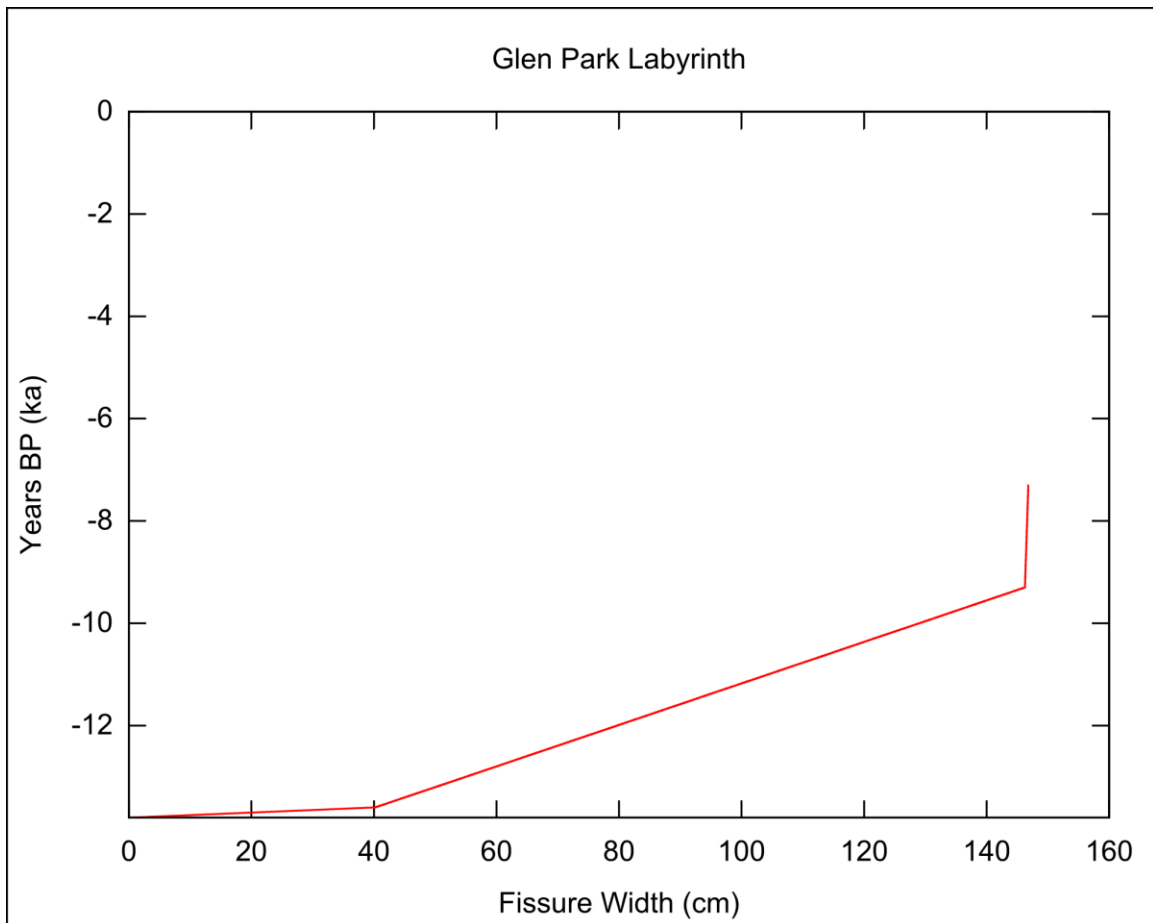


Figure 5.18 Model of possible growth path of Glen Park Labyrinth.

This model shows growth of mean passage width, and not the maximum observed passage cross-section width. This model uses a complete year in conduit conditions for the first slope, 40—50 days in conduit-full conditions per annum, and 0—1 days for the third, after river incision goes below the cave level.

CHAPTER VI

DISCUSSION

Verification of the post-glacial cave origin model

The model proposed by Mylroie and Carew (1987) (Fig. 2.12) hypothesizes that a cave can be shown to be post-glacial if it is completely controlled by glacial landforms, and thus can be said to post-date these landforms. The proposed schematic diagram in Figure 2.12 shows this, with water being channelized off of glacial landforms such as drumlins, movement through post-glacial deranged drainage, and into sinkholes to form a cave.

Fieldwork performed in this study verified water being channelized into the deranged drainage, and into caves. The path however, is different from the schematic diagram of Mylroie and Carew (1987). The path still takes route off of landforms that would only be exposed post-glacially (in this case ice-aligned ridges), and into deranged drainage. For the case of the caves studied for verification of this model, the placement is located next to the swamps ponded in glacial depressions on the model (Fig. 5.3), as demonstrated by flow analysis of Figure 5.2. Figure 6.1 shows a schematic representation of this in similar style to Figure 2.12.

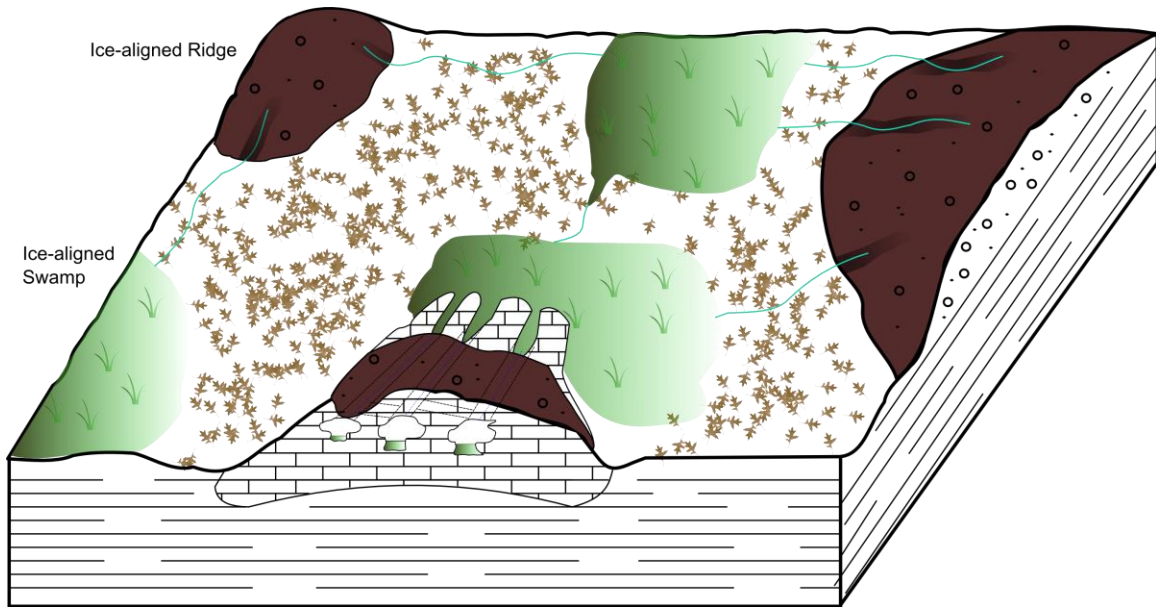


Figure 6.1 Schematic model similar to the model given by Mylroie and Carew (1987).

This model shows Hannacroix Maze in the deranged drainage, with brown till capped ice-aligned ridges and ice-aligned swamps. This cave exists within the ice-aligned swamps and show congruence and agreement with the model.

This study verifies this model, but with a different placement within the deranged drainage. It is possible that a karst terrain is currently analogous to the representation on Figure 2.12, however as this study focused on maze caves, this aspect was not observed. This possibility however, could be the case for Tetanus Shot Cave in the Joralemon Park karst area, and any passage existing between the sinkhole and the karst window of this area (Fig. 3.1).

As maze caves are a special case of caves, requiring maximum chemical enlargement, these demonstrate that enterable cave is possible, producing cross-sectional areas up to $4.4 \times 10^4 \text{ cm}^2$ (Table 5.1) in a time window less than that since the time since glacial retreat (Fig. 5.18). A question for the representation in Figure 2.12 then can be posed as follows: are there enterable post-glacial single passage or branchwork caves of

non-floodwater origins that are an explorable size and thus fit the definition of a cave given by Curl (1964)? The methods used herein could be used to model the growth history of such a cave, and field examples searched for.

The combination of time windows for formation less than the time since glacial retreat for the caves (Figures 5.5, 5.6, 5.8, Tables 5.2, 5.3) congruent with deranged drainage at Hannacroix Maze and Merritts Cave (Figures 5.1, 5.2) supports this model, and gives strong evidence to conclude these caves are post-glacial. This allows the assessment of further caves studied to determine if they are of pre-glacial or post-glacial origin.

Potential issues in methods determining post-glacial origins

Use of time plots and calculations

The time plots and calculations used for each of these caves are a simplistic view of mean conditions for the entire development of a cave passage. Conditions after glacial retreat produce larger amounts of precipitation, and meltwaters from glaciers contribute to high discharges and larger wet periods per year. These can be accounted for by modeling such as Figure 5.6, with evolving days in conduit-full condition per annum. This model does not account for handling less discharge when passages have smaller cross-sections, but does show the formation with current size as a boundary condition.

These calculations are also simplistic in the use of wall-retreat rate values. Wall-retreat rates can vary in being both higher, or lower than the 0.1 cma^{-1} used. Colder waters such as those from glacial melt can produce wall-retreat rates of up to 0.2 cma^{-1} , and organic acids such as those found in swamps (and thus affecting caves such as Hannacroix Maze and Skips Sewer) also raise these retreat rates. Lower wall-retreat rates

can also form maze caves as the radius of passage increases, as long as the Q/L ratio is above 0.001 cms^{-1} . The simplistic calculation using a value between the range is therefore appropriate.

An additional consideration for these plots is the boundary condition of time since glacial retreat as the time window to fit within. Relict caves such as Glen Park Labyrinth are further bound by the incision of rivers and change in base level as a result of this incision. These maze caves can only form when passage is near this base level or during high flooding conditions when rivers rise enough to flood the caves. While this is an issue, it can be demonstrated that these caves can form within a time window of river incision (Fig. 5.16, Table 5.6).

Sample size

The sample size of this study cannot establish statistical distribution showing that most/all maze caves in glaciated areas post-glacial. This was limited by the time available for study, and cave accessibility. While statistical analysis cannot be performed to a high significance, the caves visited fit into end-member conditions allowing a conclusion to this question. These end-members are one cave that appears relict for most of the year, only receiving water at extreme conditions (Barber Cave); three caves congruent with current drainage (Hannacroix Maze, Merritts Cave, Skips Sewer); one cave in marble (Big Loop Cave); and a completely relict cave located adjacent to an 18 meter gorge with the smallest time window since glacial retreat (Glen Park Labyrinth).

Time discrepancy between Hannacroix Maze and Merritts Cave

The time plots for Hannacroix Maze (Figs. 5.5, 5.6) and Merritts Cave (Fig. 5.8) show a discrepancy between the times of formation of two currently hydrologically connected caves. The current passage width of Merritts Cave is smaller than that of Hannacroix Maze, with the same time window to form in. An additional complication of this outcome is the time in which these caves currently experience conduit-full conditions, as Merritts Cave experiences conduit-full conditions more days per annum.

This discrepancy can be explained in several ways. One such explanation is a longer breakthrough time for Merritts Cave. If these caves were not completely initiated by isostatic rebound and tectonics, then Merritts Cave has a longer flow length to begin initiation. Additionally, a decrease in hydraulic head due to distance from the lake originally inundating Hannacroix Maze would change breakthrough times. One further explanation is the creation of inefficiencies in Hannacroix Maze. A similar condition to this situation is the formation of mazework superimposed on Skull Cave due to blockages by glacial material (Fig. 2.11). As Hannacroix Maze became larger, this would allow more and larger material to pass through it. This material could move through and create inefficiency, thus superimposing another maze cave on a preexisting maze cave.

Post-glacial origins of maze caves in glaciated areas

Each cave in this study can be evaluated by the criteria of Table 2.2 to be pre-glacial, sub-glacial, or post-glacial in origins.

From the methods used in this study it can be concluded if the maze caves evaluated are post-glacial. Hannacroix Maze, Merritts Cave, and Skips Sewer are congruent with the current drainage regimes of their locations, with glacially created

landforms completely controlling them. These caves also have cross-sectional areas that are possible to form in a time less than that of the time since glacial retreat (Figs. 5.5, 5.8), strongly suggesting post-glacial origins. While Hannacroix Maze contains glacial sediments, these could have been emplaced here during flooding or from the exposed till cap at the ceiling of the cave, and does not negate a post-glacial origin of this cave.

Barber Cave appears relict, though fits in the current drainage during high flooding conditions. Prior to the downcutting of the gully to which Barber Cave is adjacent, this cave likely received conduit-full conditions for a greater amount of time, allowing the mean days in conduit-full conditions per annum to be greater than current. A higher mean time supports the time window of development less than that of the time since glacial retreat in this area (Fig. 5.11), giving support to post-glacial origins of this cave.

Big Loop Cave accepts a sinking stream within the deranged drainage of the Adirondack Park, and has no indication of adjustment to this deranged drainage from a previous drainage regime. Current observed days in conduit-full conditions per annum could form this cave within the time window since the glacial retreat in that area. Flooding can easily have transported sediment within this cave, as large trees have also been emplaced here. The congruence with current drainage and formation time possible within the time window since last glaciation strongly suggests a post-glacial origin of this cave.

Glen Park Labyrinth is completely relict in the current hydrology of the Black River. While the Black River near this cave does not appear to be part of deranged drainage, it is fed by streams with deranged patterns. The apparent non-congruence with

deranged drainage however is not an issue with this cave; as the channel of the river itself is post-glacial in origin due to cross-cutting a pre-glacial drainage divide. Without the Black River being in this location, there would be no cave, requiring Glen Park Labyrinth to be post-glacial. While the discussion on this could immediately end due to the cave being controlled by a post-glacial channel, the cross-sectional area should be discussed as it provides calibration for other maze caves in this study, and extrapolation of post-glacial origins to other maze caves in glaciated areas. As Glen Park Labyrinth is the most extensive known maze cave in New York, and has the largest cross-sectional area, this cave provides an end-member for these maze caves. This cross-section can be established within the time since glacial retreat (Figs. 5.15, 5.17), thus lending evidence that caves with smaller cross-sections could have formed since retreat.

As previously discussed, the sample size of this study limits the statistical conclusions that can be made about the majority of maze caves in glaciated areas as being post-glacial in origin. While this is the case, both a cave that is currently only in conduit-full conditions for a maximum of one or two days per annum (Barber Cave), and the maze cave with the largest cross-sectional area (Glen Park Labyrinth) can form in the time since glacial retreat. That these caves form post-glacially give end-members of the possible maze caves that can be studied. This study shows that the spectrum in between these can form post-glacially, and thus a conclusion can be reached that a majority of maze caves in glaciated areas of New York are post-glacial in origin.

Time and maze caves

Transience of maze caves in glaciated areas

Of careful note throughout this study has been the depth and surface geology of maze caves. Each of the caves in the study had ceilings within the first 10 meters of the surface, with many ceilings only existing at 1 to 3 meters depth. Observations of the surficial geology at each study area show limestone pavements with dissolutionally enlarged joints. Caves such as Hannacroix Maze, Merritts Cave, Skips Sewer, and Glen Park Labyrinth have entrances directly in these joints.

Karst terrains have several factors of time limitations for caves, including both chemical and mechanical weathering. The shallowness of the caves in this study further limit the time they are within the landscape. Denudation is a direct reduction of a topographic soluble surface through dissolution, and can remove caves over large time periods. Figure 6.2 shows a chart of denudation rates in mm ka^{-1} as a function of climate type and precipitation minus evapotranspiration (White 1988). Another chemical process affecting the transience is the formation of passages in these caves themselves. As seen in Hannacroix Maze, dissolution can occur all the way up to an insoluble surface, in this case, consolidated glacial till (Fig. 3.12a).

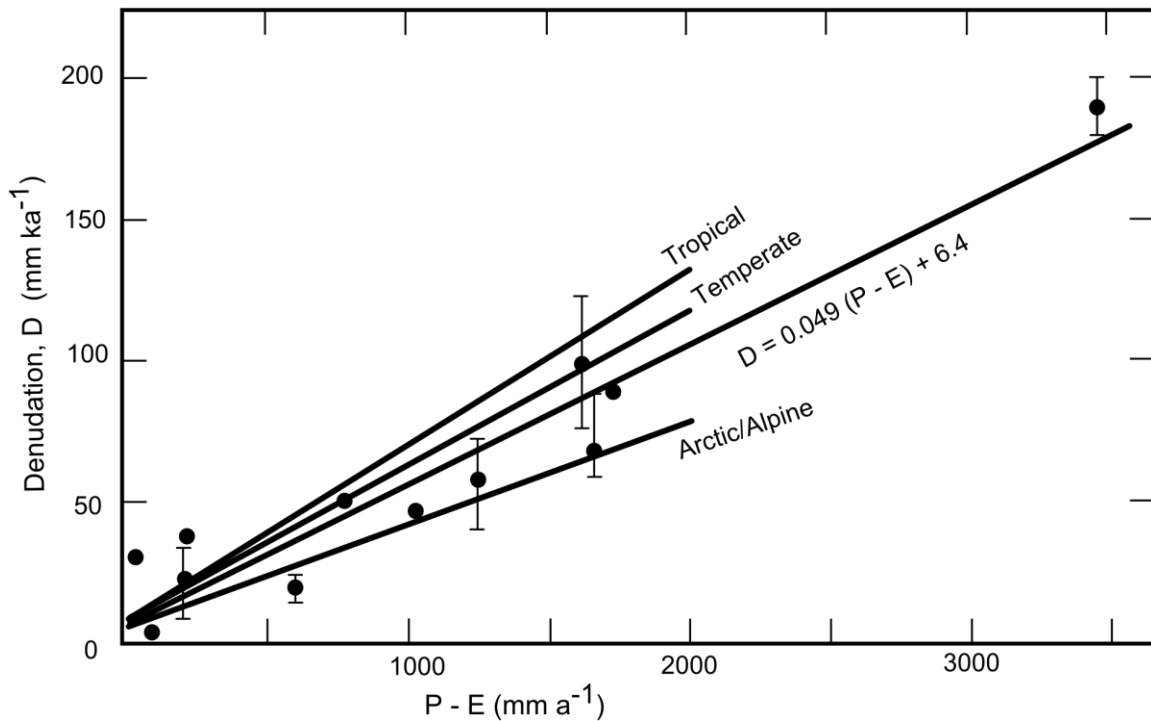


Figure 6.2 Denudation rates as a function of climate type and precipitation minus evapotranspiration.

For temperate climates (typical of New York, and other previously glaciated regions) denudation can be up to 125 mm ka⁻¹. At the maximum rate denudation could remove shallow caves in as little as 10—20 ka. Redrawn from White (1988).

Glaciations have dramatic mechanical effects on all terrains, including karst terrains. Glacial quarrying removes large amounts of surface material, and enhances jointing. Surficially exposed limestone joints can be enlarged chemically, and therefore are very vulnerable to quarrying. With maze caves being associated with jointing, this can enhance their removal during glacial periods, affecting their transience. Compared to denudation, this can occur rapidly with introduction of glaciers in an area. Interglacial times can last 20 ka, with ice advance after the onset of further glaciation. This 20 ka window allows surface denudation above these maze caves, but rates are limited in the

study areas to a maximum of around 50 mm ka^{-1} , where precipitation minus evaporation is highest (near Big Loop Cave). The limited time window therefore does not allow enough surface denudation to reach the ceilings of the maze caves, and thus the dominant limitation on the time of maze caves in glaciated areas are the glaciation events. Though glacial quarrying removes larger amounts of material, some maze caves of large extent (such as Glen Park Labyrinth) could leave relict, truncated passage in the terrain.

Rapidity of growth

The caves visited in this study show time limitations for their growth, especially in the case of Glen Park Labyrinth. Glen Park Labyrinth has a cross-sectional passage area in some places as high as 4.4 m^2 . While not as dramatic as pre-glacial cave cross-sectional areas seen elsewhere in glaciated karst terrains, this cross-sectional area has set limits in the time to form that can be measured. The cross-sectional area for Glen Park Labyrinth is not only bound by the time since the last glaciation, but also of its relict position. The time limitation for the formation of this cave can be estimated at less than 7 ka. Even at current discharges of the Black River, this cave could form in less than 9 ka. This rapid growth is due to the enlargement of joints due to rebound and associated tectonics after glaciation, and the large wall-retreat rates associated with maze caves.

This study therefore shows a rapid process on geologic timescales. In areas that are not glaciated maze caves can form rapidly, become relict, and then be untouched by large mechanical weathering processes. These caves can then persist into millions of years, but the actual formative processes only requiring on the order of thousands to tens of thousands of years.

Similar time limitations of growth exist in other karst terrains. These time limitations can include changing base level, and position of sea level. Mylroie and Carew (1987) discussed this with caves in young, eogenetic rocks being bound by sea level fluctuations. This paper gives tens of thousands of year boundary conditions in which to form the caves presented. Further work has limited the formation of these caves to 9 ka. This limited time has produced voluminous caves with large cross-sectional areas known as flank margin caves. The methods and results presented here show that this rapid development can occur not only in porous eogenetic rocks, but also dense telogenetic rocks.

Future work

Both the methods of this study and the results of this study produce opportunities for further work. This study only looks at maze caves for post-glacial origins. The methods presented here could also apply to branchwork and single conduit caves. Modeling can show the evolution of such passage, though the complexity is greater due to varying wall-retreat rates that are mostly set as constant for maze caves. This could show if enterable and explorable cave passages can be produced in the time since last glaciation.

Determination of discharges that passages can handle can also be further elaborated upon. This method was developed after the fieldwork for this study, and thus had limited data for computation. Scallops in each parallel passage can be measured, along with mean cross-sectional passage areas in each of these passages to determine variability in discharges, allowing quantification of flow behavior through these maze caves.

One further opportunity is the modeling of glacial quarrying affecting maze caves, as joint controlled caves can be quantified by joint spacing, porosity, and depth and can be modeled for probability of removal.

CHAPTER VII

CONCLUSIONS

A model proposed by Mylroie and Carew (1987) suggested that post-glacial caves would be controlled by glacial landforms such as drumlins, with caves being congruent with deranged drainage. This model had not been tested since the hypothesis was proposed. Maze caves offered an opportunity to demonstrate this model, as the retreat rates required to form these caves produce explorable dimensions in the time since deglaciation. Shallow depths further allow entrances to form within this timeframe.

Using GIS analysis, this model was verified for the maze caves Hannacroix Maze, Merritts Cave, and Skips Sewer. The GIS analysis showed water being channelized into deranged drainage from glacially aligned ridges that would not exist without the prior glaciation. These caves are additionally controlled by floodwaters of a swamp located in a glacial depression. While the location of the maze caves on the schematic diagram proposed by Mylroie and Carew (1987) was not completely demonstrated, these caves show congruence with the post-glacial drainage, and do not have any indication of modification of pre-existing cave. These caves further satisfy the criteria proposed in Table 2.2 to demonstrate post-glacial origins of caves.

An additional hypothesis was proposed that maze caves would be predominantly post-glacial in age for glaciated areas. This hypothesis was proposed due to the shallow nature of epigenic maze caves creating vulnerability to glacial quarrying upon subsequent

glaciation. The methods used herein demonstrated cross-sectional passages areas could be formed in a time since the retreat of the last glaciers for each cave in the study, and that these caves are congruent with either deranged drainage or post-glacial channels. While the caves visited do not produce a statistical conclusion to this hypothesis, end-members were observed in the form of a cave that only experiences conduit-full conditions a limited time per year, and the most extensive maze cave in New York with the largest cross-sectional area being able to form in the time since glacial retreat. The spectrum between these end-members should therefore also be able to form post-glacially, allowing it to be concluded that a majority of maze caves in glaciated regions (that are not protected and relict at high elevations, such as the maze caves in the stripe karst of Norway) are post-glacial in origin.

A final conclusion to be made is that these maze caves are not likely to survive future glaciation. Fieldwork demonstrated shallow depths for each maze cave in the study, with jointing leaving these vulnerable to quarrying by future glaciation.

REFERENCES

- Adams, C.S., Swinnerton, A.C., 1937, The solubility of limestone: *Transactions of the American Geophysical Union*, v. 11, p. 504–508
- Baker, V.R., 1973, Geomorphology and hydrology of karst drainage basins and cave channel networks in East Central New York: *Water Resources Research*, v.9, p. 695–706
- Baker, V. R., 1976, Hydrogeology of a cavernous limestone terrane and the hydrochemical mechanisms of its formation, Mohawk River Basin, New York: *Empire State Geogram*, v. 12, p. 2–65
- Carroll, R.W., 1969a, Discovery and Mapping of Tunnel-Rat Special at Glen Park: *The Northeastern Caver*, v. 1, no. 8, p. 95
- Carroll, R.W., 1969b, Map of Three Falls Complex and Commercial Cave, Glen Park, NY: *The Northeastern Caver*, v. 1, no. 10, p. 118
- Carroll, R.W., 1972, Some Recommended Caves for the Fall NRO: *The Northeastern Caver*, v. 3, no. 9, p. 115
- Choquette, P.W., Pray, L.C., 1970, Geologic nomenclature and classification of porosity in sedimentary carbonates: *American Association of Petroleum Geologists Bulletin*, v. 54, p. 207–250
- Curl, R.L., 1964, On the Definition of a Cave: *Bulletin of the National Speleological Society*, v. 26, no. 1, p. 1–6
- Cushing, H.P., Fairchild, H.L., Ruedemann, R., Smyth, C.H., 1910, Geology of the Thousand Islands Region: *New York State Museum Bulletin*, no. 145, 194 p.
- Dasher, G.R., 1994, On Station: Huntsville, Alabama, National Speleological Society, Inc., 242 p.
- Dumont, K.A., 1995, Karst hydrology and Geomorphology of the Barrack Zourie cave system, Schoharie County, New York: *Bulletin V of the New York Cave Survey*, 71 p.
- Engel, T. 1989, Big Loop Cave: *The Northeastern Caver*, v. 20, no. 1, p. 31–35

- Engel, T., 2009, New York State: in Palmer, A.N., Palmer, M.V. (Eds.), *Caves and Karst of the USA: Huntsville, Alabama National Speleological Society*, p. 27-32
- Ford, D.C., 1977, Karst and glaciation in Canada, *Proceedings, 7th International Speleological Congress*, p. 188–189
- Ford, D.C., 1983, Effects of glaciation upon karst aquifers in Canada: *Journal of Hydrology*, v. 61, p. 149–158
- Ford, D.C., 1987, Effects of glaciation and permafrost on the development of karst in Canada: *Earth Surface Processes and Landforms*, v. 12, p. 507–521
- Ford, D.C., Smart, P.L., Ewers, R.O., 1983, The physiography and speleogenesis of Castle Guard Cave, Columbia Icefields, Alberta, Canada: *Arctic and Alpine Research*, v. 15, p. 437–450
- Goldring, W., 1935, Geology of the Berne Quadrangle, New York: *New York State Museum Bulletin no. 303*, 238 p.
- Goldring, W., 1943, Geology of the Cocksackie Quadrangle, New York: *New York State Museum Bulletin no. 332*, 374 p.
- Groves, C.G., Howard, A.D., 1994, Minimum hydrochemical conditions allowing limestone cave development: *Water Resources Research*, v. 30, no. 3, p. 607–615
- Faulkner, T., 2006a, Tectonic inception in Caledonide Marbles: *Acta Carsologica*, v. 35, n. 1, p. 7–21
- Faulkner, T., 2006b, Limestone dissolution in phreatic conditions at maximum rates and in pure, cold, water: *Cave and Karst Science*, v. 33, n. 11, p. 11–20
- Faulkner, T., 2008, The top-down, middle-outwards, model of cave development in central Scandanavian marbles: *Cave and Karst Science*, v. 34, n. 1, p. 3–16
- Faulkner, T., 2009, Speleogenesis in New England marble caves: *Proceedings of the fifteenth International Speleological Congress, Kerryville, USA*, v. 2, p. 855–862
- Harland, W., 1957, Exfoliation joints and ice action: *Journal of Glaciology*, v. 3, no. 21, p. 8–10
- Isacshen, Y.W., Landing, E., Lauber, J.M., Rickard, L.V., Rogers, W.B., 2000, *Geology of New York: A Simplified Account, Second Edition*: Albany, New York, New York State Museum, 294 p.
- Jennings, J.N., 1971, *Karst*: Cambridge, Mass., M.I.T. Press, 252 p.

- Kastning, E.H., 1975, Cavern development in the Helderberg Plateau, east-central New York: *Bulletin I of the New York Cave Survey*, 194 p.
- LaFleur, R.G., 1968, Glacial Lake Albany: in Fairbridge, R.W. (ed.) *Encyclopaedia of Geomorphology*, Reinhold, New York, p. 1295
- Lauriol, B., Ford, D.C., Cinq-Mars, J., Morris, W.A., 1997, The chronology of speleothem deposition in northern Yukon and its relationship to permafrost: *Canadian Journal of Earth Science*, v. 34, p. 902–911
- Lauritzen, S.-E., 1981, Glaciated karst in Norway: *Proceedings, 8th. International Speleological Congress*, Bowling Green, v. 2, p. 410–411
- Lauritzen, S.-E., 1984, Evidence of subglacial karstification in Glomdal, Svartisen, Norway: *Norsk Geografisk Tidsskrift*, v. 38, p. 169–170
- Lauritzen, S.-E., 2001, Marble stripe karst of the Scandinavian Caledonides: An end-member of the contact karst spectrum: *Acta Carsologica*, v. 20, no. 2, p. 47–76
- Lauritzen, S.-E., Mylroie, J.E., 2000, Results of a speleothem U/Th dating reconnaissance from the Helderberg Plateau, New York: *Journal of Cave and Karst Studies*, v. 62, no.1, p. 20–26
- Lauritzen, S.-E., Skoglund, R.Ø., 2013, Glacier Ice-Contact Speleogenesis in Marble Stripe Karst: in *Treatise on Geomorphology* volume 6, Elsevier, p. 363–396
- Muller, E.H., Calking, P.E., 1993, Timing of Pleistocene glacial events in New York State: *Canadian Journal of Earth Sciences*, v. 30, p. 1829–1845
- Mylroie, J.E., 1977, Speleogenesis and karst geomorphology of the Heldeberg Plateau, Schoharie County, New York: *Bulletin II of the New York Cave Survey*, 336 p.
- Mylroie, J.E., 1984, Pleistocene climatic variation and cave development: *Norsk Geografisk Tidsskrift*, v. 38, p. 151–156
- Mylroie, J.E., Carew, 1987, Field evidence for the minimum time for speleogenesis: *National Speleological Society Bulletin*, v. 49, no. 2, p. 67–72
- Mylroie, J.E., Mylroie, J.R., 2004, Glaciated karst: How the Helderberg Plateau revised the geologic perception: *Northeastern Geology and Environmental Sciences*, v. 26, p. 82–92
- Nardacci, M., 1994, The hydrology of the Hannacroix Maze Karst; Albany County, New York: *Northeastern Caver*, v. XXV, no.3, p. 75–83
- Palmer, A.N., 1972, Dynamics of a sinking stream system, Onesquethaw Cave, New York: *National Speleological Society Bulletin*, v. 34, no. 3, p. 89–110

- Palmer, A.N., 1975, The origin of maze caves: *National Speleological Society Bulletin*, v. 37, no. 3, p. 56–76
- Palmer, A.N., 1984, Geomorphic interpretation of karst features in LaFleur, R.G. (Ed.) *Groundwater As a Geomorphic Agent*: Allen and Unwin, Boston, Mass., p. 173–209
- Palmer, A.N., 1991, Origin and morphology of limestone caves: *Geological Society of American Bulletin*, v. 103, p. 1–21
- Palmer, A.N., 2000, Maze Origin By Diffuse Recharge Through Overlying Formations patterns in Klimchouk, A.B., Ford, D.C., Palmer, A.N., Dreybrodt, W. (Eds.), *Speleogenesis: Evolution of Karst Aquifers*: National Speleological Society, Huntsville, Alabama, p. 387–390
- Palmer, A.N., 2001, Dynamics of cave development by allogenic water: *Acta Carsologica*, v. 30, no. 2, p. 13–32
- Palmer, A.N., 2007, *Cave Geology*: Dayton, Ohio, Cave Books, 454 p
- Palmer, A.N., Palmer, M.V., Porter, C.O., Rubin, P.A., and Mylroie, J.E., 1991, A geologic guide to the karst and caves of the Helderberg Mountains, Schoharie and Albany Counties, New York, in Nardacci, M. (Ed.), *Guide to the caves and karst of the Northeast*: Huntsville, Alabama, National Speleological Society, p. 105–167
- Palmer, M.V., 1976, Ground-water flow patterns in limestone solution conduits [M.A. Thesis]: State University of New York at Oneonta, 150 p.
- Rayburn, J.A., Cronin, T.M., Franzi, D.A., Knuepfer, P.L.K., Willard, D.A., 2011, Timing and duration of North American glacial lake discharges and the Younger Dryas climate reversal: *Quaternary Research*, v. 75, p. 541–551
- Ridge, J.C., 2004, The Quaternary glaciation of Western New England with correlations to surrounding areas: *Developments in Quaternary Sciences*, v. 2, p. 169–199
- Rubin, P.A., Engel, T., Nardacci, M., 1995, Geomorphology, Paleoclimatology and Land Use Considerations of a Glaciated Karst Terrain; Albany County, New York: in Garver, J.I., Smith, J.A. (eds.) *Field Trips for the 67th annual meeting of the New York State Geological Association*, p. 81-107
- Ryder, P.F., 1975, Phreatic network caves in Swaledale, Yorkshire: *Transactions of the British Cave Research Association*, v. 2, no. 4, p. 177–192
- Sasowsky, I.D., Bishop, M.R., 2006, Empirical study of conduit radial cross-section determination and representation methods of cavernous limestone porosity characterization: *Journal of Cave and Karst Studies*, v. 68, no. 3, p. 130–136

- Skoglund, R.Ø., Lauritzen, S.-E., 2005, Maze caves in stripe karst: Examples from Nonshauggrotta, northern Norway: *14th International Congress of Speleology*, O-64, 6 p.
- Skoglund, R.Ø., Lauritzen, S.-E., 2011, Subglacial maze origin in low-dip marble stripe karst: Examples From Norway: *Journal of Cave and Karst Studies*, v. 73, no. 1, p. 31–43
- Skoglund, R.Ø., Lauritzen, S.-E., Gabrovšek, F., 2010, The impact of glacier-ice contact and subglacial hydrochemistry on evolution of maze caves: A modeling approach, *Journal of Hydrology*, v. 388, p. 157–172
- Steadman, D.W., Craig, L.J., Engel, T., 1993, Late Pleistocene and Holocene vertebrates from Joralemon's (Fish Club) Cave, Albany County, New York: *Bulletin of the New York State Archaeological Association*
- Stewart, D.P., 1958, The Pleistocene Geology of the Watertown and Sackets Harbor Quadrangles, New York: *New York State Museum Bulletin*, no. 369, 79 p.
- Sweeting, M.M., 1973, Karst Landforms: New York, New York, Columbia University Press, 362 p.
- Tranter, M., 2003, Geochemical weathering in glacial and proglacial environments: in Drever, J.I., (ed.), *Treatise on Geochemistry*, Amsterdam, Elsevier, p. 189–205
- Tranter, M., Brown, G., Raiswell, R., Sharp, M., Gurnell, A., 1993, A conceptual model of solute acquisition by alpine glacial meltwaters: *Journal of Glaciology*, v. 39, no. 11–13, p. 1229–1271
- Twidale, C.R., 2004, River patterns and their meaning: *Earth-Science Reviews*, v. 67, p. 159–218
- United States Geological Survey, USGS Current Conditions for Black River at Watertown, NY: http://waterdata.usgs.gov/ny/nwis/uv?site_no=04260500 (accessed October 2013).
- Weremeichik, J.M., 2013, Paleoenvironmental reconstruction by identification of glacial deposits, Helderberg Plateau, Schoharie County, New York [M.S. Thesis]: Mississippi State University, 171 p.
- Walther, A.C., 1974, The limestone and caves of North-west England: Newton Abbot, U.K., David & Charles for the BCRA, 477 p.
- White, W.B., 1969, Conceptual Models for Carbonate Aquifers, *Groundwater*, v. 50, no. 2, p. 180–186

White, W.B., 1988, *Geomorphology and Hydrology of Karst Terrains*: Oxford, Oxford University Press, 464 p.

White, W.B., 2007, Cave sediments and paleoclimate: *Journal of Cave and Karst Science*, v. 69, no. 1, p. 76–93

Zimmerman (Ed.), 1992, *The Lesser Caves of Watertown*: Northeast Regional Organization Publication

APPENDIX A
A PYTHON PROGRAM FOR PASSAGE GROWTH MODELING

```

import math
import numpy as np
import random as r

plot = np.array([[0.0,0.0]])
x = 0.0
y = -16.2

while (y <= 0):

    if (y+16.2) <= 0.4:
        x += 0.1

    elif ((y+16.2) >= 0.4) and ((y+16.2) <= 1):
        rand = r.uniform(30.0,50.0)
        x += 0.1*(rand/365.25)

    else:
        rand = r.uniform(5.0,15.0)
        x += 0.1*(rand/365.25)

    plot = np.append(plot, [[x*2, y]], axis=0)
    y += 1.0/1000.0

print plot[-1]

```

Figure A.1 Code listing to generate points for Hannacroix Maze model.

```

import math
import numpy as np
import random as r

plot = np.array([[0.0,0.0]])
x = 0.0
y = -17.4

while (y <= 0):

    if (y+17.4) <= 1.5:
        rand = r.uniform(15.0,30.0)
        x += 0.1*(rand/365.25)

    elif ((y+17.4) > 1.5) and ((y+17.4) <= 4):
        rand = r.uniform(2.0,15.0)
        x += 0.1*(rand/365.25)

    else:
        rand = r.uniform(0.0,2.0)
        x += 0.1*(rand/365.25)

    plot = np.append(plot, [[x*2, y]], axis=0)
    y += 1.0/1000.0

print plot[-1]

```

Figure A.2 Code listing to generate points for Barber Cave model.


```

import math
import numpy as np
import random as r

plot = np.array([[0.0,0.0]])
x = 0.0
y = -13.8

while (y <= -13.8 + 6.5):

    if (y+13.8) <= 0.2:
        x += 0.1

    elif ((y+13.8) > 0.2) and ((y+13.8) <= 4.5):
        rand = r.uniform(40.0,50.0)
        x += 0.1*(rand/365.25)

    else:
        rand = r.uniform(0.0,1.0)
        x += 0.1*(rand/365.25)

    plot = np.append(plot, [[x*2, y]], axis=0)
    y += 1.0/1000.0

print plot[-1]

```

Figure A.3 Code listing to generate points for Glen Park Labyrinth.

APPENDIX B
CROSS-SECTION SKETCHES, MEASUREMENTS, AND CALCULATIONS

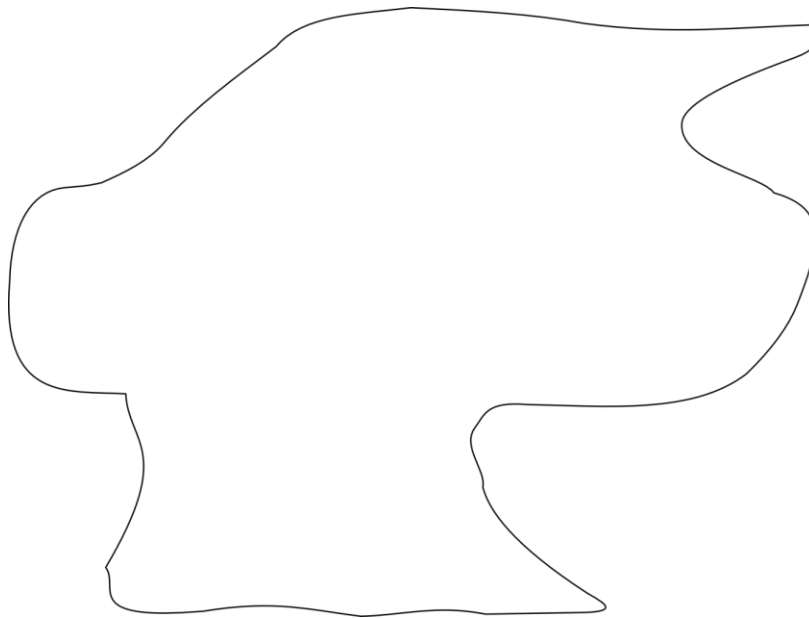


Figure B.1 Sketch of passage cross-section in Hannacroix Maze in Fungus Footpath.

Table B.1 Measurements of Hannacroix Maze cross-section

Angle	Distance to Wall (m)
0	0.854
45	0.514
90	1.156
135	0.696
180	0.515
225	0.308
270	0.628
315	0.47

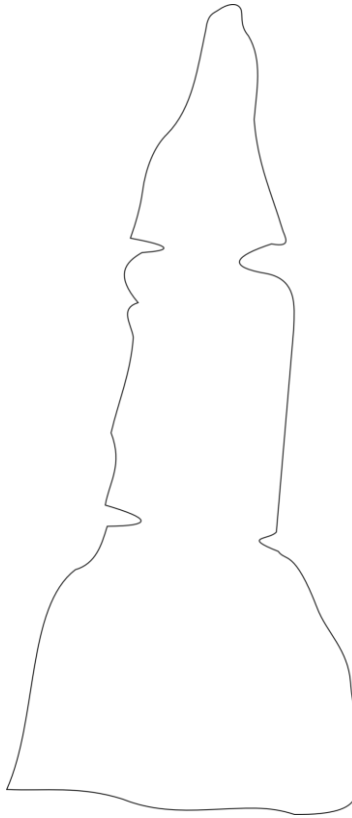


Figure B.3 Sketch of passage cross-section in Merritts Cave along MC-MC'.

Table B.3 Measurements of Merritts Cave cross-section.

Angle	Distance to Wall (m)
22.5	0.928
45	1.145
67.5	0.657
90	0.563
112.5	0.565
135	0.745
157.5	1.096
180	2.855
202.5	1.006
225	0.511
247.5	0.416
270	0.353
292.5	0.388
315	0.506
337.5	0.933

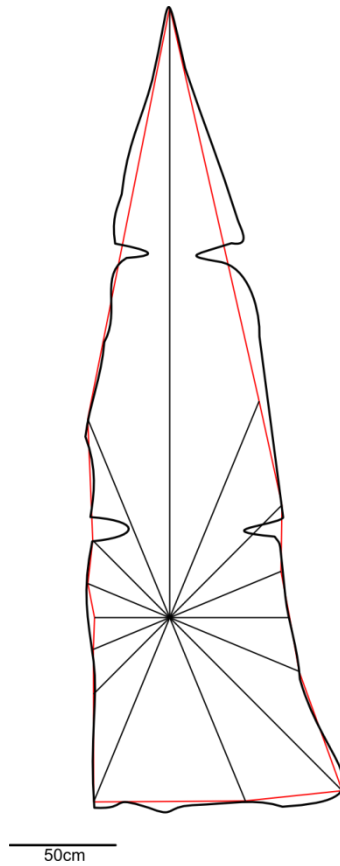


Figure B.4 Transformed cross-section in Merritts Cave along MC-MC'.

Table B.4 Computations based on Equation 4.1 to compute cross-sectional area for Merritts Cave.

Shot Angle	Distance	Angle Between	A	B	C ²	C	S	T ²	T	Area
22.5	0.928	22.5	1.145	0.928	0.209	0.457	1.265	0.041	0.203	2.491
45	1.145	22.5	0.657	1.145	0.353	0.594	1.198	0.021	0.144	
67.5	0.657	22.5	0.563	0.657	0.065	0.255	0.738	0.005	0.071	
90	0.563	22.5	0.565	0.563	0.048	0.220	0.674	0.004	0.061	
112.5	0.565	22.5	0.745	0.565	0.096	0.311	0.810	0.006	0.081	
135	0.745	22.5	1.096	0.745	0.248	0.498	1.169	0.024	0.156	
157.5	1.096	22.5	2.855	1.096	3.570	1.890	2.920	0.358	0.599	
180	2.855	22.5	1.006	2.855	3.856	1.964	2.912	0.302	0.550	
202.5	1.006	22.5	0.511	1.006	0.323	0.569	1.043	0.010	0.098	
225	0.511	22.5	0.416	0.511	0.041	0.203	0.565	0.002	0.041	
247.5	0.416	22.5	0.353	0.416	0.026	0.162	0.466	0.001	0.028	
270	0.353	22.5	0.388	0.353	0.022	0.149	0.445	0.001	0.026	
292.5	0.388	22.5	0.506	0.388	0.044	0.209	0.552	0.001	0.038	
315	0.506	22.5	0.933	0.506	0.254	0.504	0.972	0.008	0.090	
337.5	0.933	-315	0.928	0.933	0.507	0.712	1.287	0.094	0.306	
22.5	0.928									

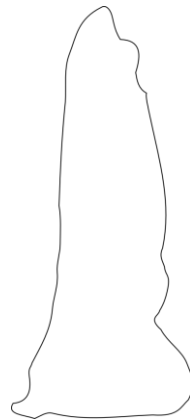


Figure B.5 Sketch of passage cross-section along BC-BC' in Barbers Cave.

Table B.5 Measurements for cross-section BC- BC' in Barbers Cave.

Angle	Distance to Wall (m)
0	0.553
90	0.201
180	0.924
270	0.152

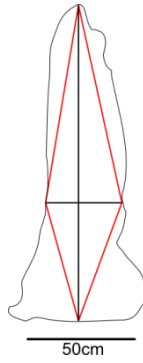


Figure B.6 Transformed cross-section along BC-BC' in Barbers Cave.

Table B.6 Computations for cross-sectional area along BC-BC' using Equation 4.1.

Shot Angle	Distance Between	Angle Between	A	B	C ²	C	S	T ²	T	Area
0	0.553	90	0.201	0.553	0.346	0.588	0.671	0.003	0.056	0.261
90	0.201	90	0.924	0.201	0.894	0.946	1.035	0.009	0.093	
180	0.924	90	0.152	0.924	0.877	0.936	1.006	0.005	0.070	
270	0.152	-270	0.553	0.152	0.329	0.574	0.639	0.002	0.042	
0	0.553									

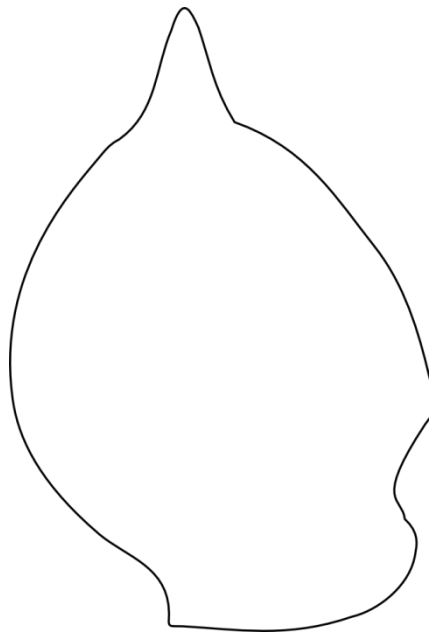


Figure B.7 Sketch of passage cross-section along BLC-BLC' in Big Loop Cave.

Table B.7 Measurements for cross-section BLC-BLC' in Big Loop Cave.

Angle	Distance to Wall (m)
0	0.522
22.5	0.628
45	0.693
67.5	0.856
90	0.719
112.5	0.798
135	0.914
157.5	1.142
180	1.922
202.5	1.111
225	0.821
247.5	0.688
270	0.582
292.5	0.486
315	0.51
337.5	0.577

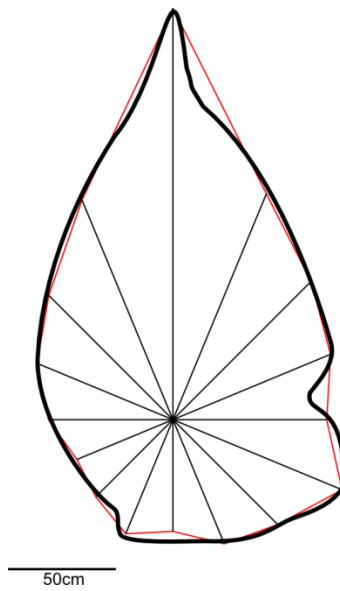


Figure B.8 Transformed cross-section along BLC-BLC' in Big Loop Cave.

Table B.8 Computations for cross-sectional area along BLC-BLC' using Equation 4.1.

Shot Angle	Distance	Angle Between	A	B	C ²	C	S	T ²	T	Area
22.5	0.628	22.5	0.693	0.628	0.070	0.265	0.793	0.007	0.083	2.237
45	0.693	22.5	0.856	0.693	0.117	0.342	0.945	0.013	0.114	
67.5	0.856	22.5	0.719	0.856	0.112	0.335	0.955	0.014	0.118	
90	0.719	22.5	0.798	0.719	0.094	0.306	0.911	0.012	0.110	
112.5	0.798	22.5	0.914	0.798	0.124	0.353	1.032	0.019	0.140	
135	0.914	22.5	1.142	0.914	0.211	0.459	1.258	0.040	0.200	
157.5	1.142	22.5	1.922	1.142	0.943	0.971	2.017	0.176	0.420	
180	1.922	22.5	1.111	1.922	0.983	0.991	2.012	0.167	0.409	
202.5	1.111	22.5	0.821	1.111	0.223	0.472	1.202	0.030	0.175	
225	0.821	22.5	0.688	0.821	0.104	0.322	0.915	0.012	0.108	
247.5	0.688	22.5	0.582	0.688	0.072	0.269	0.769	0.006	0.077	
270	0.582	22.5	0.486	0.582	0.052	0.229	0.648	0.003	0.054	
292.5	0.486	22.5	0.51	0.486	0.038	0.196	0.596	0.002	0.047	
315	0.51	22.5	0.577	0.51	0.049	0.222	0.655	0.003	0.056	
337.5	0.577	-315	0.628	0.577	0.215	0.464	0.834	0.016	0.128	
22.5	0.628									

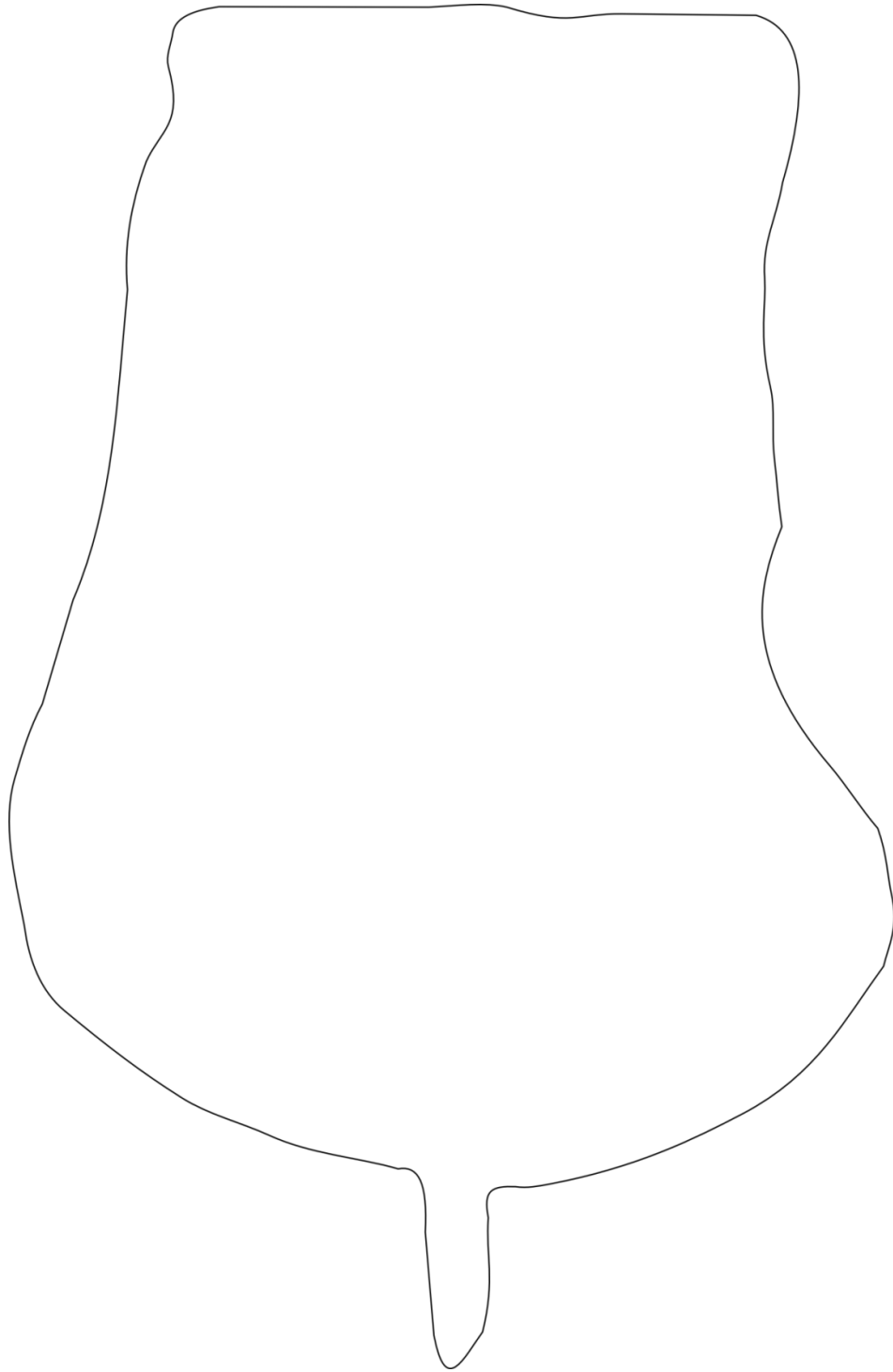


Table B.9 Sketch of passage cross-section in Glen Park Labyrinth.

Table B.10 Measurements of passage cross-section in Glen Park Labyrinth.

Angle	Distance to Wall (m)
0	0.64
45	0.861
90	1.403
135	1.502
180	2.183
225	0.773
270	0.603
315	0.64

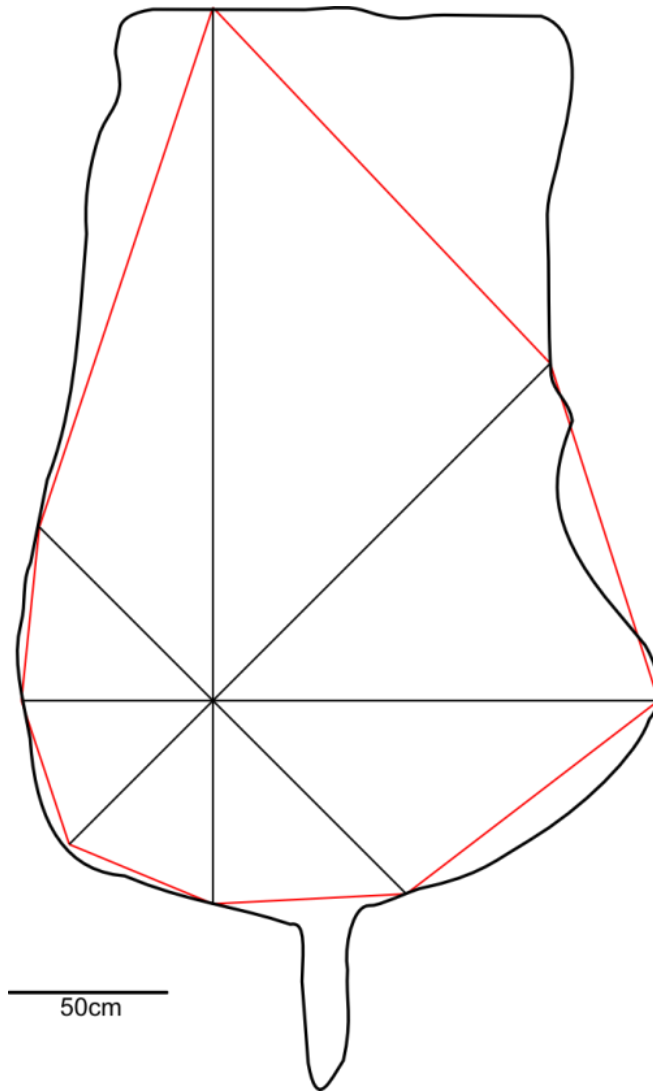


Figure B.9 Transformed cross-section of passage in Glen Park Labyrinth.

Table B.11 Calculations of cross-sectional area for passage in Glen Park Labyrinth.

Shot Angle	Distance Between	Angle Between	A	B	C ²	C	S	T ²	T	Area
0	0.64	45	0.861	0.64	0.372	0.610	1.055	0.038	0.195	3.569
45	0.861	45	1.403	0.861	1.001	1.001	1.632	0.182	0.427	
90	1.403	45	1.502	1.403	1.244	1.115	2.010	0.555	0.745	
135	1.502	45	2.183	1.502	2.384	1.544	2.615	1.344	1.159	
180	2.183	45	0.773	2.183	2.977	1.725	2.341	0.356	0.597	
225	0.773	45	0.603	0.773	0.302	0.549	0.963	0.027	0.165	
270	0.603	45	0.64	0.603	0.227	0.477	0.860	0.019	0.136	
315	0.64	-315	0.64	0.64	0.240	0.490	0.885	0.021	0.145	
0	0.64									